National Bureau of Standards
Library, N. W. Bldg.
8 SEP 1953
Reference book not to be
taken from the Library.

NBS CIRCULAR 542

Graphs of the Compton Energy-Angle Relationship and the Klein-Nishina Formula from 10 Kev to 500 Mev

UNITED STATES DEPARTMENT OF COMMERCE

NATIONAL BUREAU OF STANDARDS

UNITED STATES DEPARTMENT OF COMMERCE • Sinclair Weeks, *Secretary*
NATIONAL BUREAU OF STANDARDS • A. V. Astin, *Director*

Graphs of the Compton Energy-Angle Relationship and the Klein-Nishina Formula from 10 Kev to 500 Mev

By Ann T. Nelms

National Bureau of Standards Circular 542
Issued August 28, 1953

For sale by the Superintendent of Documents, U. S. Government Printing Office, Washington 25, D. C.
Price 55 cents

Foreword

This Circular constitutes the fourth item of a contemplated series of surveys and tabulations of information on radiation physics that are being carried out with the support of the Biophysics Branch of the Atomic Energy Commission. Three previous items have been given limited circulation as in formal reports.

This Circular represents primarily a tabulation in graphical form of certain well-known and rather simple mathematical relationships. The goal of displaying these relationships for large ranges of the independent variables and in a manner that lends itself readily to interpolation accurate to 2 percent has required considerable development of methods and an amount of labor of nearly two man-years. This effort need not seem unduly large when compared to the aggregate effort represented by a number of partial tabulations prepared in the past by other groups. It was undertaken in the hope of providing a rather definitive reference capable of fulfilling most anticipated needs except for yet undetermined correction factors and extension to energies beyond 500 million electron volts.

It is hoped that the decision to undertake an effort of this magnitude and to utilize a graphical, rather than tabular, presentation will prove justified. Critical comments and suggestions by the public will be particularly welcome, in view of the difficulty of assessing the priority of different possible tasks in this series and of estimating the number and the type of workers who may utilize similar publications.

U. Fano, *Chief*,
Nuclear Physics Section,
National Bureau of Standards.

Contents

	Page
Foreword	III
1. Symbols	1
2. Introduction	1
2.1. Radiative correction to the Klein-Nishina formula for free electrons	2
2.2. Experimental studies of the Compton effect	2
2.3. Corrections to the Klein-Nishina formula in case of small momentum transfer	2
a. Reduction of the probability of Compton scattering	3
b. Modification of the Compton law	3
2.4. General procedure and accuracy of calculations	4
2.5. Discussion of graphs	5
a. Scattered photon energy versus angle of scattering (fig. I)	5
b. Recoil electron energy versus angle of scattering (fig. II)	5
c. Photon wavelength distribution (fig. III)	5
d. Angular distribution of the scattered radiation (fig. IV)	5
e. Angular distribution of the recoil electrons (fig. V)	6
f. Energy distribution of the photon (fig. VI)	6
g. Electron energy distribution (fig. VII)	6
h. Integral Klein-Nishina cross section (fig. VIII)	6
3. References	7
4. List of graphs	8

Graphs of the Compton Energy-Angle Relationship and the Klein-Nishina Formula from 10 Kev to 500 Mev

Ann T. Nelms

The Compton energy versus angle relationship and the differential and integral Klein-Nishina cross sections are presented graphically as functions of the energy and direction of the scattered photon and of the recoil electron. These graphs are intended to serve the purpose of tables. Unpolarized primary gamma rays in an energy range from 10 Kev to 500 Mev are considered. The accuracy of all curves is estimated at 1 percent. The advantage of this form of presentation is the convenience and accuracy of two-way interpolation. In general, interpolated values may be obtained with an accuracy of 2 percent.

1. Symbols

The following symbol notation is used throughout this paper:

ν_o = Initial photon frequency, sec^{-1}.
ν = Scattered photon frequency, sec^{-1}.
$h\nu_o$ = Initial photon energy (h = Planck's constant), Mev
$h\nu$ = Scattered photon energy, Mev.
m = Electron rest-mass.
c = Velocity of electromagnetic radiation in vacuum.
$\alpha_o = h\nu_o/mc^2$ = Energy of initial photon in mc^2.
$\alpha = h\nu/mc^2$ = Energy of scattered photon in mc^2.
$\lambda_o = mc^2/h\nu_o = 1/\alpha_o$ = Wavelength of initial photon in Compton wavelength.
$\lambda = mc^2/h\nu = 1/\alpha$ = Wavelength of scattered photon in Compton wavelength.
T = Kinetic energy of the recoil electron $= h\nu_o - h\nu$, Mev.
θ = Angle between primary photon beam and scattered beam, degrees.
ψ = Angle between primary photon beam and direction of recoil electrons, degrees.
σ_0 = Thomson's classical cross section $\frac{8}{3}\pi r_0^2$, $cm^2 = 6.651 \times 10^{-25} cm^2$, where $r_0 = e^2/mc^2$, and e is the electronic charge.

Differential Klein-Nishina cross section per electron:

$f(\lambda_o, \lambda)$ = Photon wavelength distribution, Thomson cross section unit per Compton wavelength unit (see page 4).
$d\sigma/d\Omega_\theta$ = Angular distribution of the scattered photon, cm^2/steradian.
$d\sigma/d\Omega_\psi$ = Angular distribution of the recoil electron, cm^2/steradian.
$d\sigma/dh\nu$ = Energy distribution of the scattered photon, cm^2/Mev.
$d\sigma/dT$ = Energy distribution of the recoil electron, cm^2/Mev.

Integral Klein-Nishina cross section:

σ_T = Total Compton cross section, cm^2/electron.
σ_a = Effective cross section for the energy absorbed by the electron, cm^2/electron. (See sec. 2.5-h, page 6).

2. Introduction

After discussions with various members of the National Bureau of Standards Radiation Physics Laboratory who expressed a desire for tabulations of the Compton energy versus angle relationships and differential and integral Klein-Nishina cross section for unpolarized [1] [2] gamma rays, a survey of the literature [1] was made. This study included available information over the last decade. There are two unfavorable characteristics common to all of the presentations of such data; namely, the energy range of the primary radiation is limited and the forms of presentation do not yield accurate interpolated values of the cross section.

This report strives to eliminate these undesirable features. The data are expressed in the units used most often by experimentalists. All calculations and curves are believed to be accurate to 1 percent, taking as a basis the values of constants from DuMond and Cohen.[3] The actual form of the plots is such that interpolated values can be obtained in general within 2-percent accuracy.

The Compton effect depicts the scattering of a photon of initial energy α_o by a "free" electron, so that the photon has a degraded energy α, and the recoil electron has acquired a kinetic energy equal to $\alpha_o - \alpha$. The expression for α as a function of α_o and of the angle of photon scattering θ is given by

$$\alpha = \alpha_o/[1 + \alpha_o(1 - \cos\theta)]. \quad (1)$$

[1] For a discussion of polarization, see U. Fano, J. Opt. Soc. Am. **39**, 859 (1949).

[2] Figures in brackets indicate the literature references at the end of this paper.

[3] J. W. M. DuMond and E. R. Cohen, Phys. Rev. **82**, 555 (1951).

The differential Klein-Nishina cross section [2] for the scattering of a photon in the direction θ per unit solid angle is expressed as

$$\frac{d\sigma}{d\Omega}=\frac{r_0^2}{2}\frac{(1+\cos^2\theta)}{[1+\alpha_o(1-\cos\theta)]^2}\left\{1+\frac{\alpha_o^2(1-\cos\theta)^2}{(1+\cos^2\theta)[1+\alpha_o(1-\cos\theta)]}\right\}. \quad (2)$$

This cross section can be expressed in terms of the energy from eq (1).

$$\frac{d\sigma}{d\alpha}=\frac{\pi r_0^2}{\alpha_o^2}\left[\frac{2}{\alpha_o}-\frac{2}{\alpha}+\frac{1}{\alpha_o^2}+\frac{1}{\alpha^2}-\frac{2}{\alpha_o\alpha}+\frac{\alpha_o}{\alpha}+\frac{\alpha}{\alpha_o}\right] \quad (3)$$

for $\alpha_o\geq\alpha\geq\alpha_o/[1+2\alpha_o]$. The total Compton cross section can be obtained from eq (3) by integrating over all scattered energies. Hence

$$\sigma_T=2\pi r_0^2\left\{\frac{1+\alpha_o}{\alpha_o^2}\left[\frac{2(1+\alpha_o)}{1+2\alpha_o}-\frac{\ln(1+2\alpha_o)}{\alpha_o}\right]+\frac{\ln(1+2\alpha_o)}{2\alpha_o}-\frac{1+3\alpha_o}{(1+2\alpha_o)^2}\right\}. \quad (4)$$

2.1. Radiative Correction to the Klein-Nishina Formula for Free Electrons

The Compton scattering by free electrons is described to a very good approximation by the Klein-Nishina formula. "Radiative corrections" arise from high-order electrodynamic effects and are associated with the weak bremsstrahlung generated in the sudden recoil of the electron. These corrections have been calculated by Schafroth [3] and by Brown and Feynman [4] up to terms proportional to e^6 (giving corrections of the order $e^2/(hc/2\pi)=1/137$ to the K-N formula).

The net effect of the calculated correction is small, of the order of 1 percent or less,[4] but it consists of two appreciable portions that nearly cancel one another. On the one hand, the probability of the ordinary Compton effect is usually reduced. On the other hand, one must consider, in this approximation, the probability that the electron radiates in the course of the Compton process one (or more) photons in addition to the scattered one. This additional photon usually has a very low energy and therefore it is hard to detect, and does not appreciably affect the energy balance of the process. Therefore, the two processes, of ordinary Compton scattering and scattering with two-photon emission (sometimes referred to as double Compton effect), are not readily resolved operationally, and their combined probability must be calculated (except when the additional photon has unusually high energy)[5].

[4] Calculations for an incident photon energy of 2.62 Mev give corrections of the order of 1 percent at angles around 50°, when a photon energy of 100 Kev is assumed for the low-energy photon. The integrated correction is less than 1 percent and has been stated by Colgate [4a] as about 0.2% in his experiment.

[5] A detailed separate calculation of either effect is not even meaningful because it is based on the assumption of a fictitious photon mass. This point must be borne in mind when examining the original papers [4].

2.2. Experimental Studies of the Compton Effect

Few investigations have been made of the angular distribution of the scattered photons predicted by the Klein-Nishina formula. Of these, possibly the most conclusive test is given by the data of Hofstadter and McIntyre [5] for Co^{60} γ-radiation. They measured the number of coincidences between the recoil electron and the scattered photon as a function of the angular position of the detector (stilbene crystal). They obtained good agreement with the differential Klein-Nishina curve within their experimental error except at the smallest angles used (20° and 15°). An additional experiment by Hofstadter and McIntyre [6] yielded an indication of the energy distribution of Compton electrons.

Numerous experiments have been made to check the Klein-Nishina formula for total scattering cross section. Parkinson [7] found agreement with predictions of the theory within an experimental error of 1 percent. He reviews previous similar work where the total scattering cross section was obtained from measurements of the total attenuation coefficient. It is important in such measurements that the incident energy and absorbing material be chosen so that Compton scattering gives the main contribution to the total attenuation. Otherwise, more reliance than is justified may be placed on cross sections for the photoelectric and pair production processes.

Verification of the Compton relationship has been the aim of many experiments. Most of this work has been summarized by Cross and Ramsey [8]. Their results, in agreement with Hofstadter and McIntyre [9], indicate that the recoil electron and scattered photon emitted in a Compton scattering event are simultaneous within a time interval of less than 1.5×10^{-8} sec. The conservation of energy and momentum laws have been verified in various experiments.

2.3. Corrections to the Klein-Nishina Formula in the Case of Small Momentun Transfer

The assumption of free electrons initially at rest that underlies the Klein-Nishina formula is approximately valid only if the momentum transferred to the electron greatly exceeds the initial momentum of the electron's motion within an atom. In terms of the wavelengths of the incident radiation (λ_o) and of the atomic electron (λ_{el}), this condition reads

$$\lambda_o/2\sin\frac{\theta}{2}\ll\lambda_{el}.$$

When this condition is not satisfied, Compton scattering is complicated by the bonds that hold the atomic electrons and by their motion within the atom. As a result, Compton scattering becomes less frequent than predicted by the Klein-Nishina law.

a. Reduction of the probability of Compton scattering

In an approximate calculation one may regard the probability of Compton scattering by an atomic electron as the product of two factors. The first factor concerns the probability that the photon is deflected by a certain angle (θ) and transfers to the electron a corresponding amount of momentum p as though the electron were free. The second factor concerns the probability that the electron, having received a momentum p, will absorb a certain amount of energy and thereby become excited or leave the atom. The first factor is given by the differential Klein-Nishina cross section ($d\sigma_{K-N}$) for free electrons. The second factor has been evaluated by Heisenberg and Bewilogua [10] on the basis of the Fermi-Thomas model. They evaluated the probability $S(h\nu,\theta,Z)$ that any energy absorption whatsoever results when a photon of frequency ν is scattered by an angle θ and transfers a momentum $p \sim h\nu 2 \sin(\theta/2)/c$ to the electrons of an atom with atomic number Z. Thus the total cross section for Compton scattering with deflection θ by the Z electrons of an atom is given approximately by

$$d\sigma_Z = d\sigma_{K-N} S(h\nu,\theta,Z) \qquad (4a)$$

The dependence of S on $h\nu$, θ, and Z is expressed in terms of the single variable $V = 178.4 Z^{-2/3} h\nu \sin\theta/2$. A graph of $S(V)$ is given in figure 1.

A comparison of eq (4a) with the Klein-Nishina cross section for $Z=82$ is shown in figure 2 for an incident photon energy of 300 Kev. At very small angles the cross section per unit solid angle for bound electrons is considerably lower than that for free electrons. At $\theta=4°$, $d\nu_Z$ is about 50 percent of the Klein-Nishina cross section for Pb

$$\left(Z\frac{d\sigma_{K-N}}{d\Omega} = 648\times10^{-26};\quad S(V)=0.486,\right.$$

so that

$$\left.\frac{d\sigma_Z}{d\Omega} = Z\frac{d\sigma_{K-N}}{d\Omega}\,S(V) = 315\times10^{-26}\right).$$

The reduction of the probability of Compton scattering is more than compensated for by the probability of coherent scattering [6] (unmodified radiation) at small angles. At $\theta=4°$ and $Z=82$ the cross section per unit solid angle for coherently scattered radiation of 300-Kev energy is 86×10^{-24}, or about 13 times the Klein-Nishina cross section.

b. Modification of the Compton law

The initial state of bound motion of an atomic electron also causes a relaxation of the Compton relationship that binds the energy of a scattered photon to its direction and the direction of electron

[6] Coherent scattering is the object of an investigation in progress.

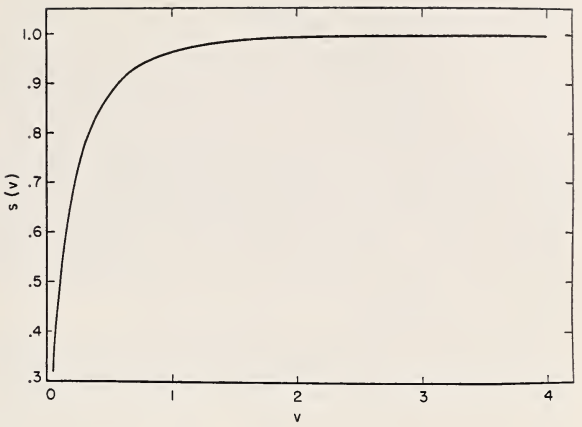

FIGURE 1. *Correction $S(V)$ to the Klein-Nishina formula in the case of a small momentum transfer as a function of $V(h\nu,\theta,Z)$.*

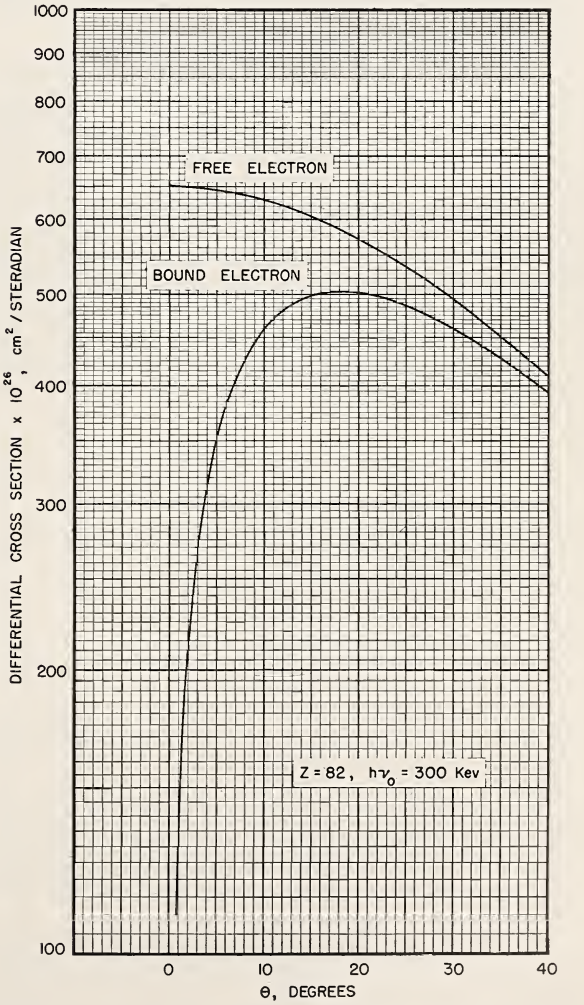

FIGURE 2. *Illustration of the effect of $S(V)$ on the Klein-Nishina cross section for* Pb *at $h\nu_0=300$ Kev.*

recoil to its energy. This effect may be visualized in two equivalent manners.

The atomic electrons may be regarded as initially free but endowed with a certain statistical distribution of velocities. Then the Compton relationship holds exactly in the moving frame of reference in which each electron happens to be at rest. As a result, photons scattered in a certain direction do not have identical energies (even though their initial energies were equal). The resulting energy spread may be regarded as a Doppler broadening because it arises from the electron's motion.

Alternately, one may consider that the momentum transferred to an electron is essentially determined by the angle of photon scattering (and by the incident photon energy). As a result of this momentum transfer, the electron may recoil out of the atom with various energies and leave the energy balance to the photon. (The reduction of Compton scattering probability mentioned in section a, page 3, corresponds to the possibility that the recoil is absorbed by the whole atom and the electron fails to be ejected.)

According to either picture, the balance of momentum, which is the basis of the Compton law, must take into account the initial momentum of the electron's motion within the atom. The direction of this momentum is random. Its magnitude, p_b, may be regarded as roughly related to the ionization potential of the electron, I, according to $p_b^2/2m \sim I$. The momentum p transferred from the photon to the electron equals approximately $h\nu_o 2 \sin(\theta/2)c$ provided $h\nu_o(1-\cos\theta) \ll mc^2$. The momentum q with which the electron recoils out of the atom is expected to lie within the approximate limits $q \sim p \pm p_b$. The recoil energy varies correspondingly within the approximate limits

$$\frac{q^2}{2m} \sim \frac{p^2}{2m} + I \pm 2\sqrt{\frac{p^2}{2m} I}.$$

The kinetic energy of the recoil electron varies within the limits

$$T = \frac{q^2}{2m} - I \sim \frac{p^2}{2m} \pm 2\sqrt{\frac{p^2 I}{2m}}.$$

More specifically, a value of $T = p^2/2m \pm (p^2 I/2m)^{1/2}$ is found by calculation to occur approximately half as frequently as the value $T = p^2/2m$ (see below).

Semiquantitative verification of the energy distribution of recoil electrons was obtained by DuMond [11] from an experimental determination of the spectral distribution of photons scattered at a given angle.

In the Compton scattering by free electrons, the energy of the scattered photon is approximately equal to the energy of the incident photon when $h\nu_o(1-\cos\theta) \ll mc^2$. This condition holds for all values of θ when $h\nu_o \ll mc^2$, for small values of θ when $h\nu_o \sim mc^2$, and for very small values of θ when $h\nu_o \gg mc^2$. For all these cases, of course, the kinetic energy acquired by the electron is small and may be evaluated approximately by the above expression with the substitution $p = h\nu_o 2 \sin(\theta/2)/c$. For example, if $h\nu_o = 300$ Kev, $I = 1$ Kev and $\theta = 30°$, then $T \approx 4 \pm 10$ Kev.

The problem of the energy distribution of recoil electrons in Compton scattering is equivalent to the corresponding problem for inelastic scattering of electrons of energy E by atomic electrons. The energy loss W of an electron scattered through a moderately large angle ($\gg\sqrt{I/E}$) falls approximately within the limits $W = Q \pm 2\sqrt{QI}$, where Q is the energy loss in scattering by a free electron, and $W = Q \pm \sqrt{QI}$ is half as frequent as $W = Q$ [12].

2.4. General Procedure and Accuracy of Calculations

The Compton energy versus angle values were calculated directly from eq (1). Corrections to the Klein-Nishina formula discussed in the preceding sections were not included in the calculations of the cross sections. The differential cross section can be expressed in terms of wavelength $\lambda_o = 1/\alpha_o$ from eq (3),

$$\frac{d\sigma}{d\lambda} = \pi r_0^2 \left(\frac{\lambda_o}{\lambda}\right)^2 \left[\frac{\lambda_o}{\lambda} + \frac{\lambda}{\lambda_o} - 2(\lambda - \lambda_o) + (\lambda - \lambda_o)^2\right], \quad (5)$$

where $\lambda_o \leq \lambda \leq \lambda_o + 2$. A rearrangement of eq (5) gives

$$f(\lambda_o, \lambda) = \frac{1}{\sigma_0}\frac{d\sigma}{d\lambda} = \frac{3}{8}\left(\frac{\lambda_o}{\lambda}\right)^2 \left[\frac{\lambda_o}{\lambda} + \frac{\lambda}{\lambda_o} - 2(\lambda - \lambda_o) + (\lambda - \lambda_o)^2\right], \quad (6)$$

for which graphs are given (figs. III, a, b, and c). This particular form was used because values are easily calculated, and the Klein-Nishina cross section in terms of all variables may be obtained by multiplying eq (6) by suitable factors. Values of $f(\lambda_o, \lambda)$ interpolated from this graph were used as a general guide in plotting the cross sections; however, the various graphs were eventually constructed from independent recalculation of $f(\lambda_o, \lambda)$ for the appropriate values of λ_o and λ.

All calculations were made to four significant figures. Considerable effort was made to place each point on the graphs with an accuracy of 1 percent. In order to have all points along the curves as accurate as the plotted points from which the smooth curves were drawn, many checks for smoothness were made. Two types of tests were used. First, transversal plots of the original graphs were made. All irregular points were checked by calculation if the deviations were greater than the stated accuracy allowed. Second, test calculations at various points were made.

TABLE 1. *Two examples of the accuracy of interpolation*

a. $h\nu_o$=0.75 Mev, $0° \leq \theta \leq 60°$

θ	$h\nu$		Error
	Interpolated	Calculated	
Degree	*Mev*	*Mev*	*Percent*
0	0.750	0.750	0.00
5	.744	.746	−.27
10	.731	.734	−.41
15	.711	.714	−.42
20	.685	.689	−.58
25	.659	.659	.00
30	.625	.627	−.32
35	.594	.593	+.17
40	.560	.558	+.36
45	.528	.525	+.57
50	.495	.492	+.61
55	.464	.461	+.65
60	.434	.433	+.23

b. θ=55°, 0.5 Mev $\leq h\nu_o \leq$ 5 Mev

$h\nu_o$	$h\nu$		Error
	Interpolated	Calculated	
Mev	*Mev*	*Mev*	*Percent*
0.5	.353	.353	0.00
.6	.401	.400	+.25
.8	.480	.480	.00
1.0	.550	.545	+.91
1.2	.600	.600	.00
1.5	.662	.666	−.60
2.0	.748	.749	−.13
2.5	.815	.810	+.61
3.0	.851	.856	−.58
3.5	.889	.893	−.45
4.0	.920	.922	−.22
5.0	.960	.967	−.72

The majority of these tests were made on the penciled graphs. There was a small sacrifice of accuracy in the reproduction. However, a few checks on the finished graphs show that the error is within the allowed deviation. Two examples of two-way interpolation are given in table 1. In the first case, which illustrates the energy-angle relationship for an initial gamma ray of 0.75 Mev, where $0° \leq \theta \leq 60°$, the points were obtained from figure I, h, by visual judgment. The second case is an interpolation from the same graph for constant angle (55°). It is well to note that more accurate values of table 1, a, can be obtained by a family of curves interpolated at constant angles. Not only the accuracy of the curves was considered but the accuracy of values obtained by interpolation.

To obtain maximum accuracy for interpolated values, the type of plot is important. For this reason different kinds of plots are given for various initial energies and in different ranges of the same energy, each section having the best plot for ease of interpolation. The tests for accuracy of interpolated values indicate that, in general, values may be obtained within an accuracy of 2 percent.

2.5. Discussion of Graphs

Each section that follows contains a discussion of a particular group of graphs that is designated by a single roman number.

249464—53——2

a. Scattered photon energy versus angle of scattering (fig. I)

A convenient form for eq (1) is

$$h\nu = h\nu_o/[1+\alpha_o(1-\cos\theta)], \tag{7}$$

where $h\nu$ and $h\nu_o$ are in Mev. For $h\nu_o \gg mc^2$, the curves decrease rapidly from the maximum value at zero degrees to a minimum value at 180° expressed as

$$h\nu_{\min} = h\nu_o/[1+2\alpha_o] \cong \tfrac{1}{2}mc^2. \tag{8}$$

In the nonrelativistic region, however, the photon does not lose an appreciable amount of energy by scattering, that is, $h\nu \sim h\nu_o$.

b. Recoil electron energy versus angle of scattering (fig. II)

Since the recoil electron energy T is the difference between the initial gamma-ray energy and the energy of the scattered photon, one can write

$$T = 2\alpha_o h\nu_o/[1+2\alpha_o+(1+\alpha_o)^2\tan^2\psi]. \tag{9}$$

The maximum value of the recoil energy is at ψ=0 when the photon is scattered by 180°. The value of the recoil energy is then expressed as

$$T_{\max} = 2\alpha_o h\nu_o/[1+2\alpha_o]. \tag{10}$$

The maximum deflection of the electron is 90°. At this limit the photon is scattered in the forward direction. Near this limit the electron energy is so low that the binding effects considered in section 2.3 must always be taken into account.

c. Photon wavelength distribution (fig. III)

The differential cross section for the scattering by a free electron of a photon with initial wavelength λ_o into the wavelength interval λ to $\lambda+d\lambda$ is given by eq (6). The original graph of this function is a large master chart from which values were taken in computing cross sections (see sec. d, page 5). Since experimentalists are less interested in this graph, a smaller chart is presented here for illustration. The accuracy desired in this report cannot be obtained from these graphs.

d. Angular distribution of the scattered radiation (fig. IV)

The differential cross section for the scattering of a photon through an angle θ into the solid angle $d\Omega$ can be expressed as a function of $f(\lambda_o, \lambda)$ in the following manner

$$\frac{d\sigma}{d\Omega_\theta} = \frac{\sigma_0 f(\lambda_o,\lambda)}{2\pi} = \frac{r_0^2}{2}\frac{(1+\cos^2\theta)}{[1+\alpha_o(1-\cos\theta)]^2} \left\{1+\frac{\alpha_o^2(1-\cos\theta)^2}{[1+\cos^2\theta][1+\alpha_o(1-\cos\theta)]}\right\}, \tag{11}$$

where $\theta=\arccos(1+\lambda_o-\lambda)$. For $h\nu_o \ll mc^2$ the cross section approaches Thomson's classical formula for scattering $\frac{1}{2}r_0^2(1+\cos^2\theta)$. In this region the curves reach a minimum at 90° about which the distribution is almost symmetrical, with maximum values of the cross section at 0° and 180°. This characteristic shape disappears as $h\nu_o \to mc^2$. A plot of the initial photon energy versus the angle at which there is a minimum value of the cross section is given in figure IV, m. As $h\nu_o$ increases beyond mc^2, the distribution is weighted in the forward direction.

e. Angular distribution of the recoil electrons (fig. V)

The differential cross section for the recoil of a free electron at angle ψ with respect to the photon's direction of propagation into the solid angle $d\Omega$ is written

$$\frac{d\sigma}{d\Omega_\psi}=\frac{\sigma_0 f(\lambda_o,\lambda)}{2\pi}\frac{(1+\alpha_o)^2(1-\cos\theta)^2}{\cos^3\psi}$$

$$=\frac{d\sigma}{d\Omega_\theta}\frac{(1+\alpha_o)^2(1-\cos\theta)^2}{\cos^3\psi}$$

$$=\frac{r_0^2}{2}\left[\frac{2(\alpha_o+1)}{(\alpha_o+1)^2\tan^2\psi+2\alpha_o+1}\right]^2\frac{1}{\cos^3\psi}\left\{1+\left[\frac{(\alpha_o+1)^2\tan^2\psi-1}{(\alpha_o+1)^2\tan^2\psi+1}\right]^2+\frac{4\alpha_o^2}{[(\alpha_o+1)^2\tan^2\psi+1][(\alpha_o+1)^2\tan^2\psi+2\alpha_o+1]}\right\}, \quad (12)$$

where $\psi=\arctan\left(\frac{1}{\alpha_o+1}\right)\left[\frac{2\alpha_o\alpha}{\alpha_o-\alpha}-1\right]^{1/2}$.

For $h\nu_o<0.2$ Mev, the curves for low primary energies lie above those for high primary energies. This trend is also true for $h\nu_o>0.2$ Mev at large angles. For initial photon energies >0.2 Mev the curves cross at small angles so that at zero degrees the curve for highest initial photon energy is above all curves for lower initial energies. In order to give the cross sections clearly at small angles, the angles are plotted on a logarithmic scale. For convenience in reading the value of the cross section at zero degrees, a few linear plots of angles were made in that region.

f. Energy distribution of the photon (fig. VI)

The differential cross section for the scattering of a photon of initial energy $h\nu_o$ into the energy interval $h\nu$ to $h\nu+dh\nu$ is given by

$$\frac{d\sigma}{dh\nu}=\frac{\sigma_0\lambda^2}{mc^2}f(\lambda_o,\lambda)=\frac{\pi r_0^2 mc^2}{(h\nu_o)^2}\left\{\frac{h\nu}{h\nu_o}+\frac{h\nu_o}{h\nu}-2\left(\frac{mc^2}{h\nu}-\frac{mc^2}{h\nu_o}\right)+\left(\frac{mc^2}{h\nu}-\frac{mc^2}{h\nu_o}\right)^2\right\}. \quad (13)$$

An analysis of this distribution shows that a minimum exists for all energies. For $h\nu_o<1.5$ Mev the minimum is well defined by the curvature. For $h\nu_o>1.5$ Mev, however, the minimum occurs about 0.5 Mev from the initial photon energy. The difference in the value of the cross section at the primary energy and at the energy where the minimum occurs is $\sim 4.88\times10^{-25}\lambda_o^4/[1-\lambda_o]$.

The graph for primary energies ≤ 400 Kev (fig. VI, i) represents $(d\sigma/dh\nu)h\nu_o/h\nu\times10^2$ as a function of the percentage of energy retained by the photon. Not to have changed the plot in this range would have resulted in the curves crossing and interpolation would have been almost impossible. To read this graph one must find the percentage of the initial energy that is scattered. The value of the ordinate obtained should be multiplied by this percentage to have the cross section in cm²/Mev. Figures VII, d to h, of the electron energy distribution curves can be used as an alternate method of obtaining values of the cross section by determining the energy of the recoil electron and reading the cross section directly in cm²/Mev. For example, let us determine the differential cross section for the scattering of a gamma ray with an initial energy of 40 Kev so that the scattered energy is 35.9 Kev. The scattered energy is 89.8 percent of the initial energy, and the corresponding ordinate reading 0.107×10^{-23} cm²/percentage of energy retained by the photon $=0.107\times89.8\times10^{-23}=9.61\times10^{-23}$ cm²/Mev. Using the alternate method, one obtains the energy of the recoil electron as 4.1 Kev. From figure VII, g, the cross section is read directly as 9.6×10^{-26} cm²/Kev.

g. Electron energy distribution (fig. VII)

The differential cross section for giving a free electron a recoil energy in the interval from T to $T+dT$ is written

$$\frac{d\sigma}{dT}=\frac{d\sigma}{dh\nu}=\frac{\sigma_0\lambda^2}{mc^2}f(\lambda_o,\lambda)=\frac{\pi r_0^2 mc^2}{(h\nu_o-T)^2}\left\{\left[\frac{mc^2T}{(h\nu_o)^2}\right]^2+2\left[\frac{h\nu_o-T}{h\nu_o}\right]^2+\frac{h\nu_o-T}{(h\nu_o)^3}[(T-mc^2)^2-(mc^2)^2]\right\}, \quad (14)$$

where $T=h\nu_o-h\nu$. The maximum value of the cross section occurs at T_{max} (see eq (10)). For $h\nu_o \gg mc^2$, the cross section decreases rapidly and gradually flattens as T approaches zero with a shallow minimum at $T\sim mc^2$ (see sec. f, page 6). At lower initial primary energies the minimum becomes more pronounced.

h. Integral Klein-Nishina cross section (fig. VIII)

The integral Klein-Nishina cross section is given by eq (4) An approximation to this equation for $h\nu_o \gg mc^2$ is given by

$$\sigma_T=\sigma_0\frac{3}{8}\frac{mc^2}{h\nu_o}[\ln 2\alpha_o+\tfrac{1}{2}].$$

This shows that the total Compton cross section decreases with increasing energy.

The attenuation of an incident beam of X-rays is determined by the total number of photons scattered out as a result of collisons with the electrons of a material. However, the probable energy transfer to a material by a beam of X-rays is determined by the product of the average fraction of the incident photon energy that is transferred to the recoil electron in a single Compton scattering process and of the total scattering cross section. This product $f\sigma_T$ is frequently referred to as the "true absorption cross section" σ_a for the Compton process. In figure VIII a plot of σ_T and σ_a is presented and figure VIII, b, shows the fraction of the incident energy that is transferred to the scattered photon and to the recoil electron in a single Compton scattering process.

I thank U. Fano for many helpful discussions, G. R. White, who offered closer guidance especially in the development of the Introduction, and the members of the Radiation Laboratory and others who made contributions through discussions and correspondence.

3. References

[1] G. Allen, Natl. Advisory Comm. Aeronaut., Tech. Notes 2026 (Lewis Flight Propulsion Laboratory, Cleveland, Ohio 1950).
C. M. Davisson and R. D. Evans, Revs. Mod. Phys. **24,** 79 (1952).
H. E. Johns, et al, Can. J. Research **30,** 556 (1952).
R. Latter and H. Kahn, U. S. Air Force Project Rand R–170 (Rand Corp., Santa Monica, Calif. 1949).
J. D. Lawson and K. Wyllie, Atomic Energy Research Establishment, Memo G–M 78 (Ministry of Supply, Harwell Berks., England).
D. W. S. Smout, Atomic Energy Research Establishment, Memo EL–R–892 (Ministry of Supply, Harwell Berks., England June 5, 1952).
G. T. P. Tarrant, Cambridge Phil Soc. **28,** 475 (1932).
J. A. Wheeler. (Unpublished).
[2] O. Klein und Y. Nishina, Z Physid Bd. 52, 853 (1929).
W. Heitler, The quantum theory of radiation (Oxford Univ. Press, Oxford, England 1944).
K. H. Spring, Photons and electrons (John Wiley & Sons, Inc., New York, N, Y. 1950).
[3] M. R. Schafroth, Helv. Phys. Acta. **23,** 542 (1950).
[4] L. M. Brown and R. P. Feyman, Phys. Rev. **85,** 231 (1952).
[4a] S. A. Colgate, Phys. Rev. **87,** 592 (1952).
[5] R. Hofstadter and J. A. McIntyre, Phys. Rev. **76,** 1269 (1949).
[6] R. Hofstadter and J. A. McIntyre, Phys. Rev. **80,** 631 (1950).
[7] W. C. Parkinson, Phys. Rev. **76,** 1348 (1949).
[8] W. G. Cross and N. F. Ramsey, Phys. Rev. **80,** 9291 (1950).
[9] R. Hofstadter and J. A. McIntyre, Phys. Rev. **78,** 24 (1950).
[10] W. Heisenberg and L. Bewilogua, Physik Z. **32,** 737 und 740 (1931).
[11] J. W. M. DuMond, Phys Rev. **5,** 1 (1933).
[12] H. A. Bethe, Handbuch der Physik **24,** 503 (Verlag von Julius Springer, Berlin, Germany 1933).

4. List of Graphs

The initial graph in several of the groups is a "picture" graph, a composite chart that indicates the complete range and general shape of the curves in the family. It is not intended to be used to obtain accurate values. The accuracy of the graphs is discussed in the Introduction.

Compton Energy-Angle Relationship:

		Page
Figure I.	Scattered photon energy versus angle	9
a, b.	$h\nu_o$, 60 to 500 Mev; θ, 0° to 12°	10
c to g.	$h\nu_o$, 5 to 500 Mev; θ, 0° to 180°	12
h, i.	$h\nu_o$, 0.5 to 5 Mev; θ, 0° to 180°	17
j.	$h\nu_o$, 50 to 500 Kev; θ, 0° to 180°	19
k.	$h\nu_o$, 10 to 50 Kev; θ, 0° to 180°	20
Figure II.	Recoil electron energy versus angle	21
a to d.	$h\nu_o$, 10 to 500 Mev; ψ, 0° to 90°	22
e to g.	$h\nu_o$, 0.8 to 10 Mev; ψ, 0° to 90°	26
h, i.	$h\nu_o$, 0.15 to 0.8 Mev; ψ, 0° to 90°	29
j, k.	$h\nu_o$, 40 to 150 Kev; ψ, 0° to 90°	31
l, m.	$h\nu_o$, 10 to 40 Kev; ψ, 0° to 90°	33

Differential Klein-Nishina Cross Section per Electron:

		Page
Figure III, a to c.	Photon wavelength distribution	35
Figure IV.	Photon angular distribution	38
a.	$h\nu_o$, 50 to 500 Mev; θ, 0° to 5°	39
b.	$h\nu_o$, 0.6 to 50 Mev; θ, 0° to 20°	40
c.	$h\nu_o$, 10 to 600 Kev; θ, 1° to 30°	41
d.	$h\nu_o$, 1 to 500 Mev; θ, 1° to 30°	42
e.	$h\nu_o$, 0.1 to 3 Mev; θ, 10° to 30°	43
f.	$h\nu_o$, 10 to 100 Kev; θ, 10° to 30°	44
g.	$h\nu_o$, 10 to 500 Mev; θ, 0° to 60°	45
h.	$h\nu_o$, 0.01 to 10 Mev; θ, 30° to 60°	46
i.	$h\nu_o$, 50 to 500 Mev; θ, 60° to 180°	47
j.	$h\nu_o$, 5 to 50 Mev; θ, 60° to 180°	48
k.	$h\nu_o$, 0.6 to 5 Mev; θ, 60° to 180°	49
l.	$h\nu_o$, 10 to 600 Kev; θ, 60° to 180°	50
m.	$h\nu_o$ versus θ at which $(d\sigma/d\Omega_\theta)_{min}$	51
Figure V.	Electron angular distribution	52
a.	$h\nu_o$, 100 to 500 Mev; ψ, 0° to 0.05°	53
b to e.	$h\nu_o$, 60 to 500 Mev; ψ, 0.0165° to 90°	54
f.	$h\nu_o$, 12 to 60 Mev; ψ, 0° to 0.5°	58
g to j.	$h\nu_o$, 5 to 60 Mev; ψ, 0.15° to 90°	59
k to m.	$h\nu_o$, 1 to 5 Mev; ψ, 0° to 90°	63
n, o.	$h\nu_o$, 0.3 to 1 Mev; ψ, 0° to 90°	66
p.	$h\nu_o$, 10 to 300 Kev; ψ, 0° to 90°	68
Figure VI.	Photon energy distribution	69
a.	$h\nu_o$, 80 to 500 Mev; $h\nu$, 10 to 500 Mev	70
b, c.	$h\nu_o$, 50 to 500 Mev; $h\nu$, 0.25 to 80 Mev	71
d.	$h\nu_o$, 8 to 50 Mev; $h\nu$, 1 to 50 Mev	73
e.	$h\nu_o$, 6 to 50 Mev; $h\nu$, 0.24 to 8 Mev	74
f.	$h\nu_o$, 2 to 6 Mev; $h\nu$, 0.22 to 6 Mev	75
g.	$h\nu_o$, 0.8 to 2 Mev; $h\nu$, 0.19 to 2 Mev	76
h.	$h\nu_o$, 0.4 to 0.8 Mev; $h\nu$, 0.15 to 0.8 Mev	77
i.	$h\nu_o$, 10 to 400 Kev; $h\nu$, 9.6 to 400 Kev	78
Figure VII.	Electron energy distribution	79
a.	$h\nu_o$, 40 to 500 Mev; T, 3 to 500 Mev	80
b.	$h\nu_o$, 15 to 500 Mev; T, 2 to 500 Mev	81
c.	$h\nu_o$, 4 to 15 Mev; T, 0.15 to 15 Mev	82
d.	$h\nu_o$, 1.2 to 4 Mev; T, 0.02 to 4 Mev	83
e.	$h\nu_o$, 0.2 to 1.2 Mev; T, 2 to 10^3 Kev	84
f.	$h\nu_o$, 100 to 200 Kev; T, 0.2 to 100 Kev	85
g.	$h\nu_o$, 15 to 100 Kev; T, 0.15 to 30 Kev	86
h.	$h\nu_o$, 10 to 100 Kev; T, 0.005 to 0.8 Kev	87

Integral Klein-Nishina Cross Section per Electron:

		Page
Figure VIII, a.	Total Compton cross section	88
	Effective cross section for energy absorption	88
Figure VIII, b.	Fraction of energy retained by the photon	89
	Fraction of energy absorbed by the electron	89

WASHINGTON, January 7, 1953.

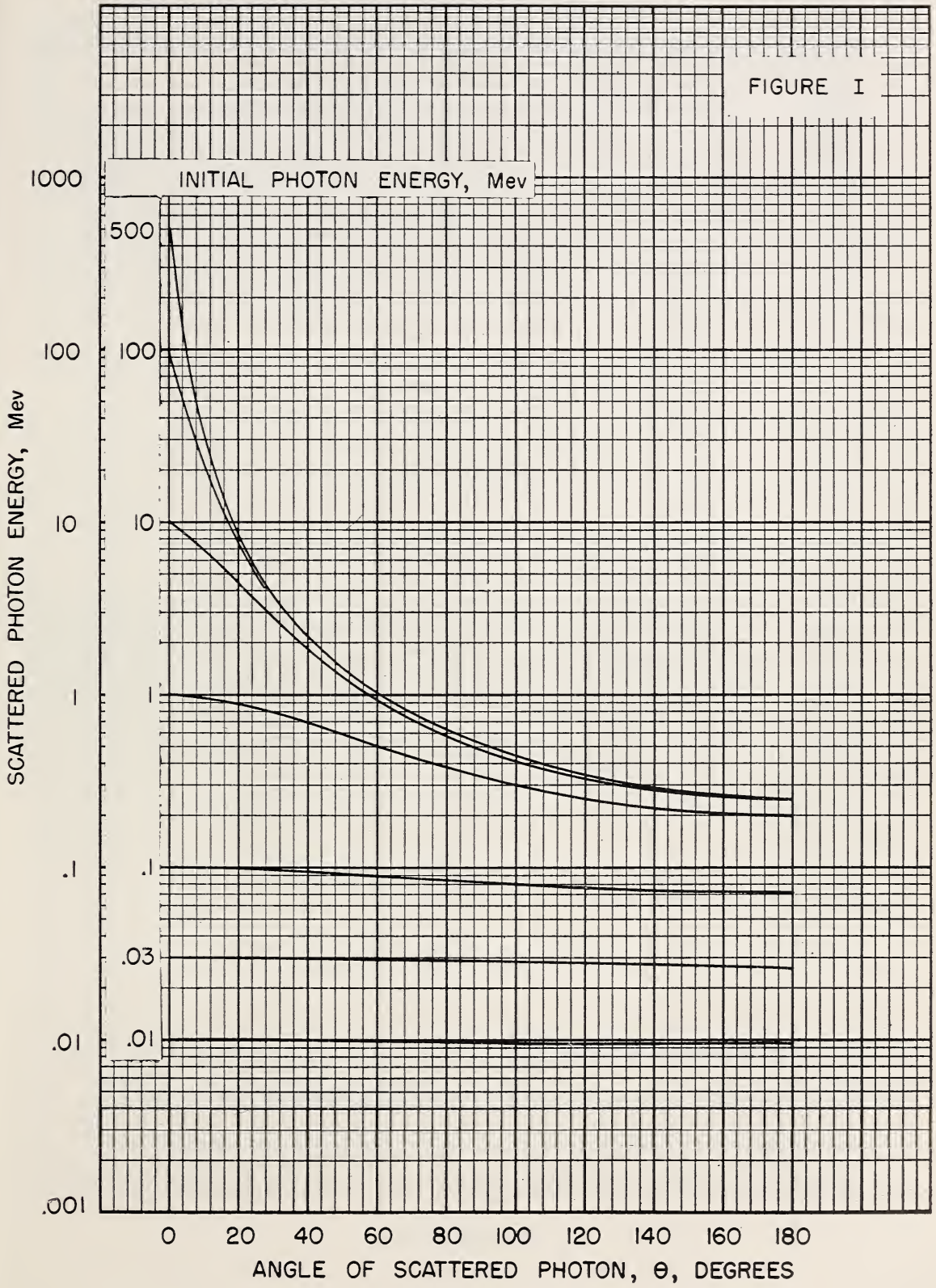
FIGURE I
INITIAL PHOTON ENERGY, Mev
500
100
10
1
.1
.03
.01
1000
100
10
1
.1
.01
.001
SCATTERED PHOTON ENERGY, Mev
0
20
40
60
80
100
120
140
160
180
ANGLE OF SCATTERED PHOTON, θ, DEGREES

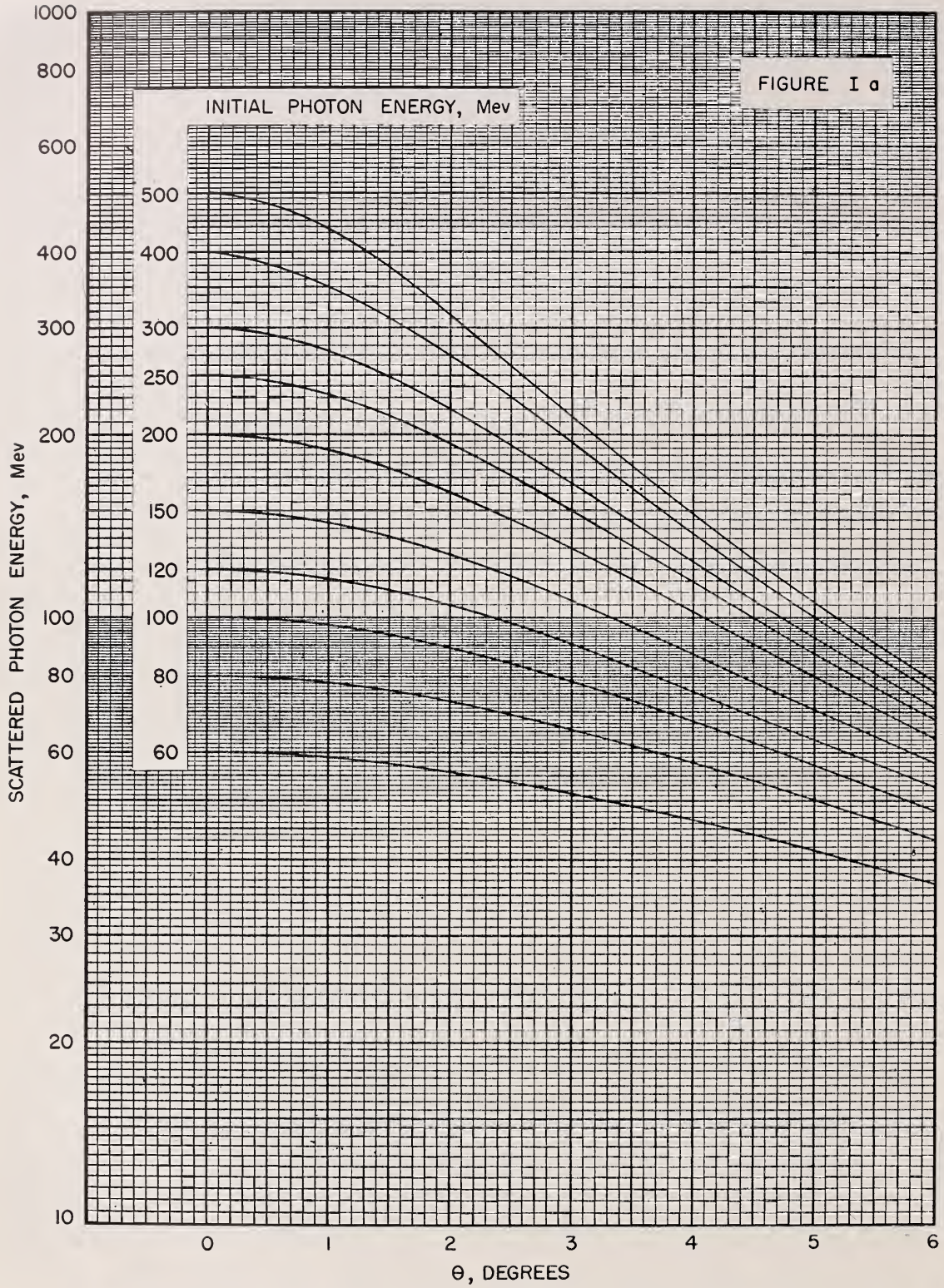
FIGURE I a
INITIAL PHOTON ENERGY, Mev
500
400
300
250
200
150
120
100
80
60
SCATTERED PHOTON ENERGY, Mev
1000
800
600
400
300
200
100
80
60
40
30
20
10
0
1
2
3
4
5
6
θ, DEGREES

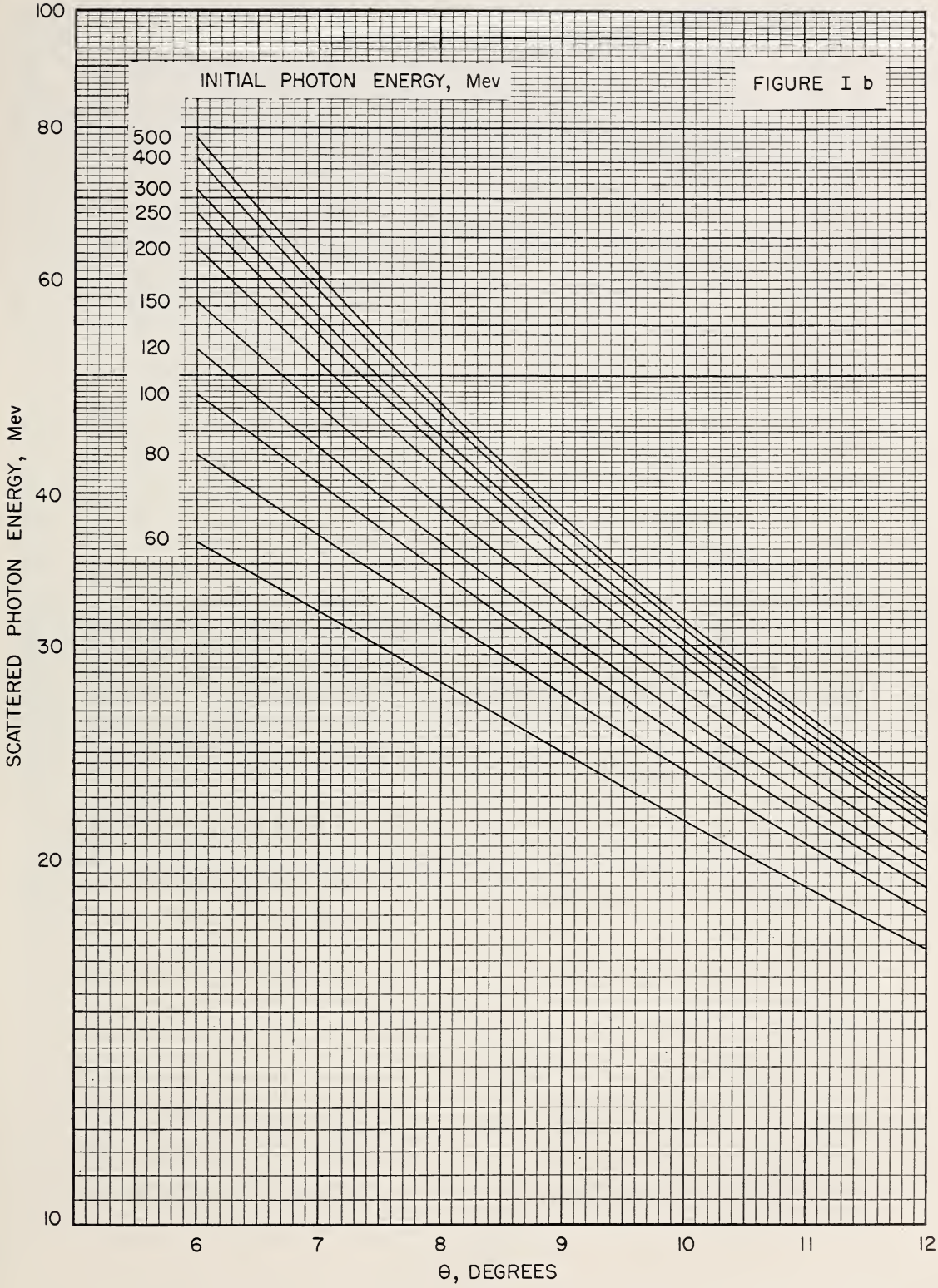
FIGURE I b
INITIAL PHOTON ENERGY, Mev
500
400
300
250
200
150
120
100
80
60
SCATTERED PHOTON ENERGY, Mev
100
80
60
40
30
20
10
6
7
8
9
10
11
12
θ, DEGREES

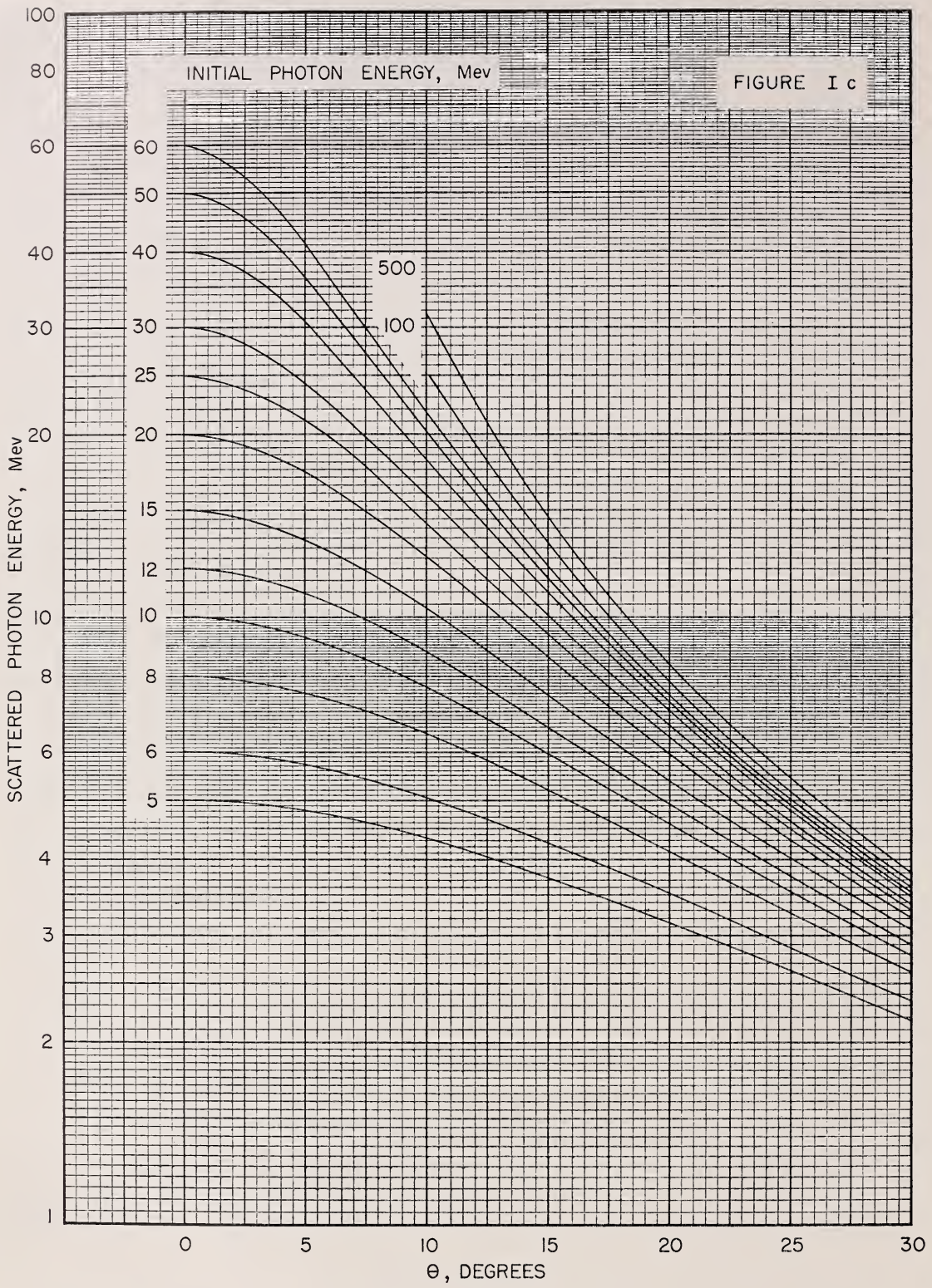
INITIAL PHOTON ENERGY, Mev
FIGURE I c
60
50
40
30
25
20
15
12
10
8
6
5
500
100
SCATTERED PHOTON ENERGY, Mev
100
80
60
40
30
20
10
8
6
4
3
2
1
0
5
10
15
20
25
30
θ, DEGREES

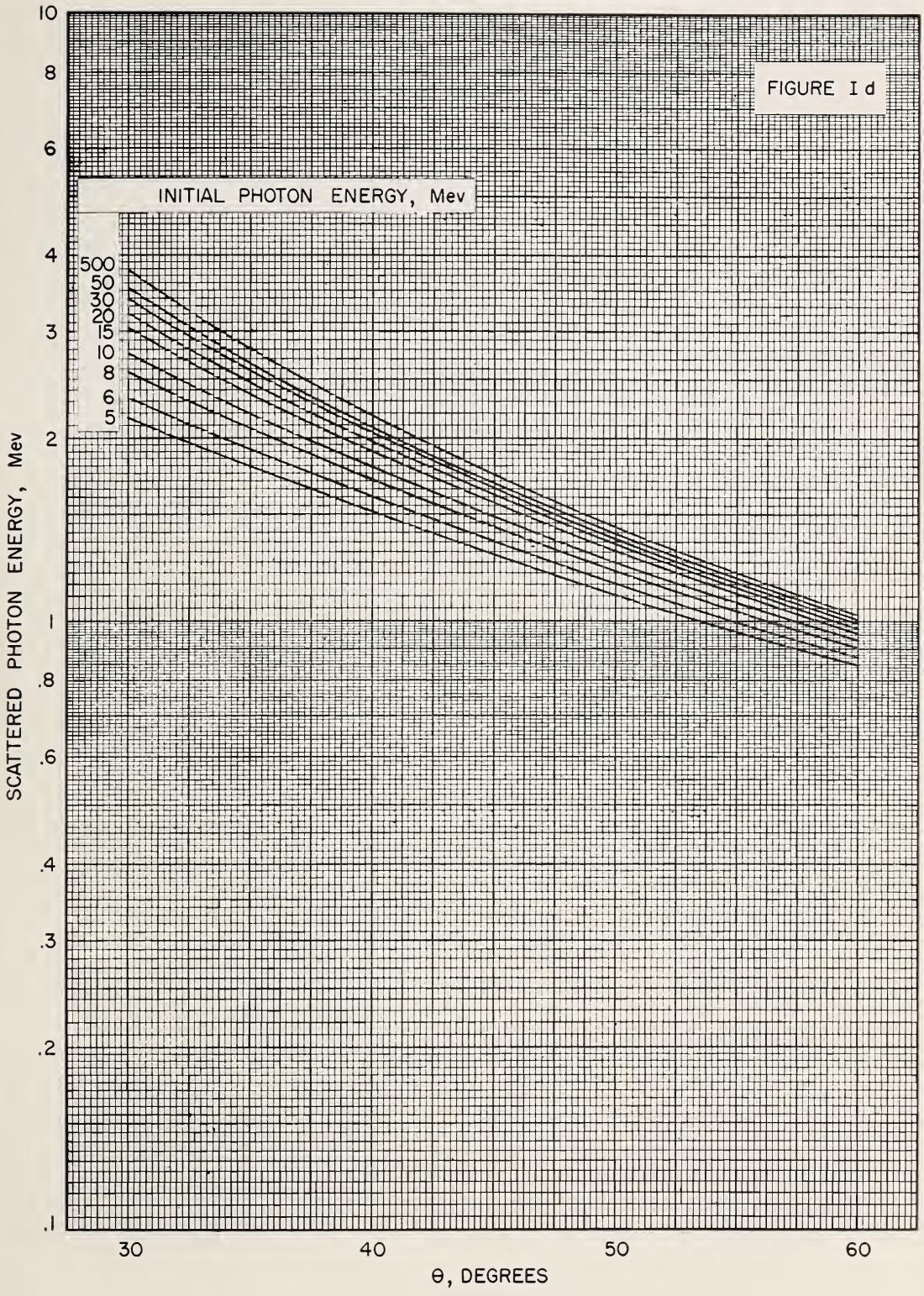
FIGURE I d
INITIAL PHOTON ENERGY, Mev
500
50
30
20
15
10
8
6
5
SCATTERED PHOTON ENERGY, Mev
10
8
6
4
3
2
1
.8
.6
.4
.3
.2
.1
30
40
50
60
θ, DEGREES

249464—53——3

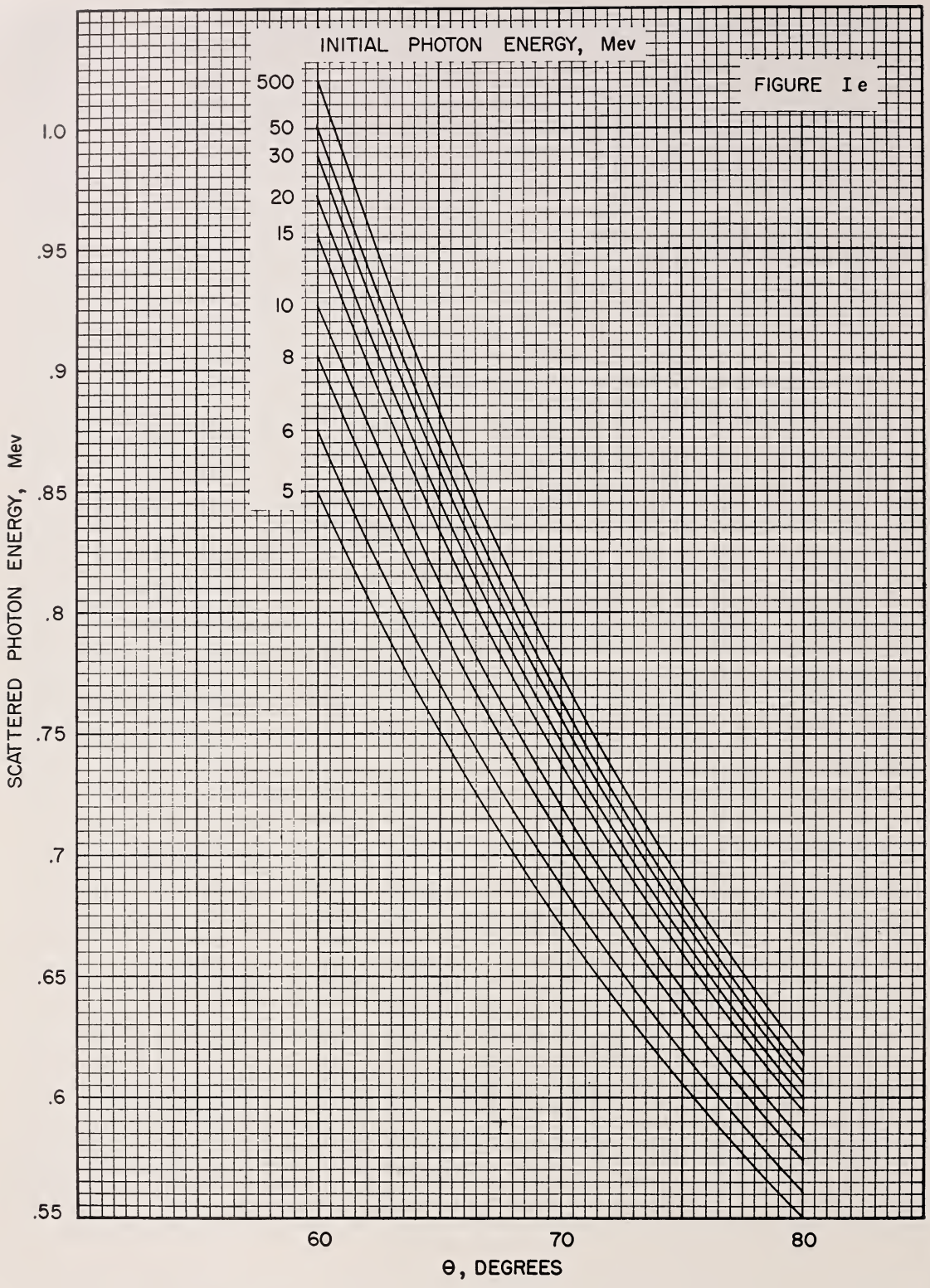
INITIAL PHOTON ENERGY, Mev
500
50
30
20
15
10
8
6
5
FIGURE Ie
1.0
.95
.9
.85
.8
.75
.7
.65
.6
.55
SCATTERED PHOTON ENERGY, Mev
60
70
80
θ, DEGREES

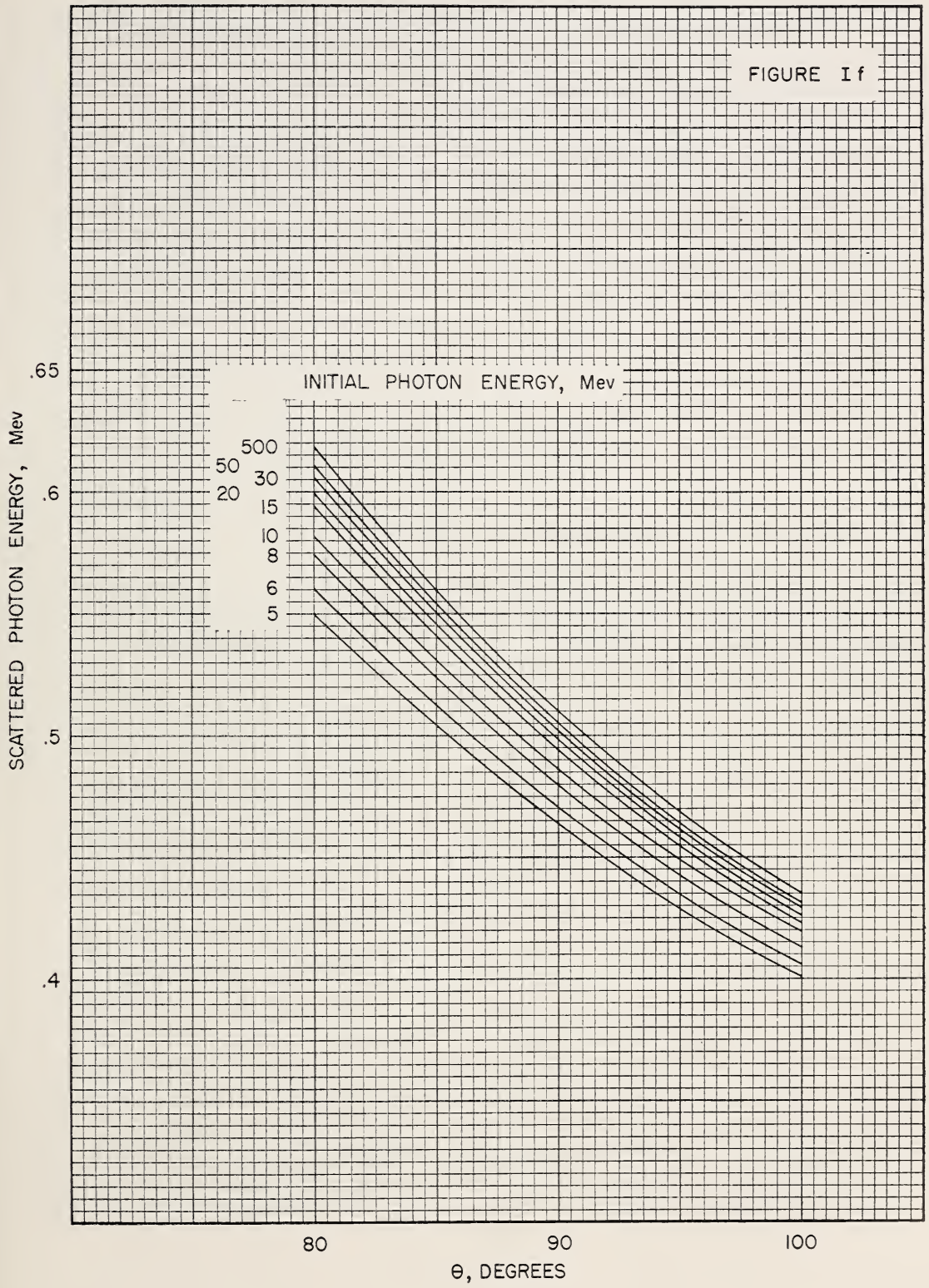
FIGURE If
INITIAL PHOTON ENERGY, Mev
500
50
30
20
15
10
8
6
5
SCATTERED PHOTON ENERGY, Mev
.65
.6
.5
.4
80
90
100
θ, DEGREES

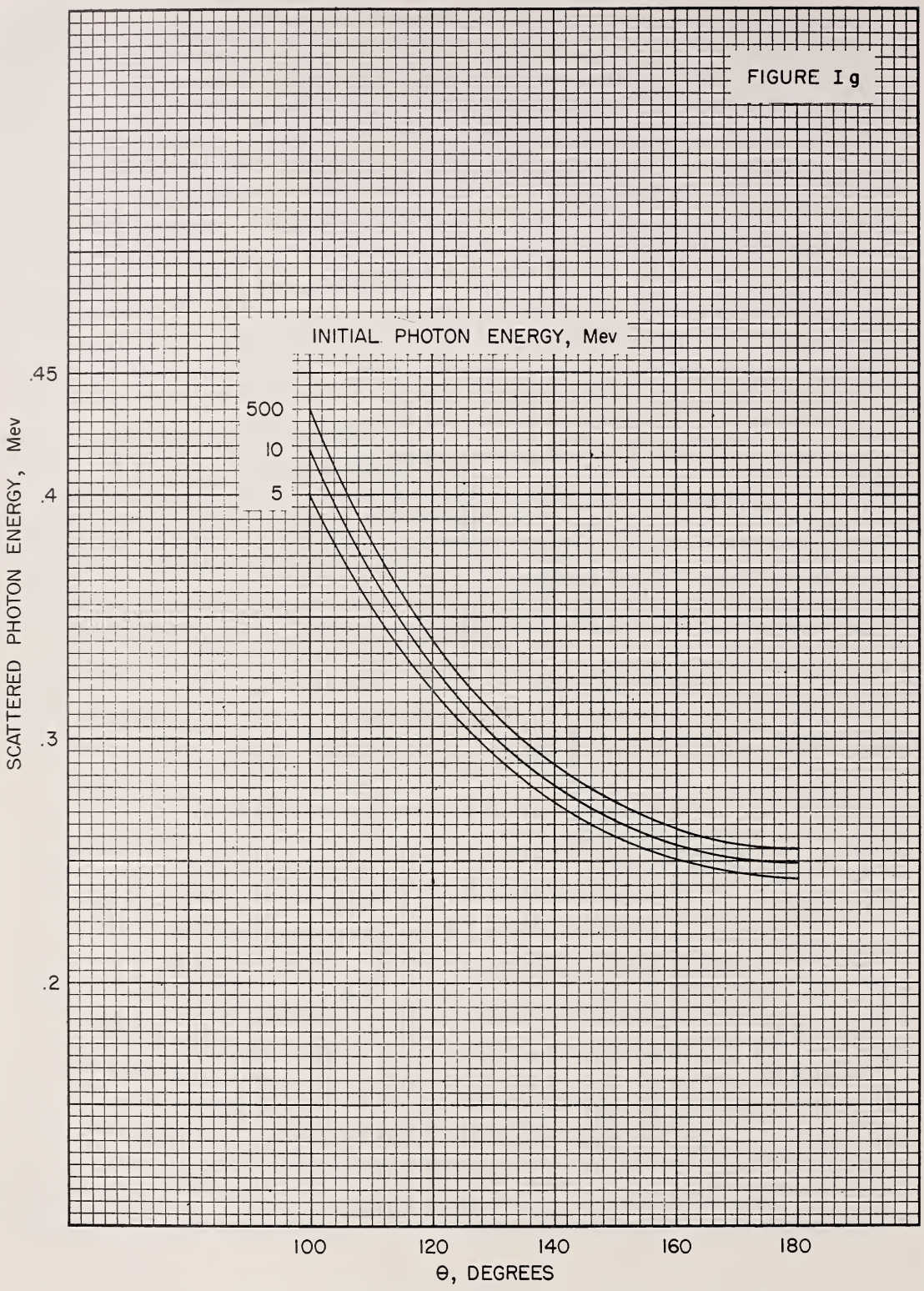
FIGURE I g
INITIAL PHOTON ENERGY, Mev
500
10
5
SCATTERED PHOTON ENERGY, Mev
.45
.4
.3
.2
100
120
140
160
180
θ, DEGREES

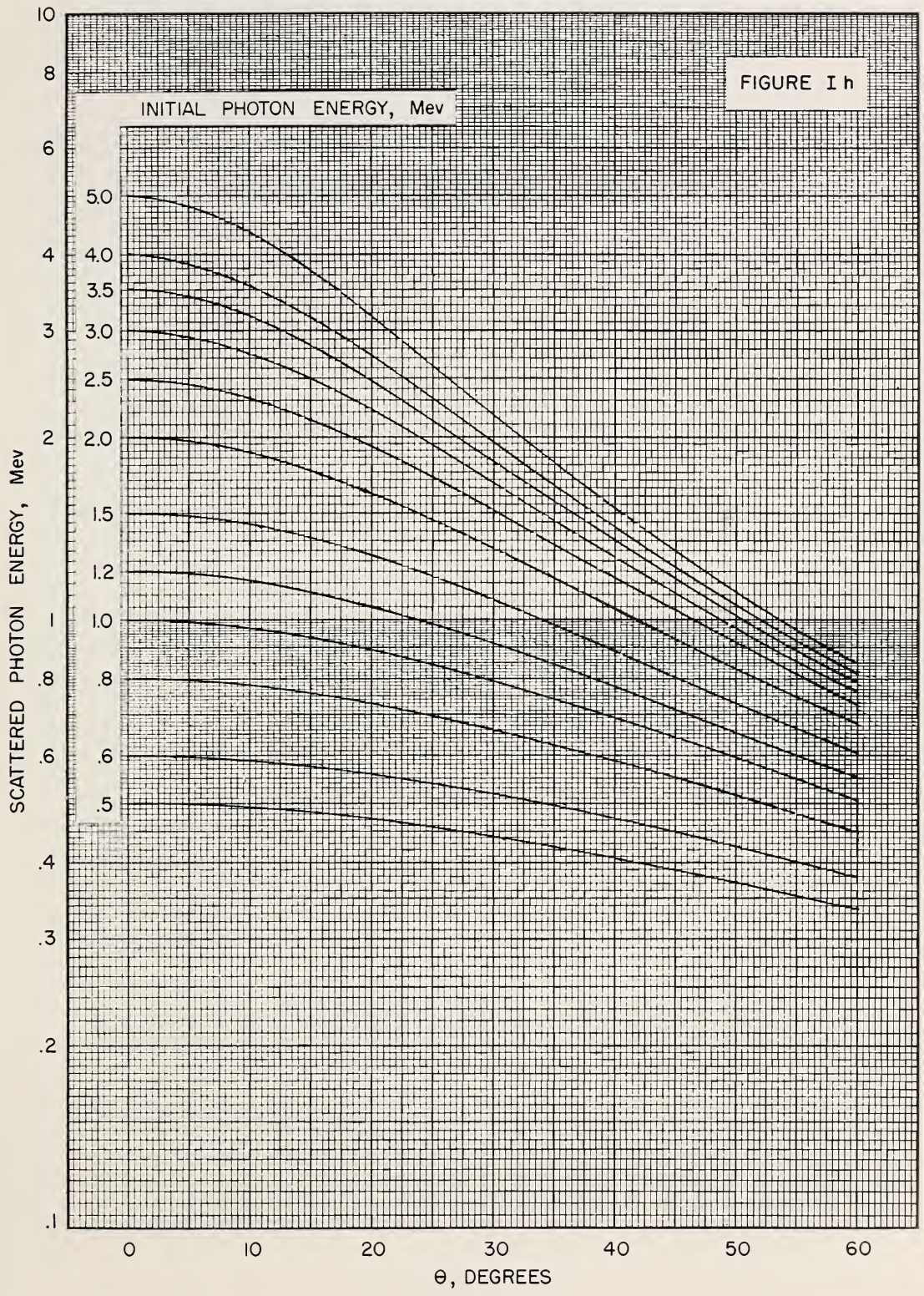
FIGURE I h
INITIAL PHOTON ENERGY, Mev
5.0
4.0
3.5
3.0
2.5
2.0
1.5
1.2
1.0
.8
.6
.5
SCATTERED PHOTON ENERGY, Mev
10
8
6
4
3
2
1
.8
.6
.4
.3
.2
.1
0
10
20
30
40
50
60
θ, DEGREES

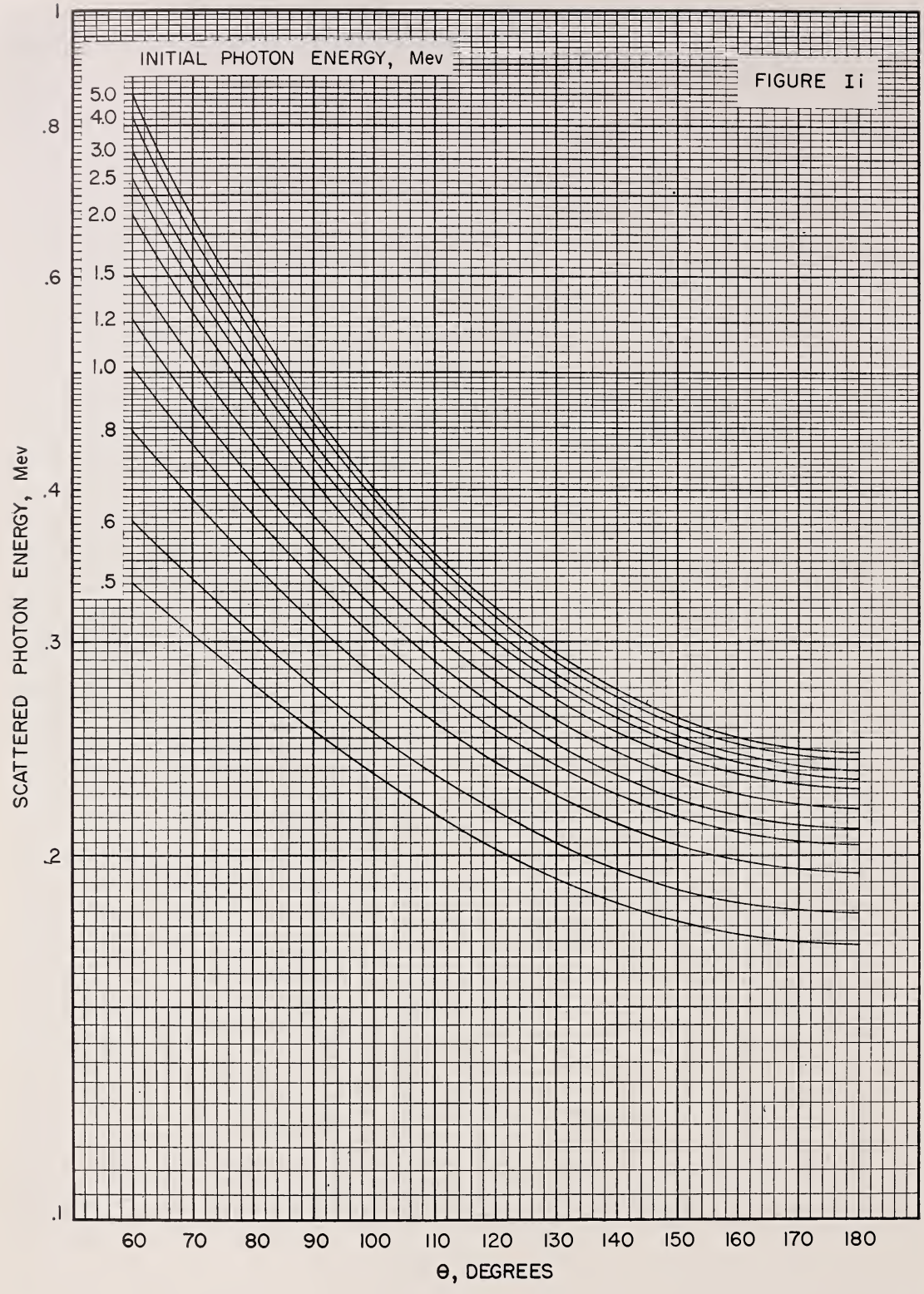
INITIAL PHOTON ENERGY, Mev
5.0
4.0
3.0
2.5
2.0
1.5
1.2
1.0
.8
.6
.5
FIGURE Ii
SCATTERED PHOTON ENERGY, Mev
1
.8
.6
.4
.3
.2
.1
60
70
80
90
100
110
120
130
140
150
160
170
180
θ, DEGREES

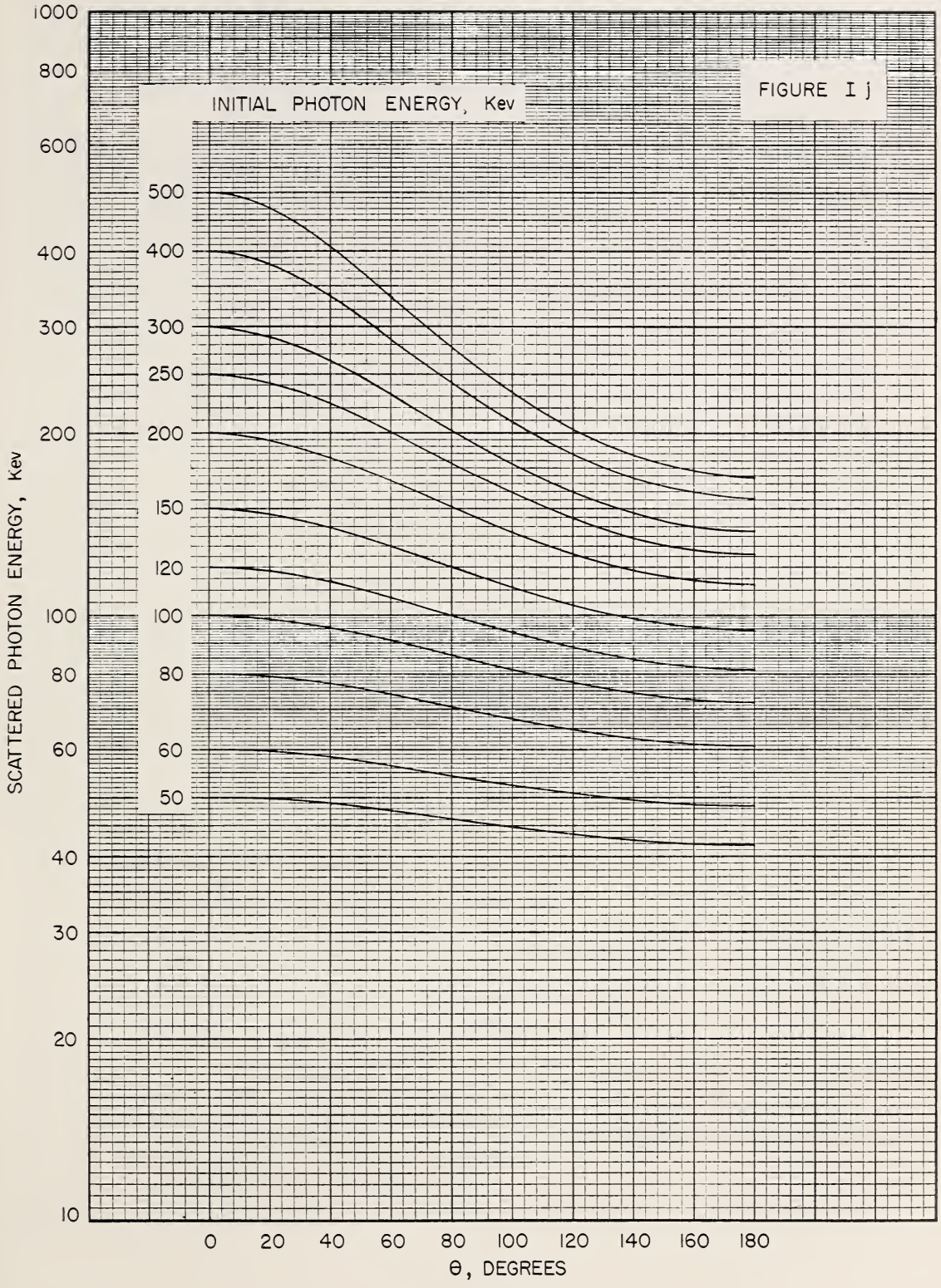
FIGURE I j
INITIAL PHOTON ENERGY, Kev
500
400
300
250
200
150
120
100
80
60
50
SCATTERED PHOTON ENERGY, Kev
1000
800
600
400
300
200
100
80
60
40
30
20
10
0
20
40
60
80
100
120
140
160
180
θ, DEGREES

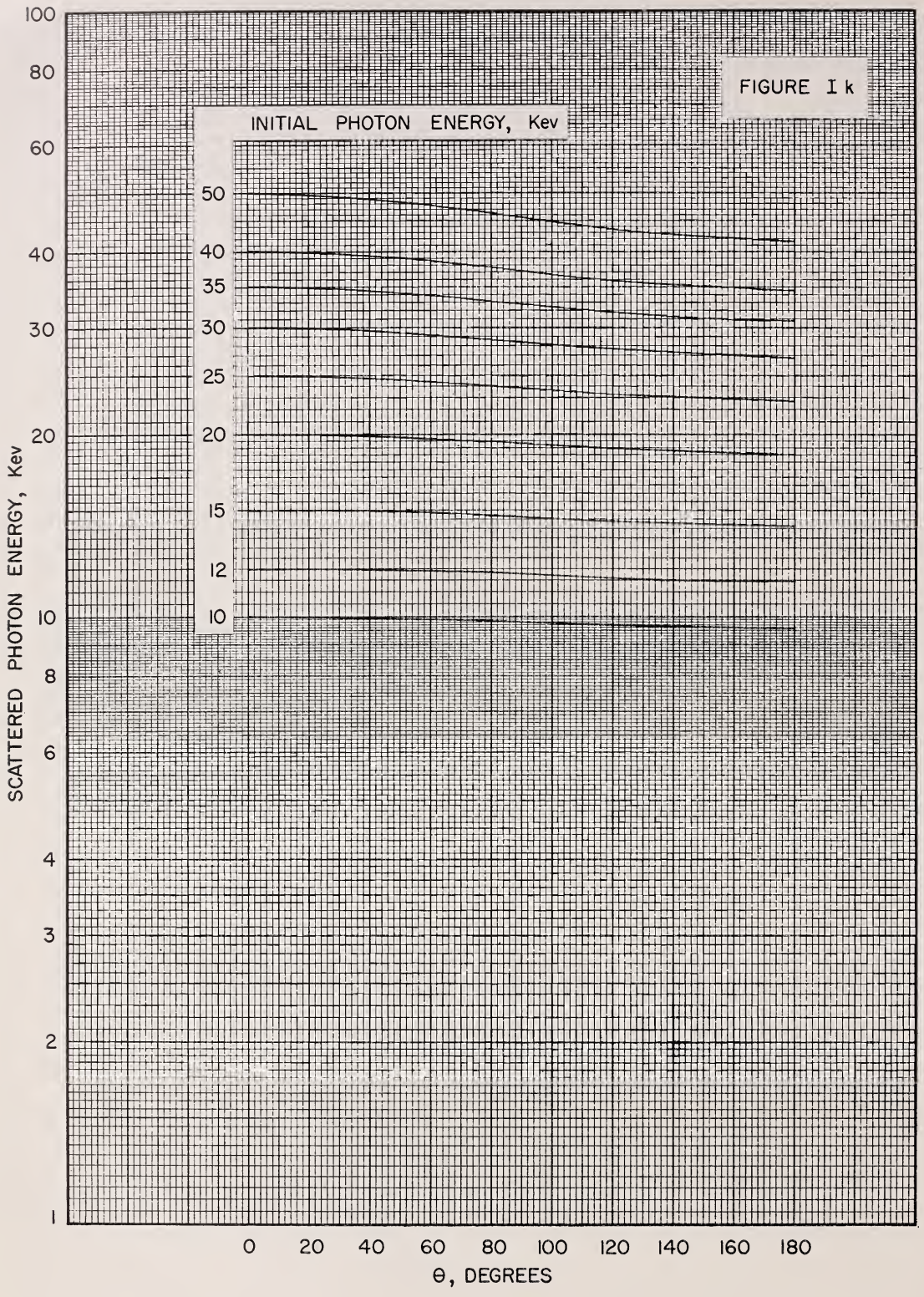
FIGURE I k
INITIAL PHOTON ENERGY, Kev
50
40
35
30
25
20
15
12
10
SCATTERED PHOTON ENERGY, Kev
100
80
60
40
30
20
10
8
6
4
3
2
1
0
20
40
60
80
100
120
140
160
180
θ, DEGREES

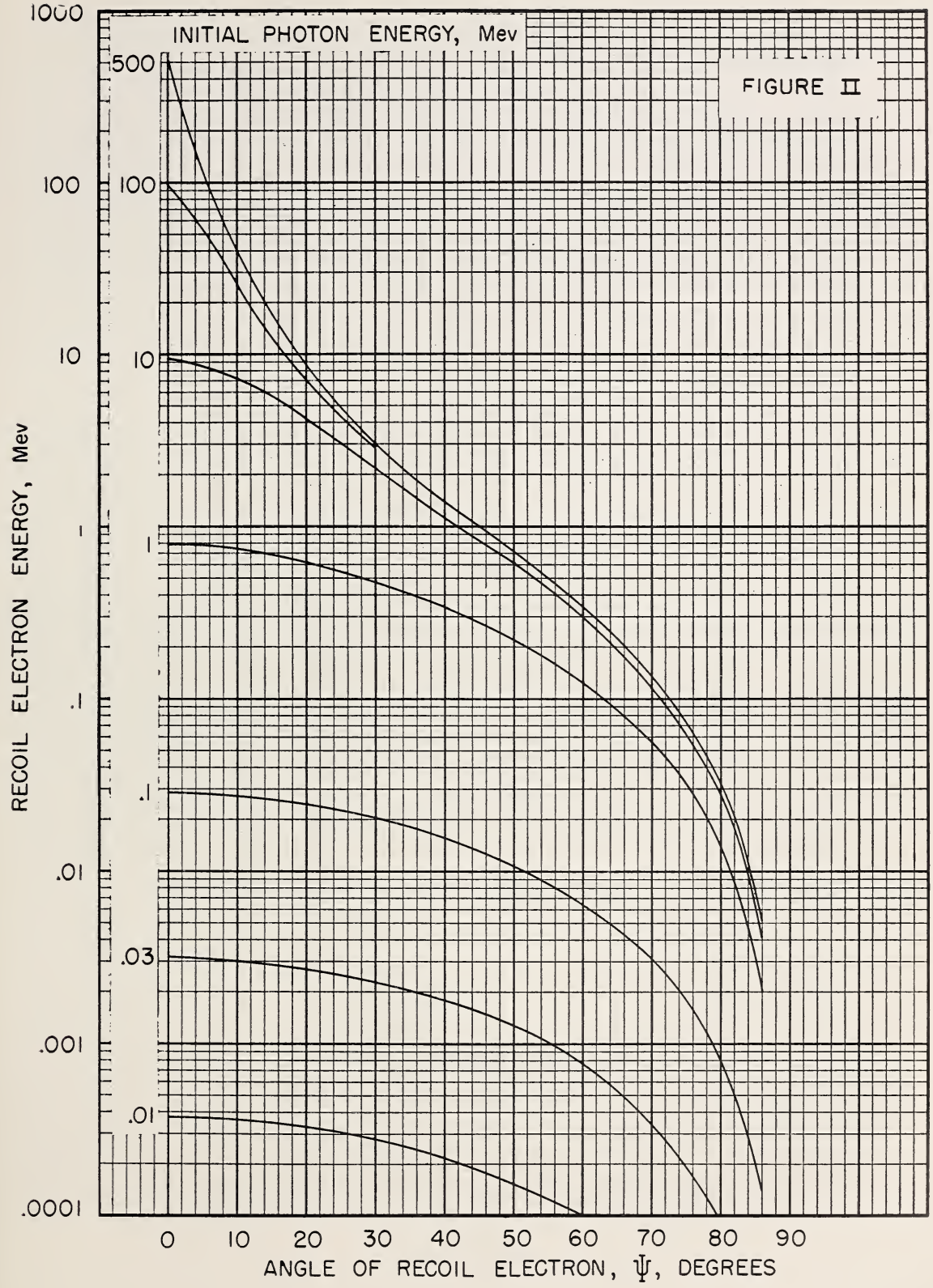
INITIAL PHOTON ENERGY, Mev
500
100
10
1
.1
.03
.01
FIGURE II
1000
100
10
1
.1
.01
.001
.0001
RECOIL ELECTRON ENERGY, Mev
0
10
20
30
40
50
60
70
80
90
ANGLE OF RECOIL ELECTRON, Ψ, DEGREES

249464—53——4

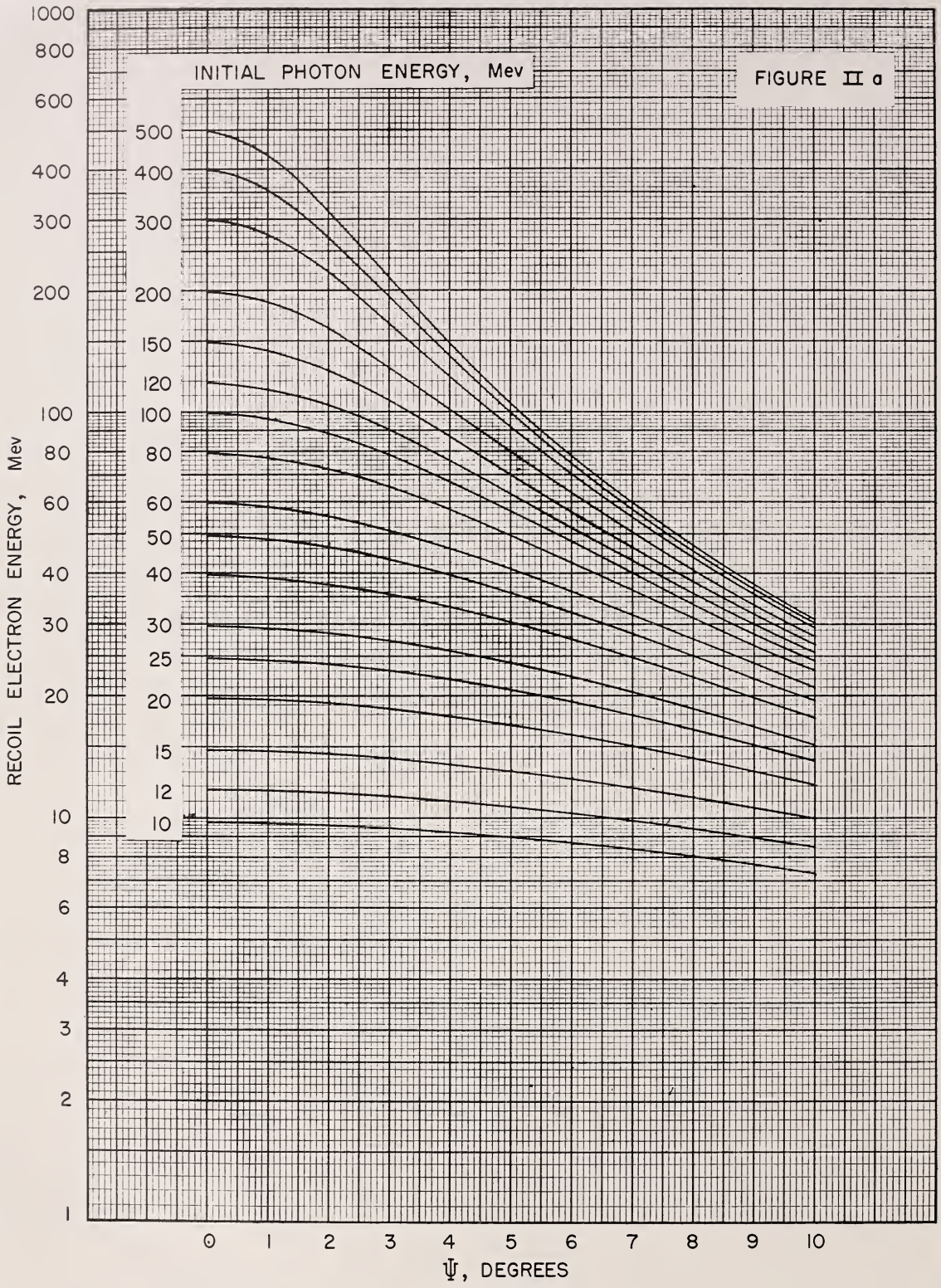
INITIAL PHOTON ENERGY, Mev
500
400
300
200
150
120
100
80
60
50
40
30
25
20
15
12
10
RECOIL ELECTRON ENERGY, Mev
1000
800
600
400
300
200
100
80
60
40
30
20
10
8
6
4
3
2
1
0
1
2
3
4
5
6
7
8
9
10
Ψ, DEGREES

FIGURE II a

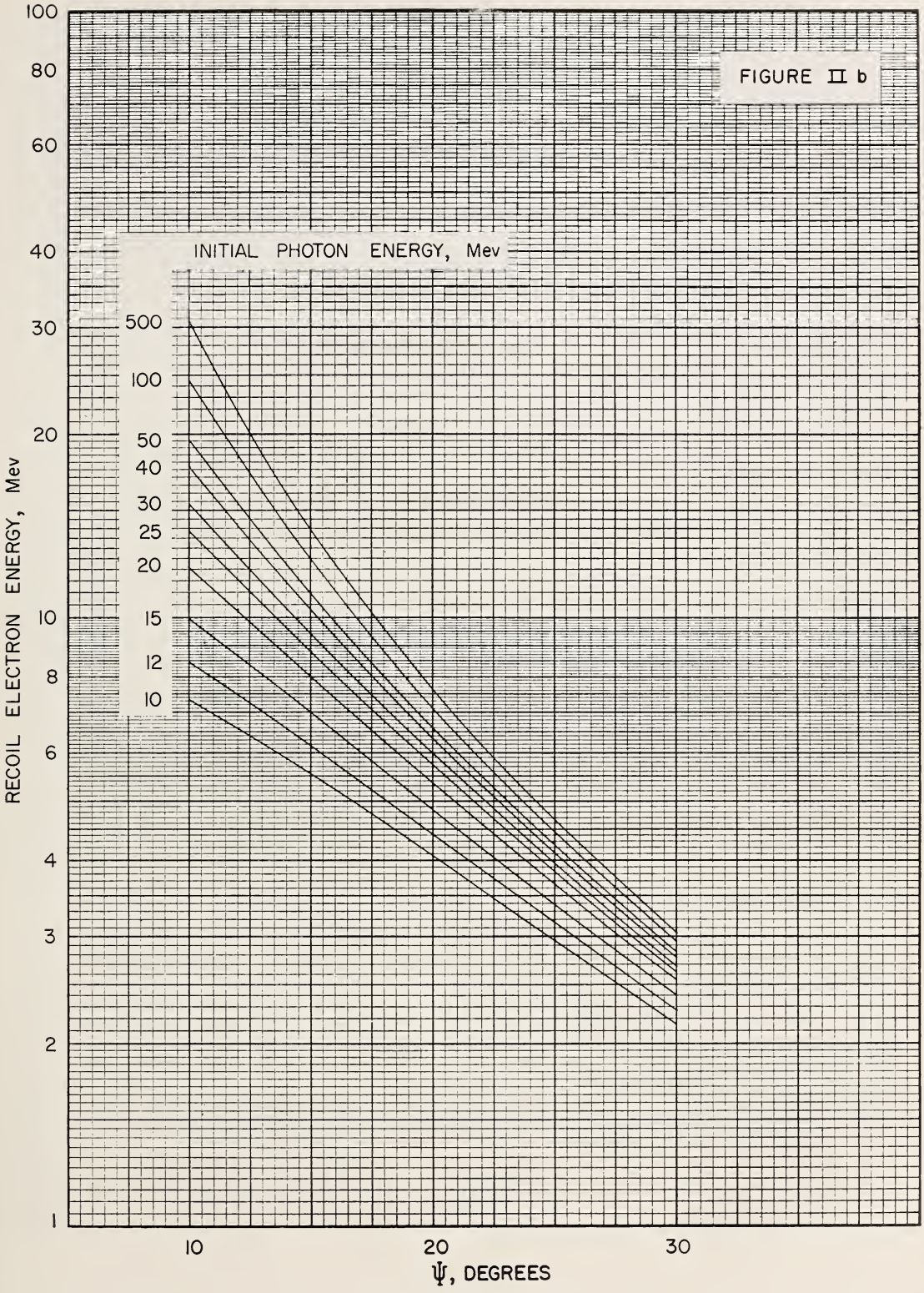
FIGURE II b
INITIAL PHOTON ENERGY, Mev
500
100
50
40
30
25
20
15
12
10
RECOIL ELECTRON ENERGY, Mev
100
80
60
40
30
20
10
8
6
4
3
2
1
10
20
30
Ψ, DEGREES

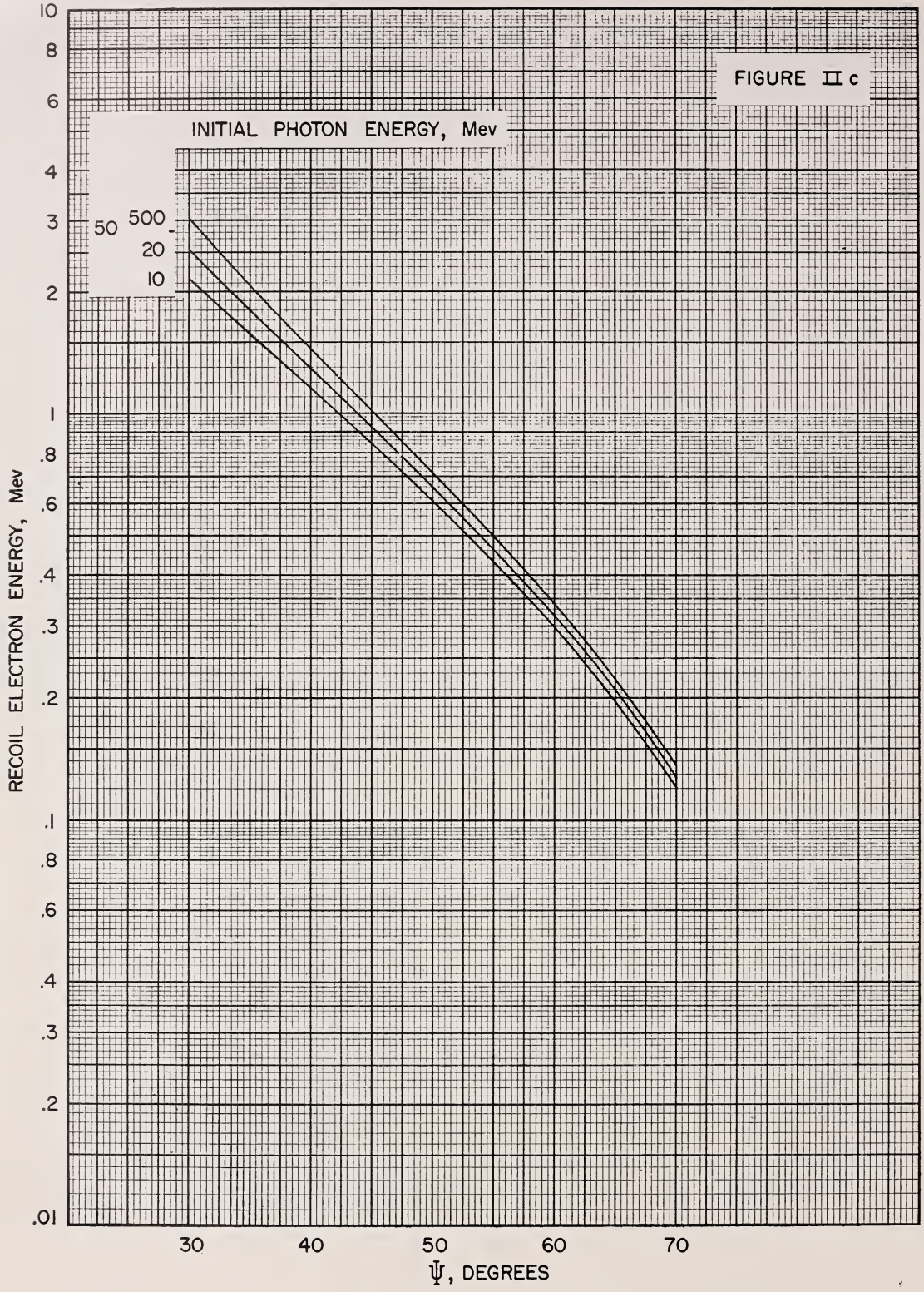
FIGURE II c
INITIAL PHOTON ENERGY, Mev
50
500
20
10
RECOIL ELECTRON ENERGY, Mev
10
8
6
4
3
2
1
.8
.6
.4
.3
.2
.1
.8
.6
.4
.3
.2
.01
30
40
50
60
70
Ψ, DEGREES

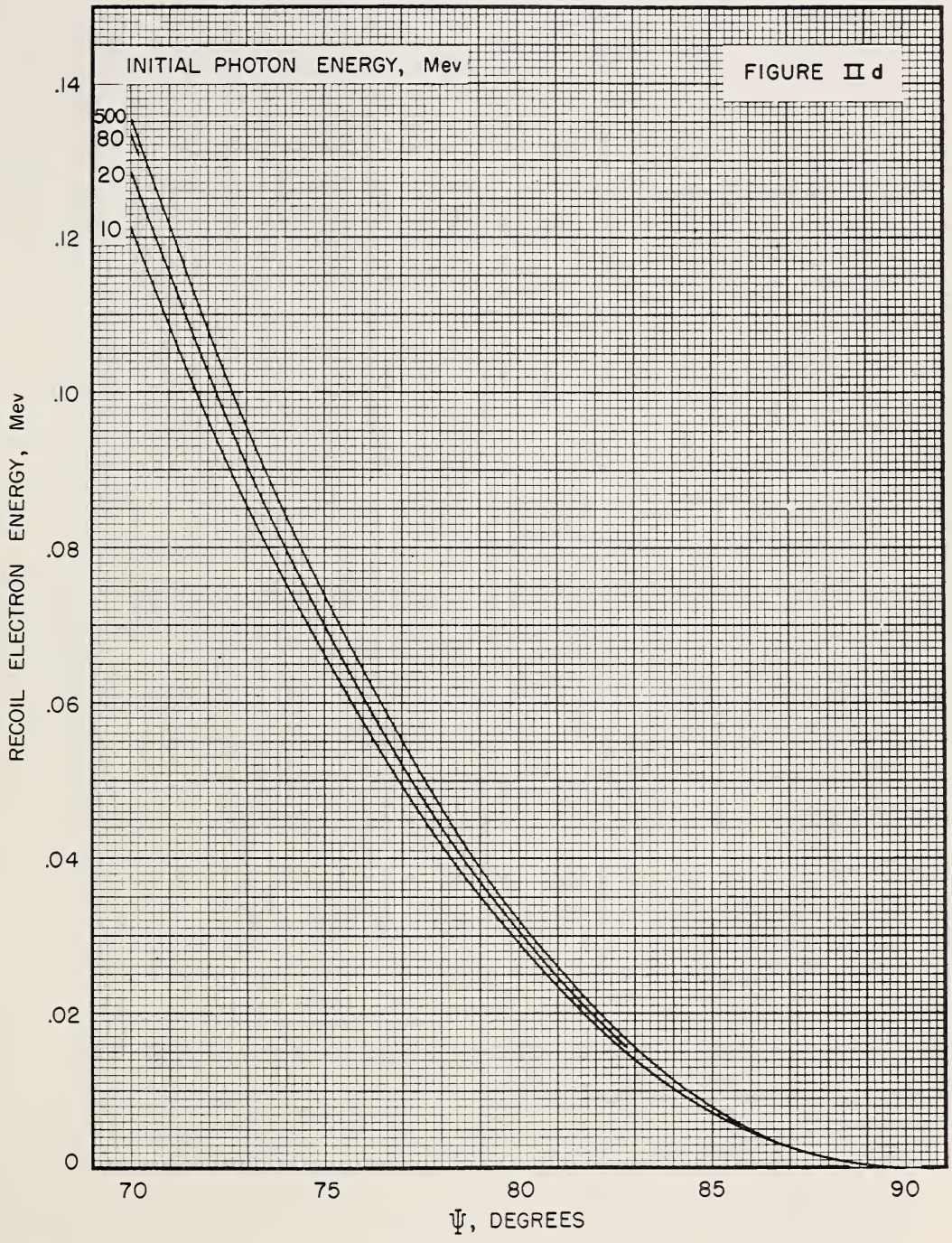
INITIAL PHOTON ENERGY, Mev
500
80
20
10
FIGURE II d
RECOIL ELECTRON ENERGY, Mev
.14
.12
.10
.08
.06
.04
.02
0
70
75
80
85
90
Ψ, DEGREES

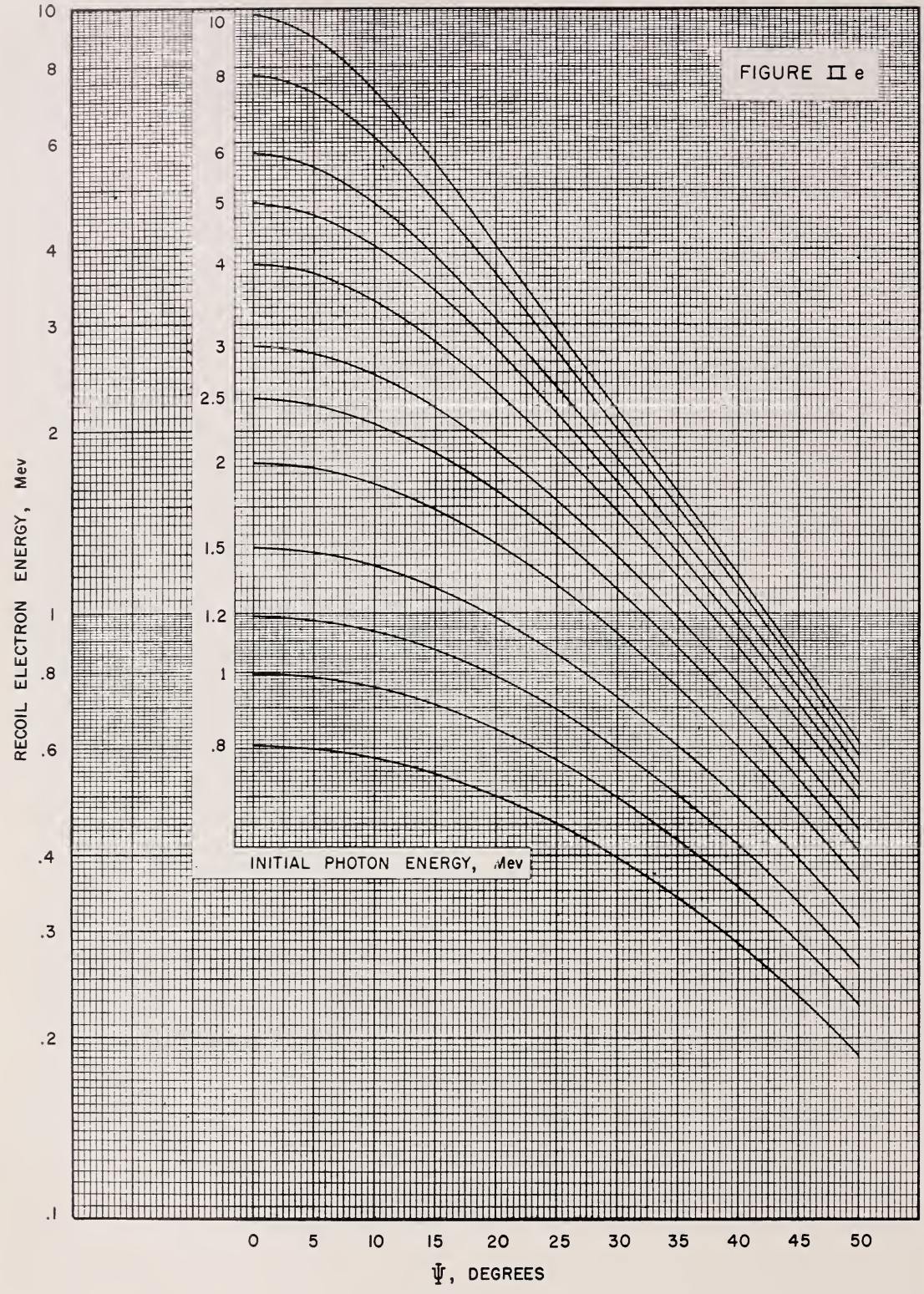
FIGURE II e
RECOIL ELECTRON ENERGY, Mev
10
8
6
4
3
2
1
.8
.6
.4
.3
.2
.1
INITIAL PHOTON ENERGY, Mev
10
8
6
5
4
3
2.5
2
1.5
1.2
1
.8
0
5
10
15
20
25
30
35
40
45
50
Ψ, DEGREES

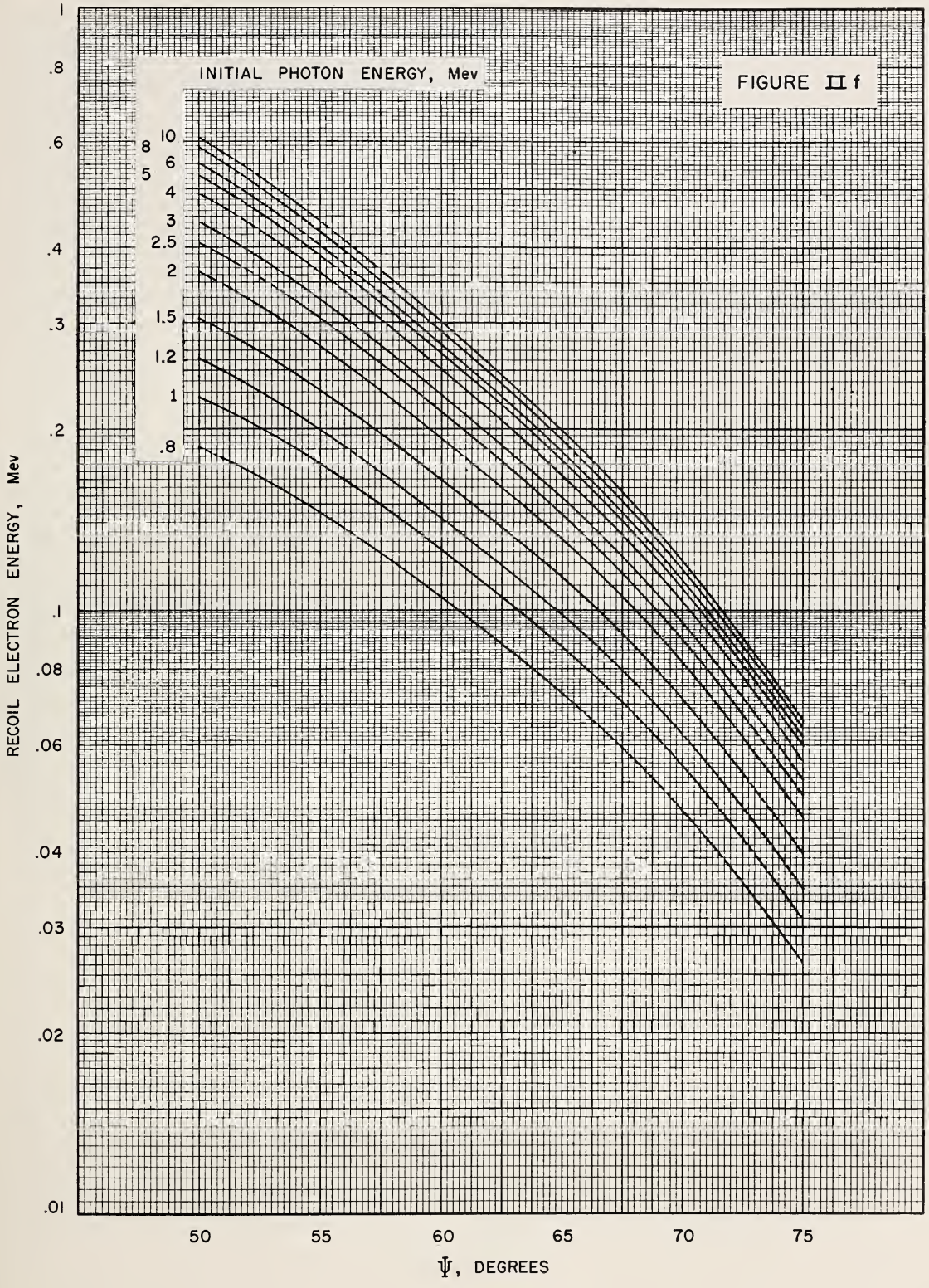
FIGURE II f
INITIAL PHOTON ENERGY, Mev
10
8
6
5
4
3
2.5
2
1.5
1.2
1
.8
RECOIL ELECTRON ENERGY, Mev
1
.8
.6
.4
.3
.2
.1
.08
.06
.04
.03
.02
.01
50
55
60
65
70
75
Ψ, DEGREES

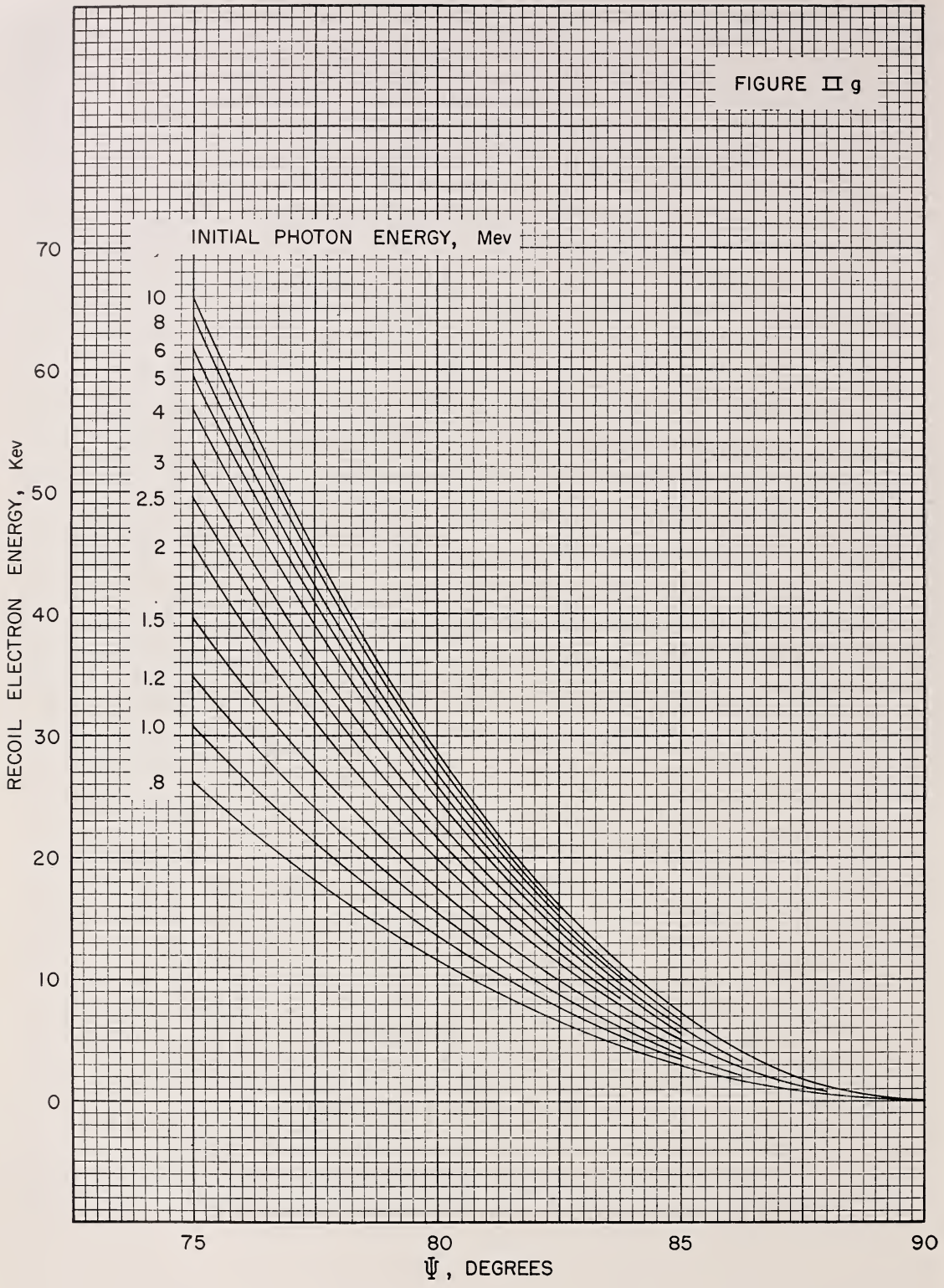
FIGURE II g
INITIAL PHOTON ENERGY, Mev
10
8
6
5
4
3
2.5
2
1.5
1.2
1.0
.8
RECOIL ELECTRON ENERGY, Kev
70
60
50
40
30
20
10
0
75
80
85
90
Ψ, DEGREES

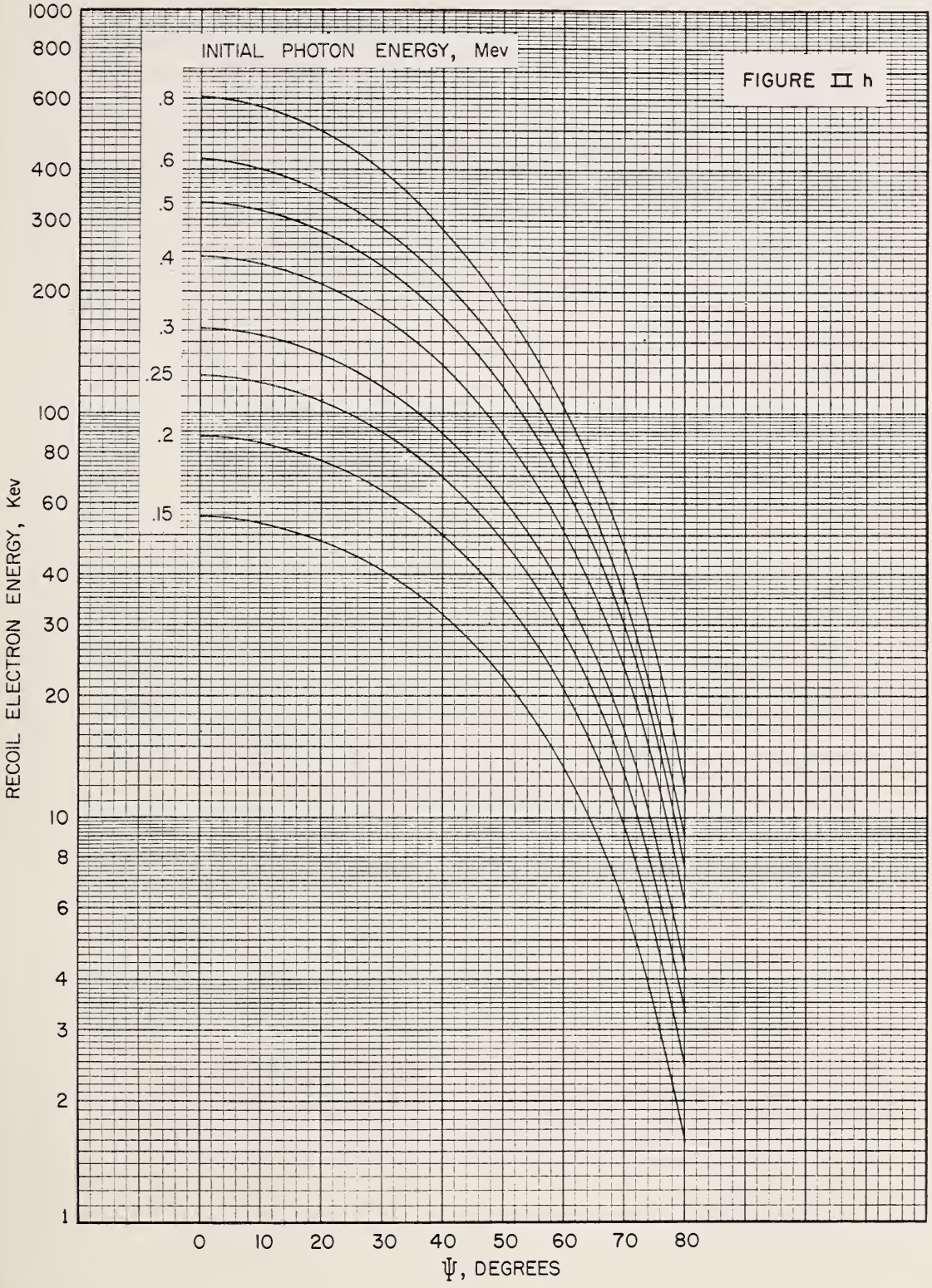

FIGURE II h

249464—53——5

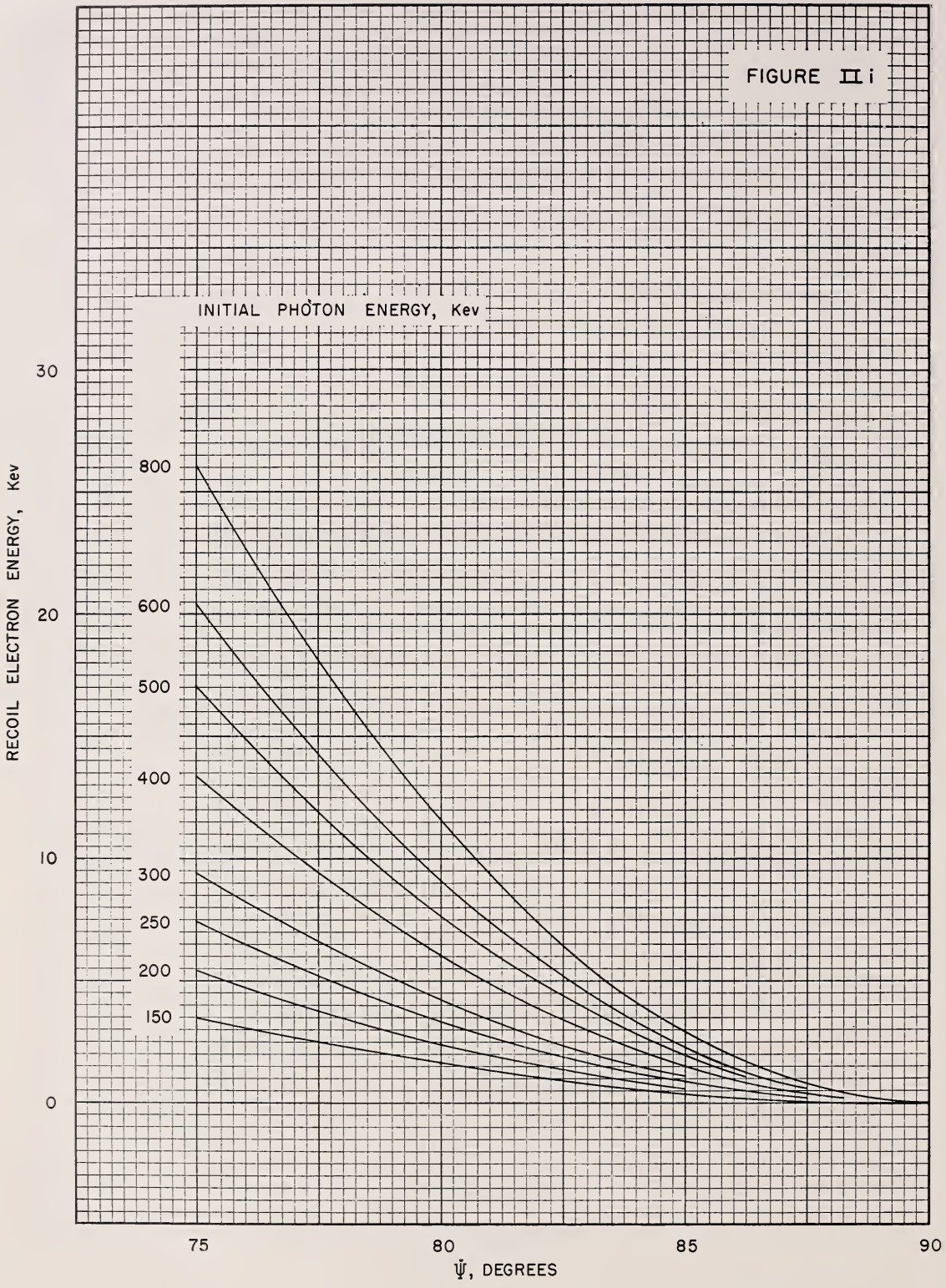
FIGURE II i
INITIAL PHOTON ENERGY, Kev
800
600
500
400
300
250
200
150
RECOIL ELECTRON ENERGY, Kev
30
20
10
0
75
80
85
90
Ψ, DEGREES

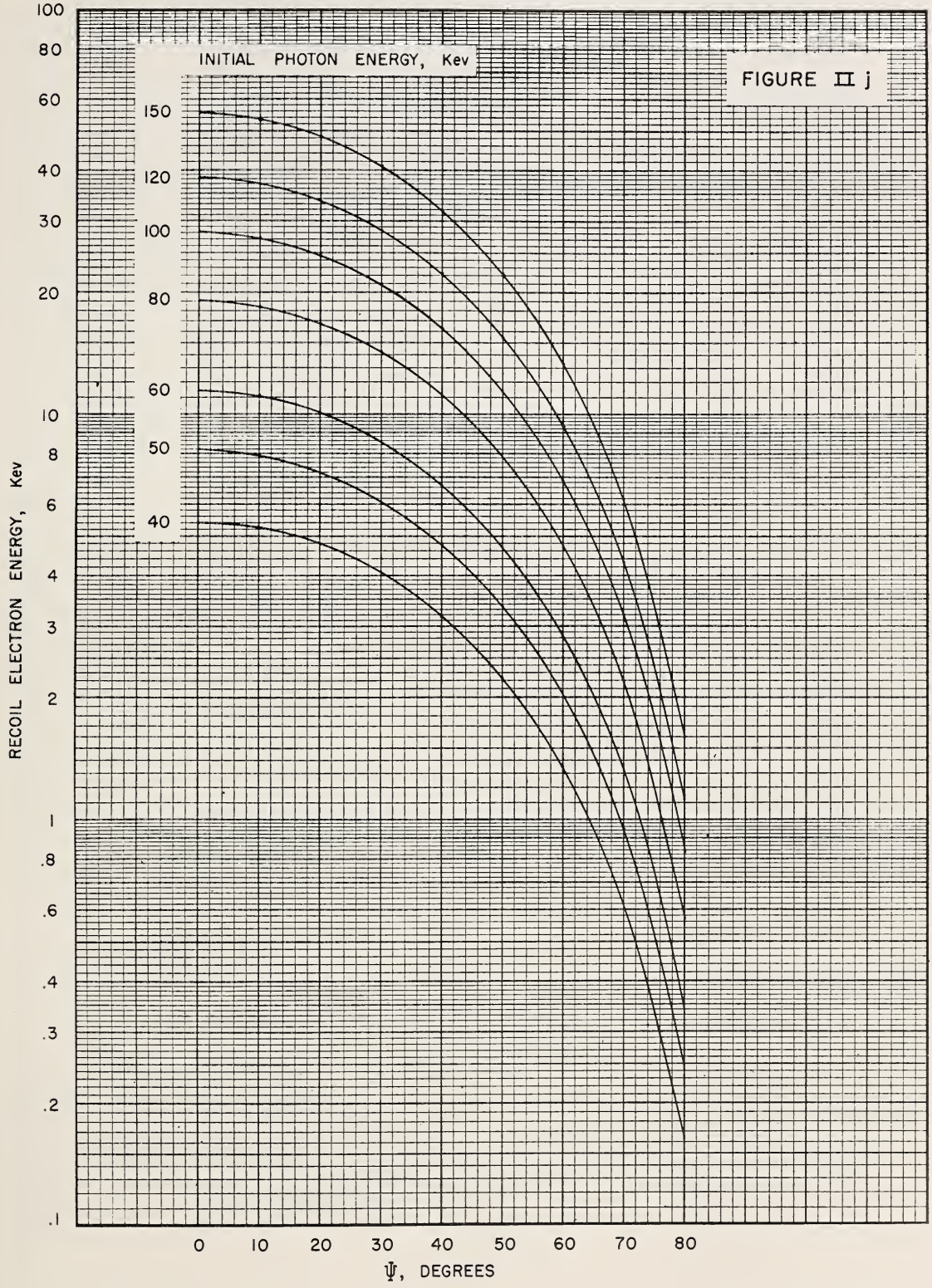
INITIAL PHOTON ENERGY, Kev
150
120
100
80
60
50
40
RECOIL ELECTRON ENERGY, Kev
100
80
60
40
30
20
10
8
6
4
3
2
1
.8
.6
.4
.3
.2
.1
0
10
20
30
40
50
60
70
80
Ψ, DEGREES

FIGURE II j

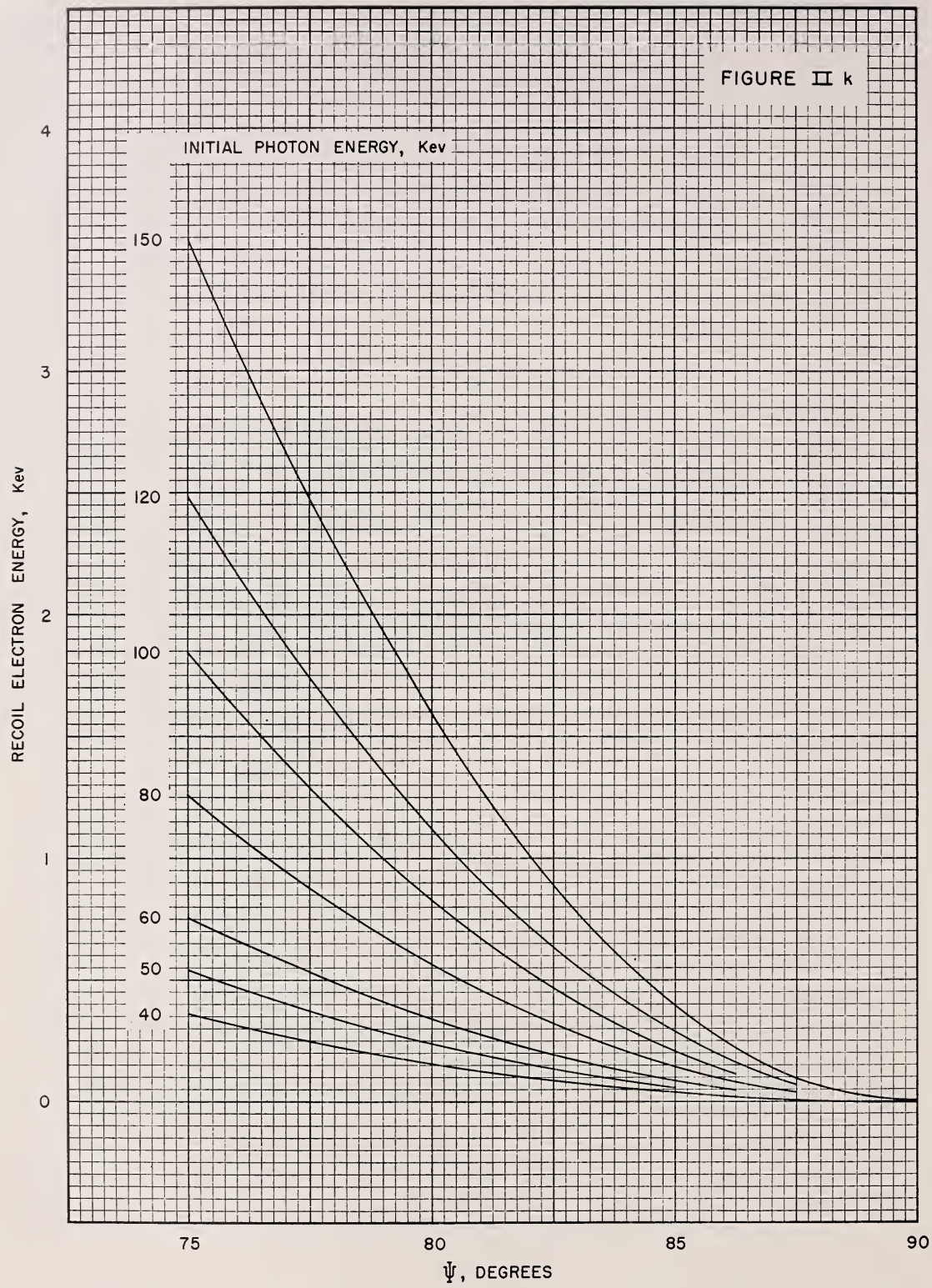
FIGURE II k
INITIAL PHOTON ENERGY, Kev
150
120
100
80
60
50
40
RECOIL ELECTRON ENERGY, Kev
0
1
2
3
4
75
80
85
90
Ψ, DEGREES

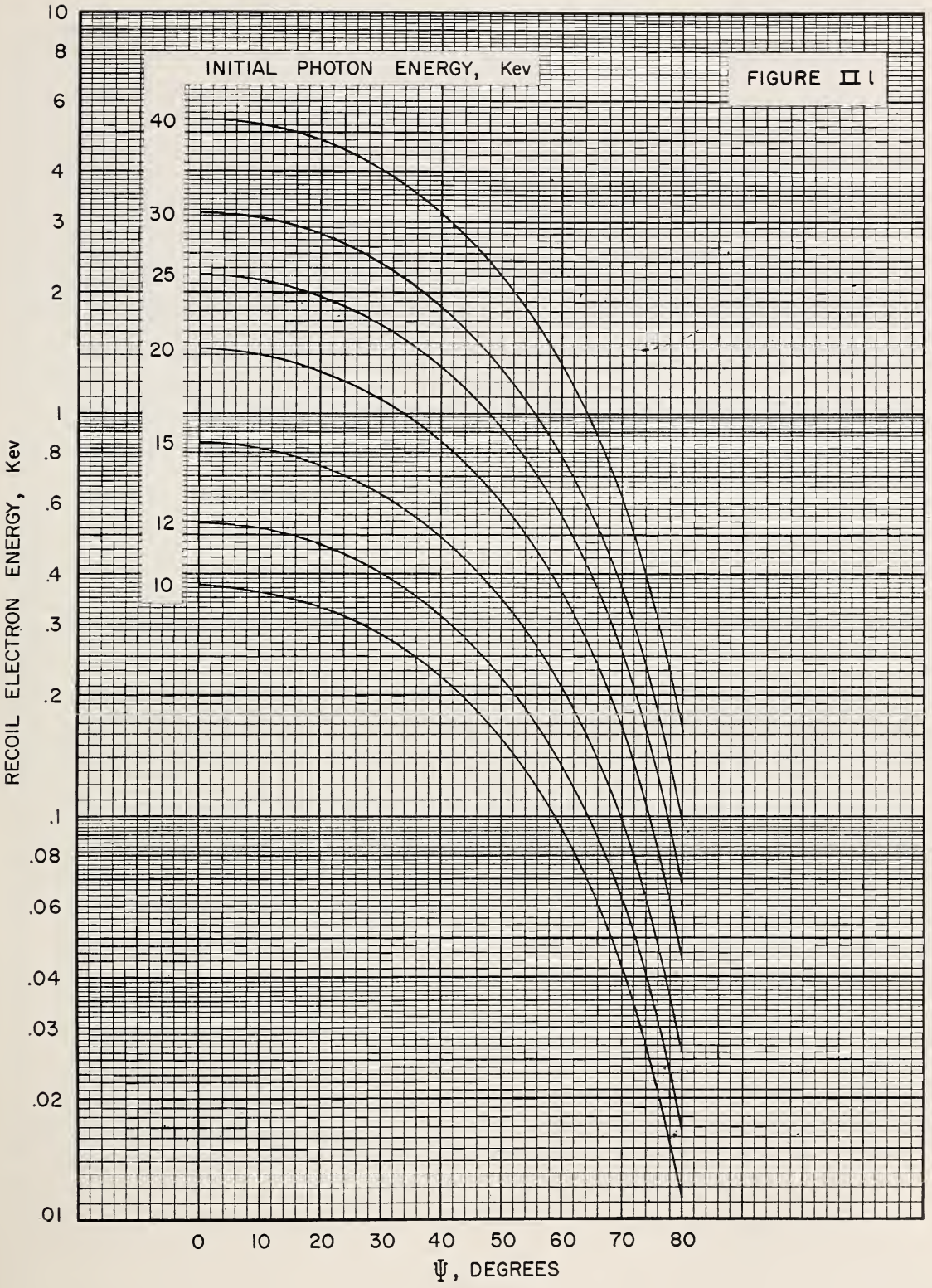
INITIAL PHOTON ENERGY, Kev
40
30
25
20
15
12
10
RECOIL ELECTRON ENERGY, Kev
10
8
6
4
3
2
1
.8
.6
.4
.3
.2
.1
.08
.06
.04
.03
.02
01
0
10
20
30
40
50
60
70
80
Ψ, DEGREES

FIGURE II l

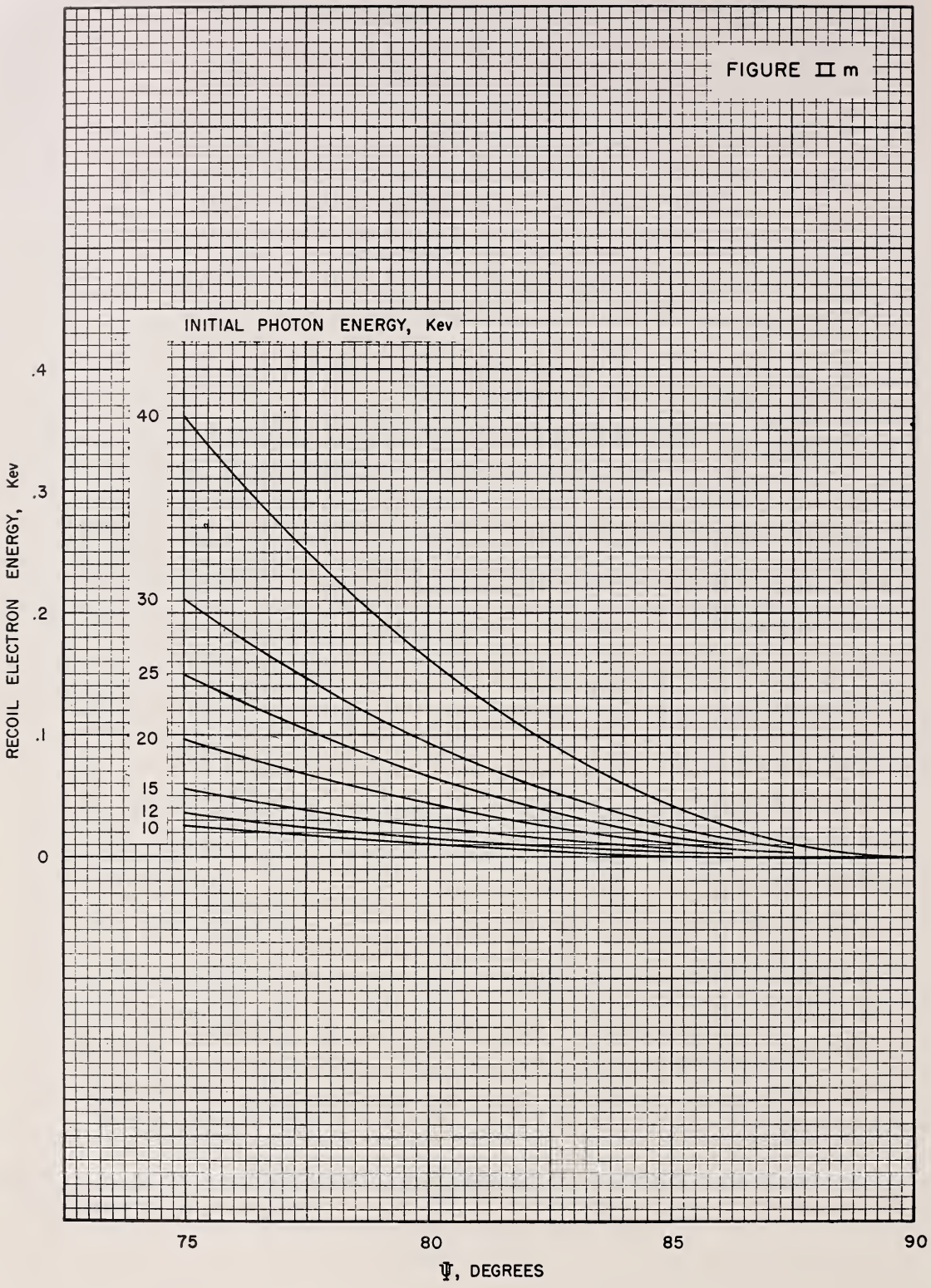
FIGURE II m
INITIAL PHOTON ENERGY, Kev
40
30
25
20
15
12
10
RECOIL ELECTRON ENERGY, Kev
.4
.3
.2
.1
0
75
80
85
90
Ψ, DEGREES

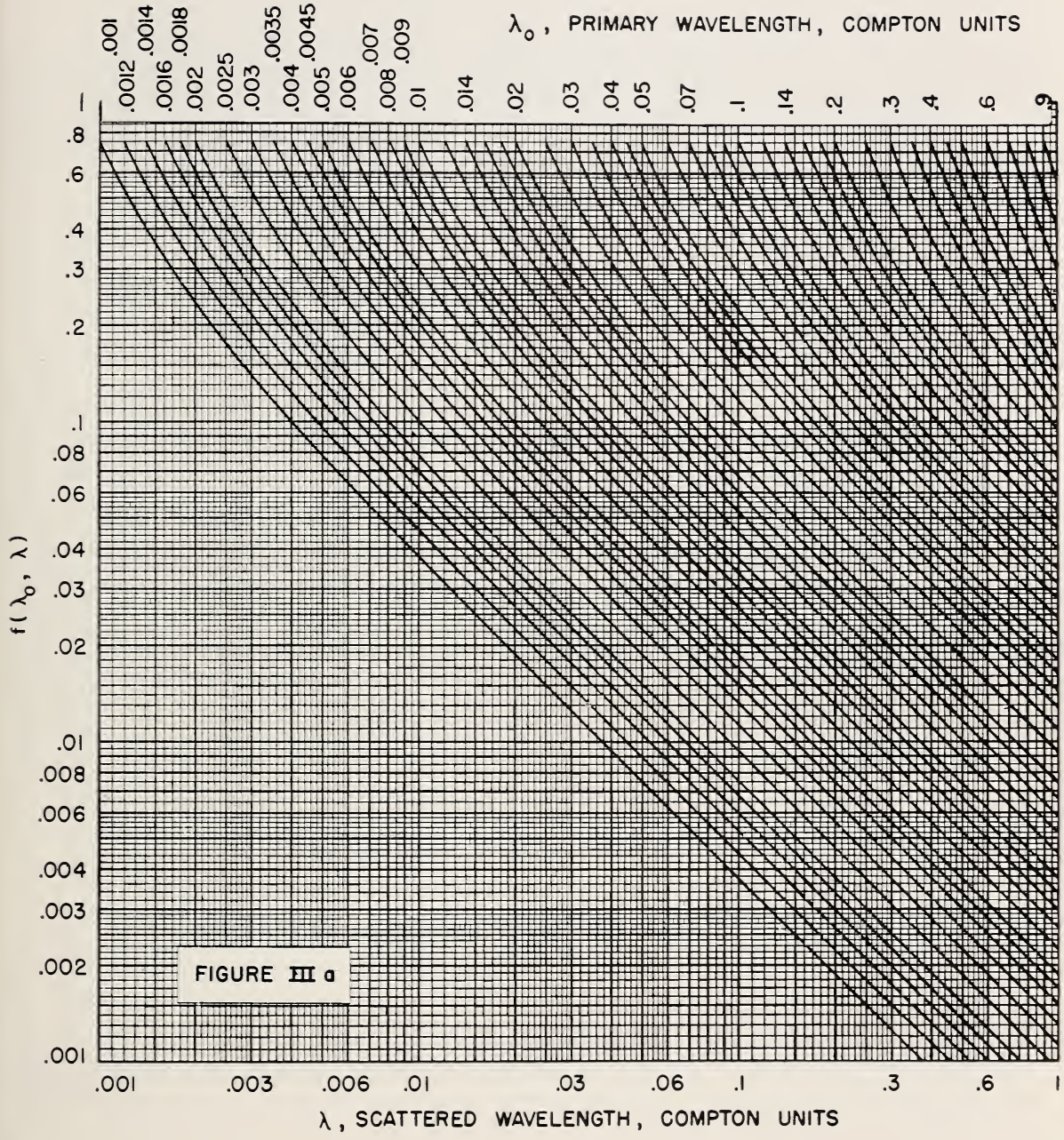
λ_o, PRIMARY WAVELENGTH, COMPTON UNITS
.001 .0012 .0014 .0016 .0018 .002 .0025 .003 .0035 .004 .0045 .005 .006 .007 .008 .009 .01 .014 .02 .03 .04 .05 .07 .1 .14 .2 .3 .4 .6 .9
1 .8 .6 .4 .3 .2 .1 .08 .06 .04 .03 .02 .01 .008 .006 .004 .003 .002 .001
$f(\lambda_o, \lambda)$
.001 .003 .006 .01 .03 .06 .1 .3 .6 1
λ, SCATTERED WAVELENGTH, COMPTON UNITS

FIGURE III a

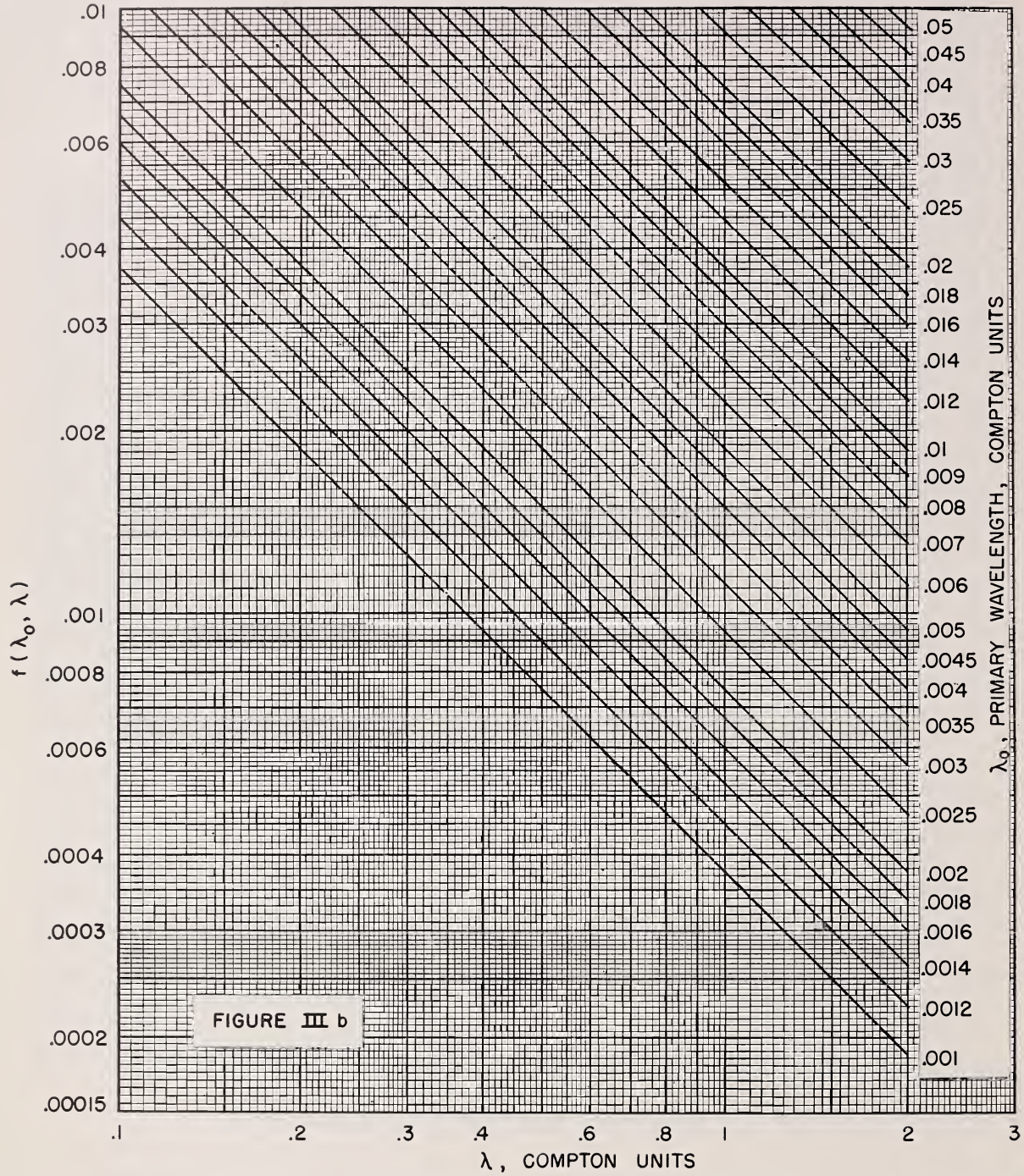
.01
.008
.006
.004
.003
.002
.001
.0008
.0006
.0004
.0003
.0002
.00015
f(λo, λ)
.1
.2
.3
.4
.6
.8
1
2
3
λ, COMPTON UNITS
.05
.045
.04
.035
.03
.025
.02
.018
.016
.014
.012
.01
.009
.008
.007
.006
.005
.0045
.004
.0035
.003
.0025
.002
.0018
.0016
.0014
.0012
.001
λo, PRIMARY WAVELENGTH, COMPTON UNITS
FIGURE III b

249464—53—6

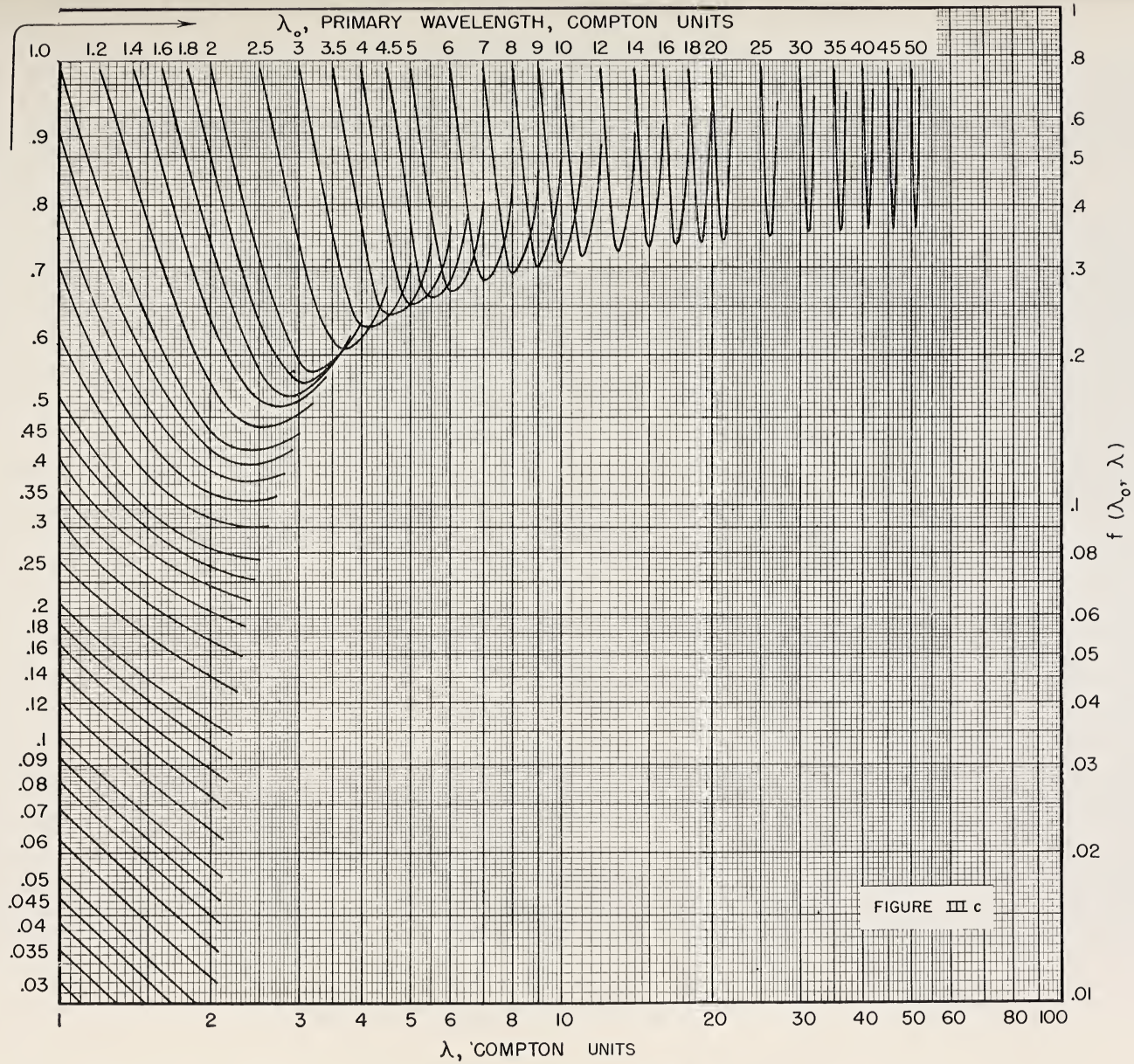

FIGURE III c

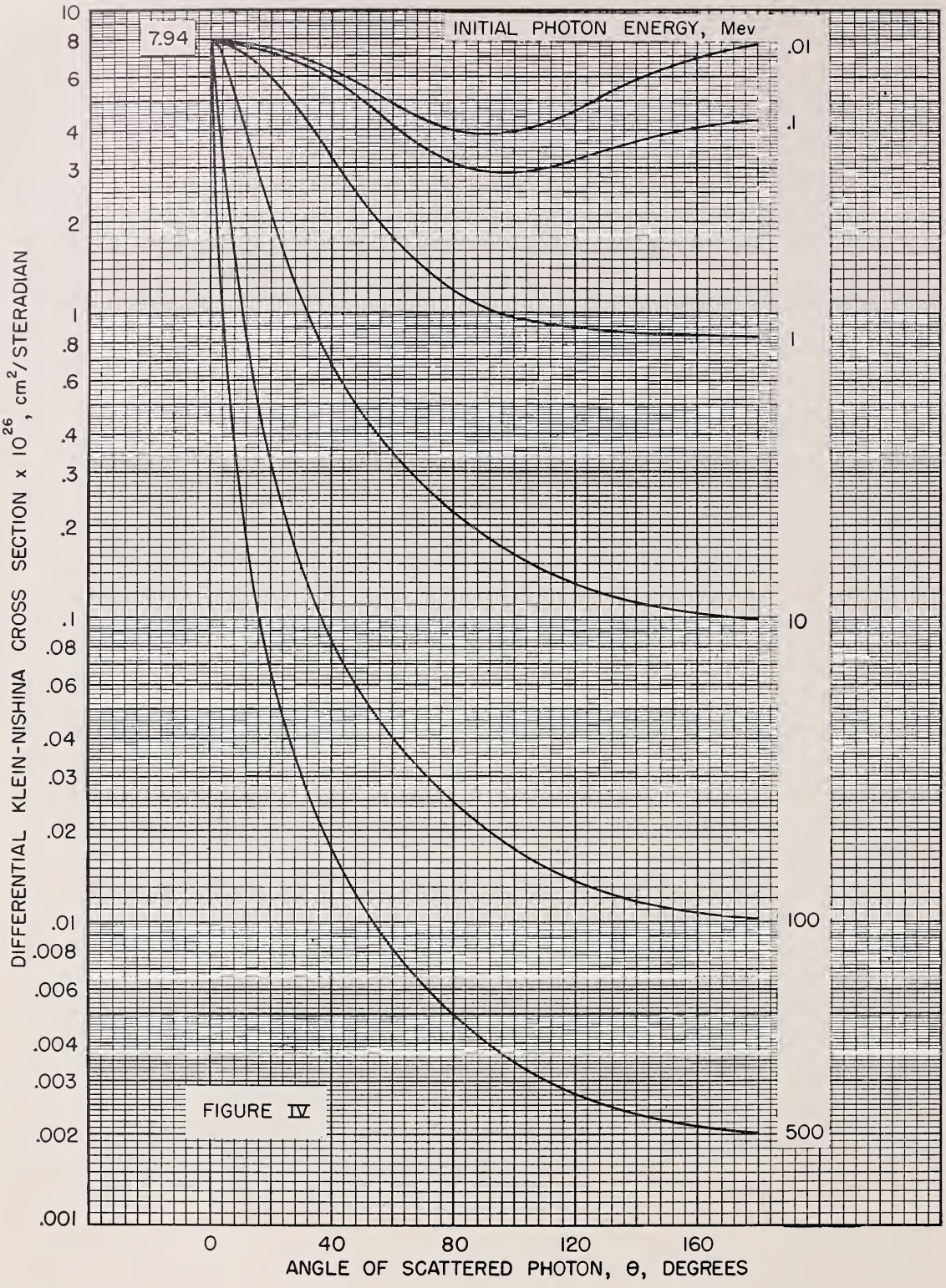
7.94
INITIAL PHOTON ENERGY, Mev
.01
.1
1
10
100
500
DIFFERENTIAL KLEIN-NISHINA CROSS SECTION x 10^{26}, cm^2/STERADIAN
10
8
6
4
3
2
1
.8
.6
.4
.3
.2
.1
.08
.06
.04
.03
.02
.01
.008
.006
.004
.003
.002
.001
0
40
80
120
160
ANGLE OF SCATTERED PHOTON, θ, DEGREES

FIGURE IV

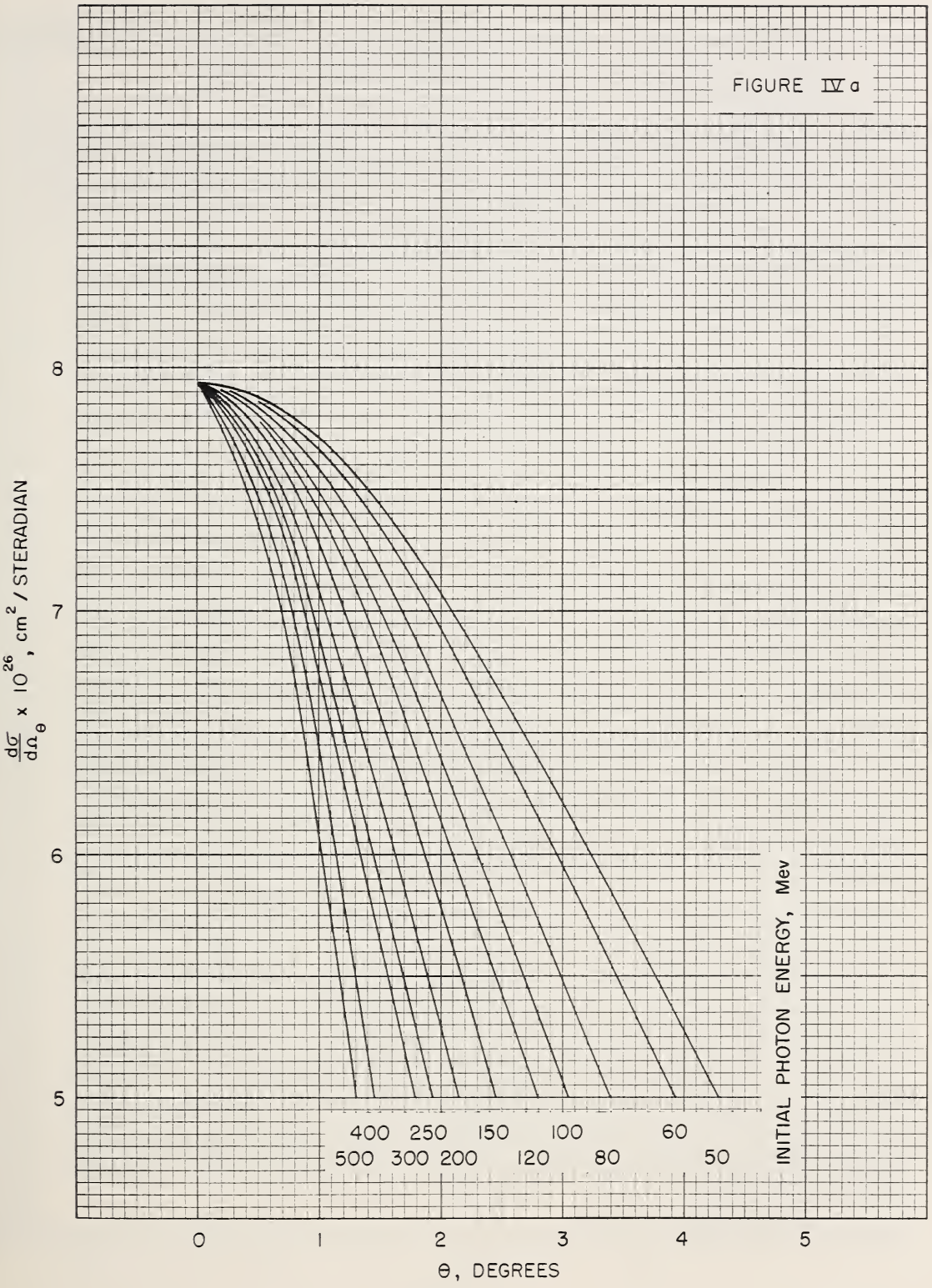
FIGURE IV a
8
7
6
5
$\frac{d\sigma}{d\Omega_\theta}$ x 10^{26}, cm^2 / STERADIAN
0
1
2
3
4
5
θ, DEGREES
400 250 150 100 60
500 300 200 120 80 50
INITIAL PHOTON ENERGY, Mev

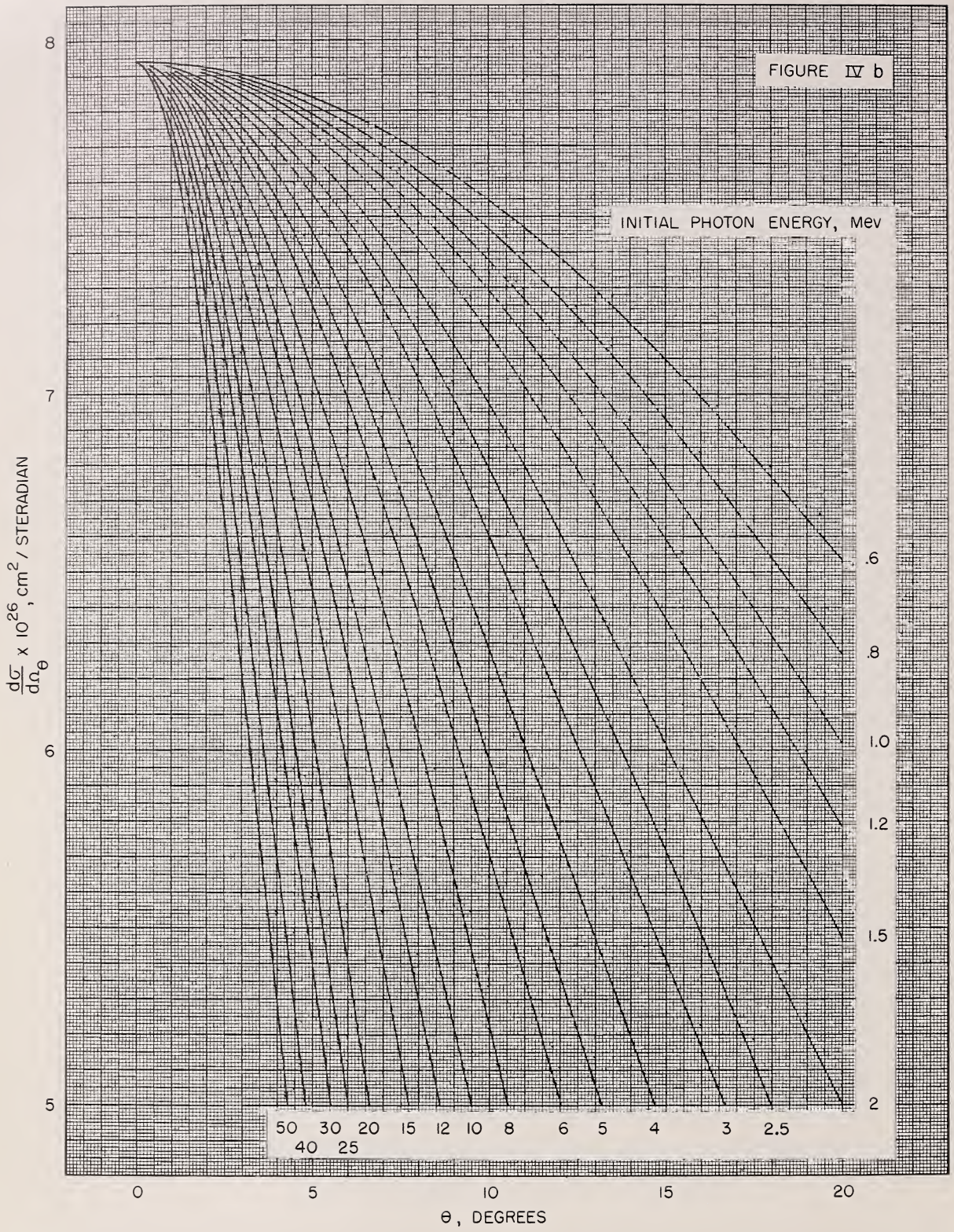
FIGURE IV b
INITIAL PHOTON ENERGY, Mev
50 40 30 25 20 15 12 10 8 6 5 4 3 2.5
.6 .8 1.0 1.2 1.5 2
8 7 6 5
0 5 10 15 20
θ, DEGREES
dσ/dΩθ x 10^26, cm^2 / STERADIAN

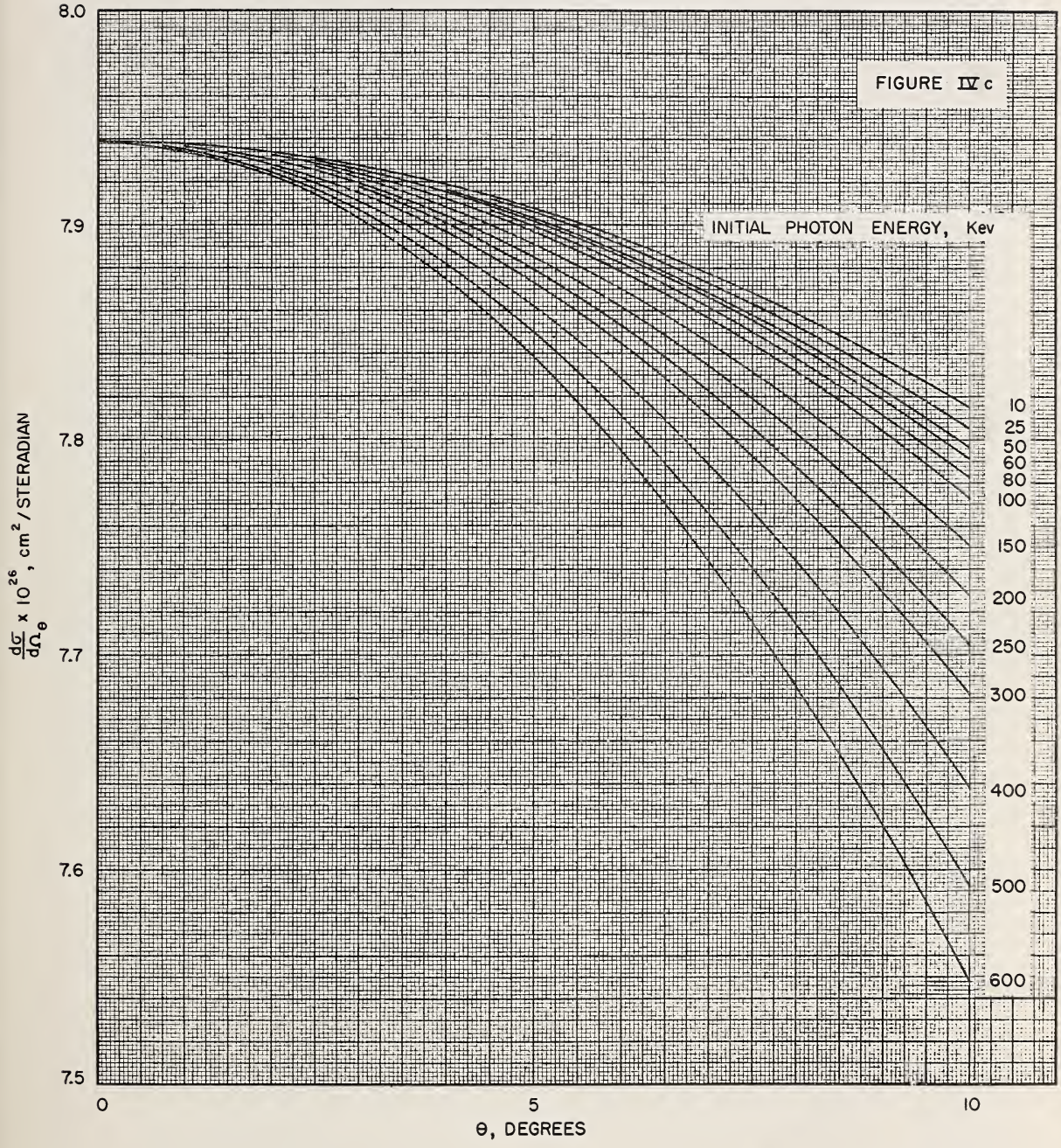
FIGURE IV c
INITIAL PHOTON ENERGY, Kev
10
25
50
60
80
100
150
200
250
300
400
500
600
8.0
7.9
7.8
7.7
7.6
7.5
0
5
10
θ, DEGREES
dσ/dΩθ x 10^26, cm^2/STERADIAN

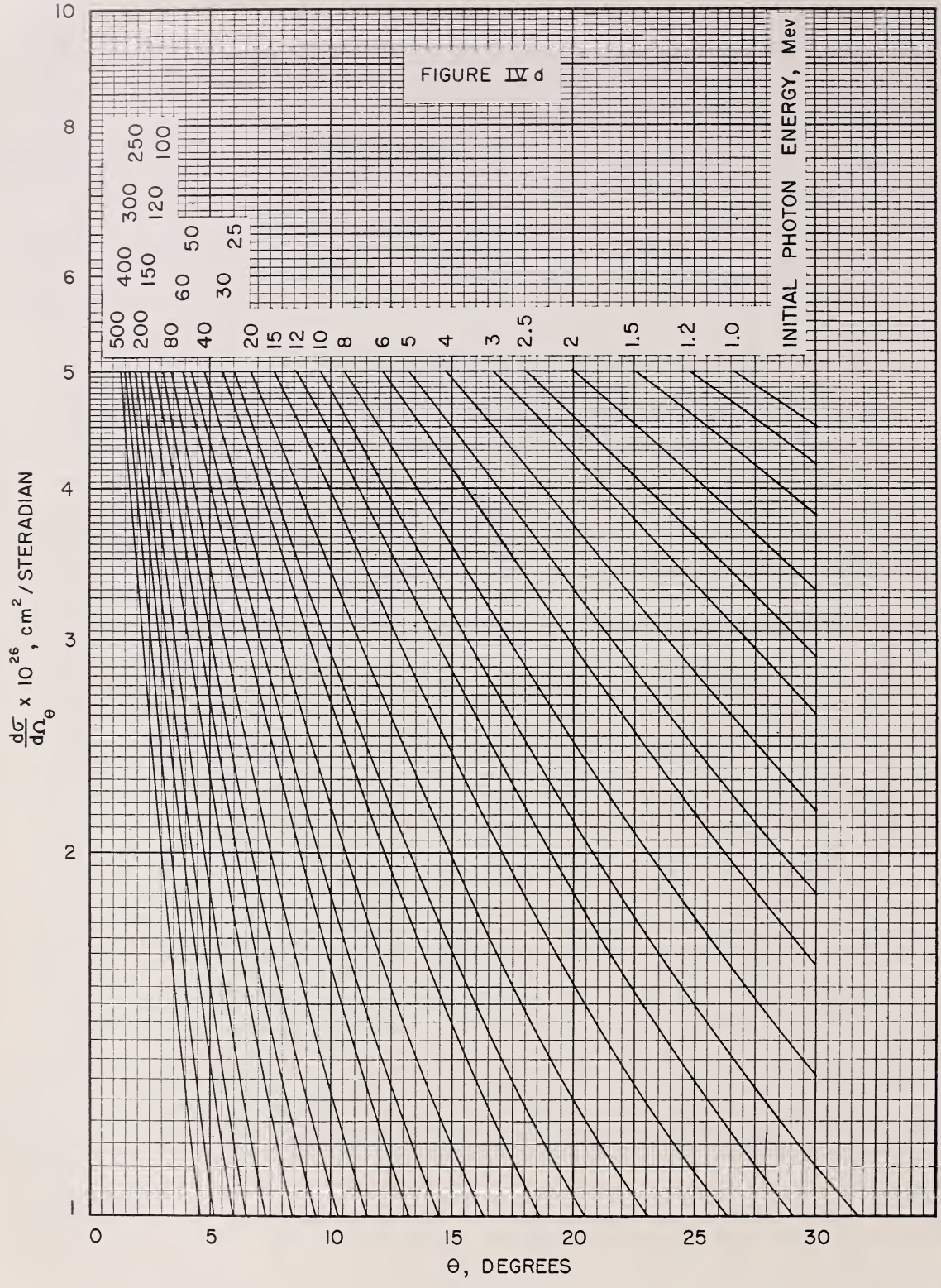
FIGURE IV d
INITIAL PHOTON ENERGY, Mev
500 200 80 40 20 15 12 10 8 6 5 4 3 2.5 2 1.5 1.2 1.0
400 150 60 30 50 25
300 120 250 100
$\frac{d\sigma}{d\Omega_\theta}$ x 10^{26}, cm^2 / STERADIAN
θ, DEGREES
0 5 10 15 20 25 30
1 2 3 4 5 6 8 10

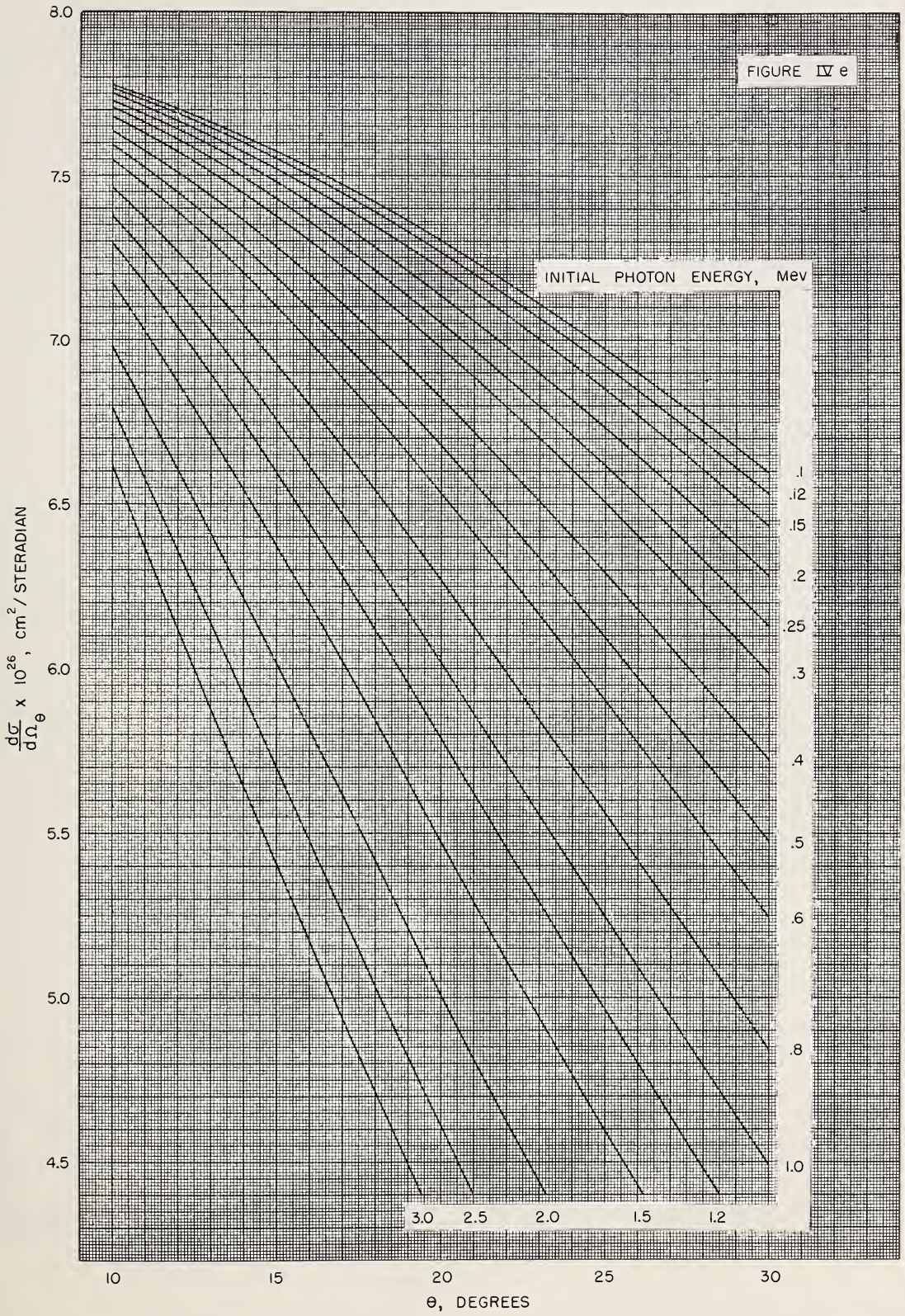
FIGURE IV e
INITIAL PHOTON ENERGY, Mev
.1
.12
.15
.2
.25
.3
.4
.5
.6
.8
1.0
3.0
2.5
2.0
1.5
1.2
8.0
7.5
7.0
6.5
6.0
5.5
5.0
4.5
10
15
20
25
30
θ, DEGREES
dσ/dΩθ x 10^26, cm^2/STERADIAN

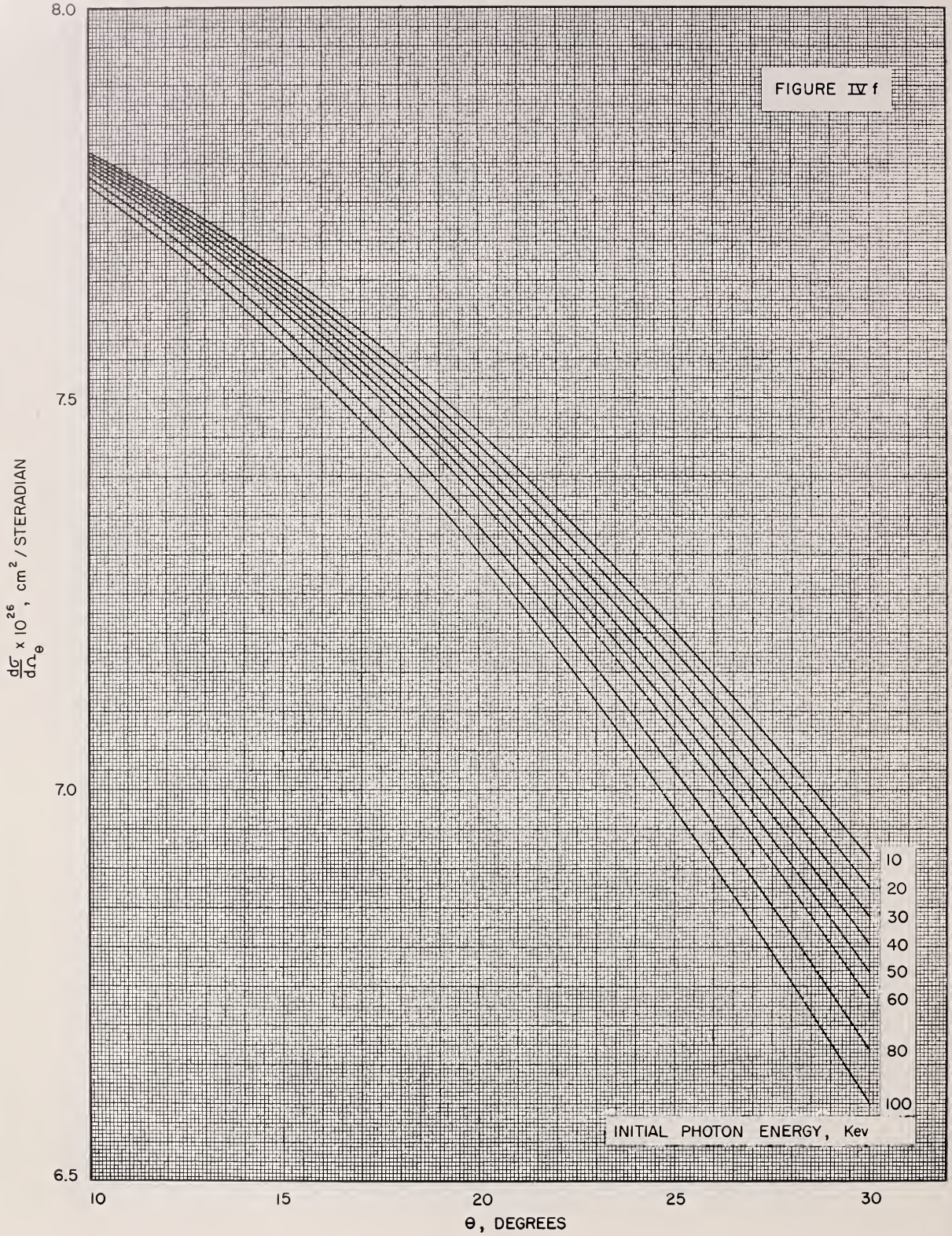
FIGURE IV f
8.0
7.5
7.0
6.5
$\frac{d\sigma}{d\Omega_\theta} \times 10^{26}$, cm^2 / STERADIAN
10
15
20
25
30
θ, DEGREES
10
20
30
40
50
60
80
100
INITIAL PHOTON ENERGY, Kev

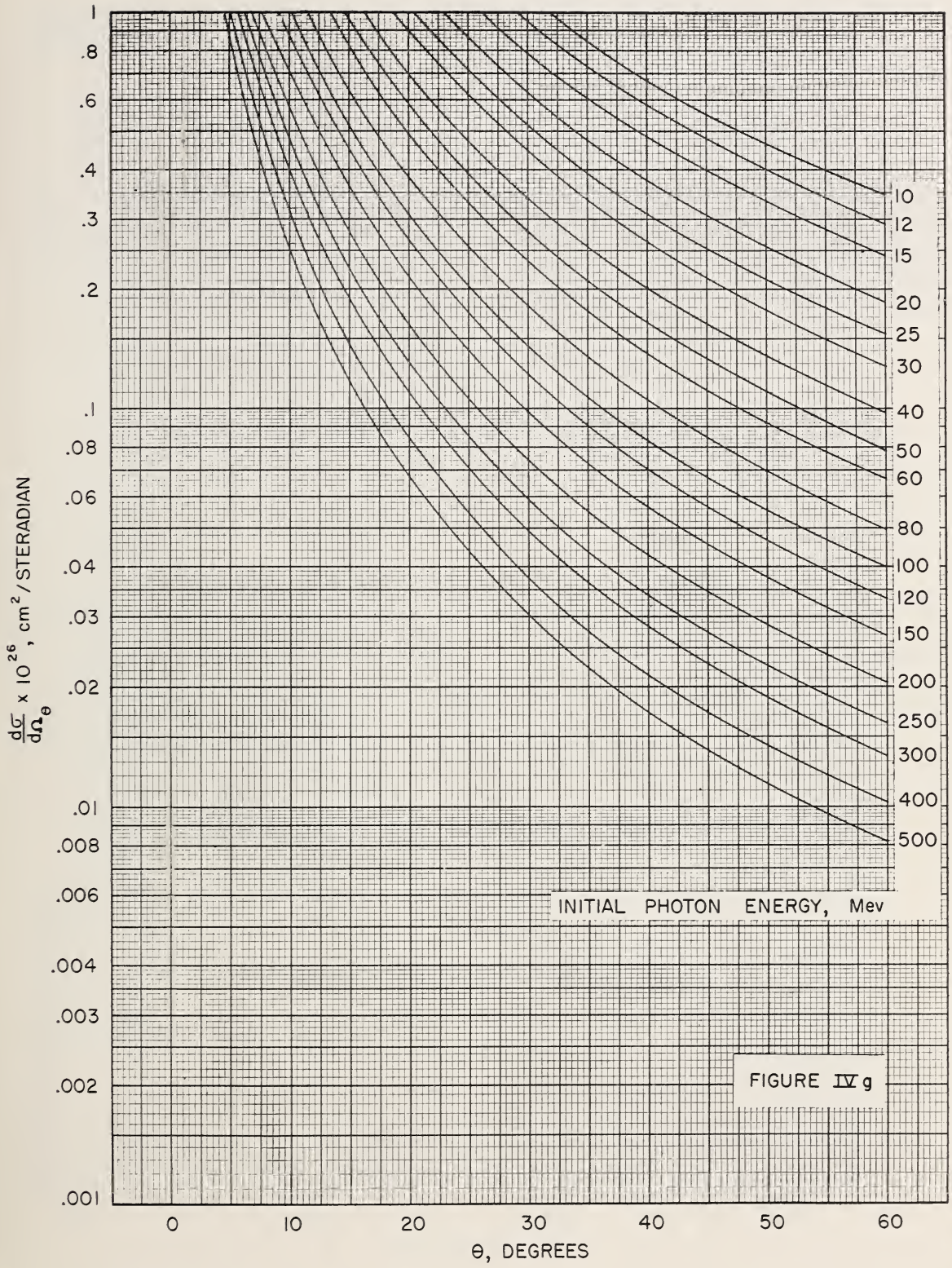
1
.8
.6
.4
.3
.2
.1
.08
.06
.04
.03
.02
.01
.008
.006
.004
.003
.002
.001
$\frac{d\sigma}{d\Omega_\theta} \times 10^{26}$, cm^2/STERADIAN
0
10
20
30
40
50
60
θ, DEGREES
10
12
15
20
25
30
40
50
60
80
100
120
150
200
250
300
400
500
INITIAL PHOTON ENERGY, Mev

FIGURE IV g

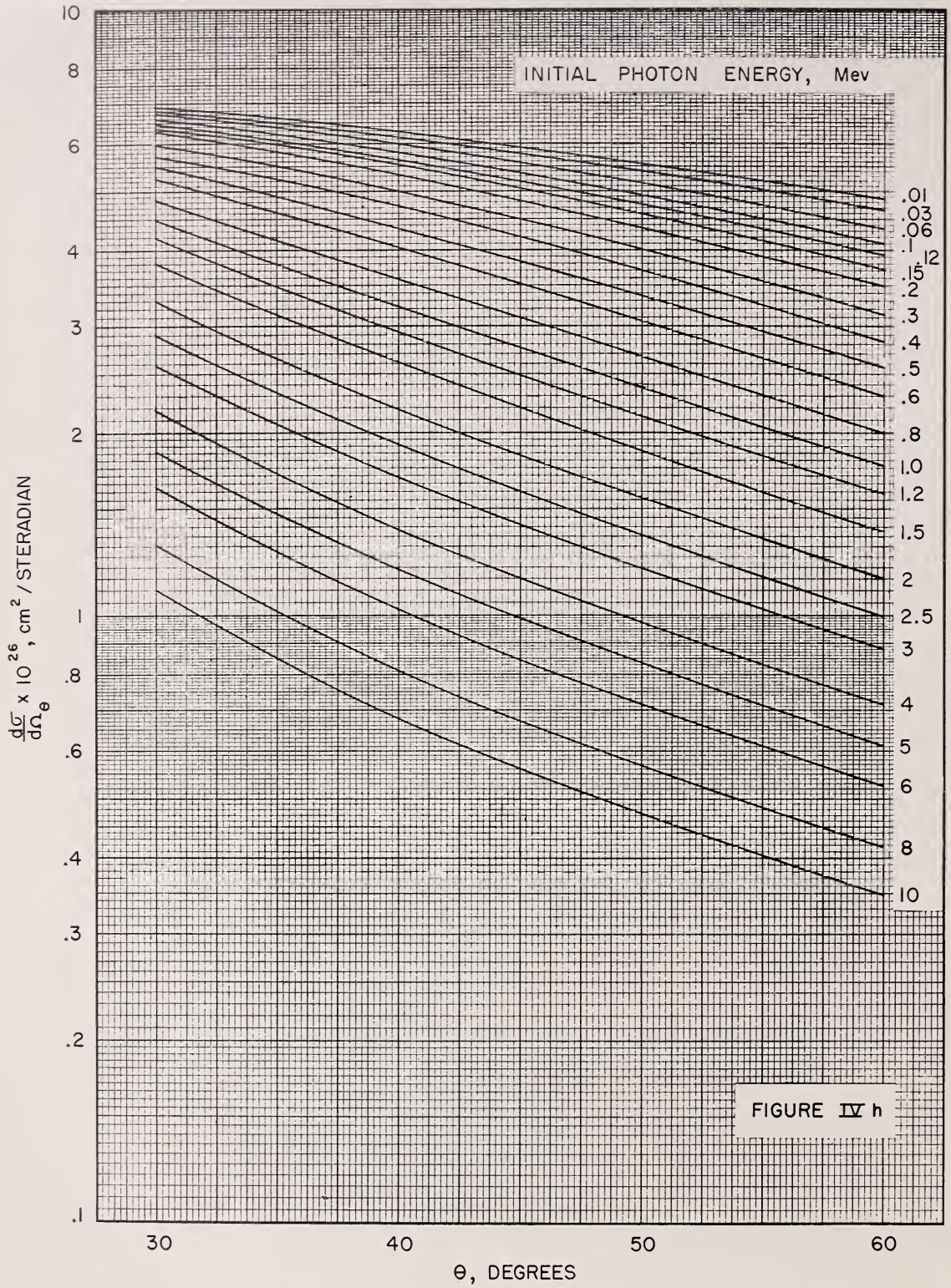
INITIAL PHOTON ENERGY, Mev
.01
.03
.06
.1
.12
.15
.2
.3
.4
.5
.6
.8
1.0
1.2
1.5
2
2.5
3
4
5
6
8
10
10
8
6
4
3
2
1
.8
.6
.4
.3
.2
.1
30
40
50
60
θ, DEGREES
dσ/dΩθ x 10^26, cm^2 / STERADIAN

FIGURE IV h

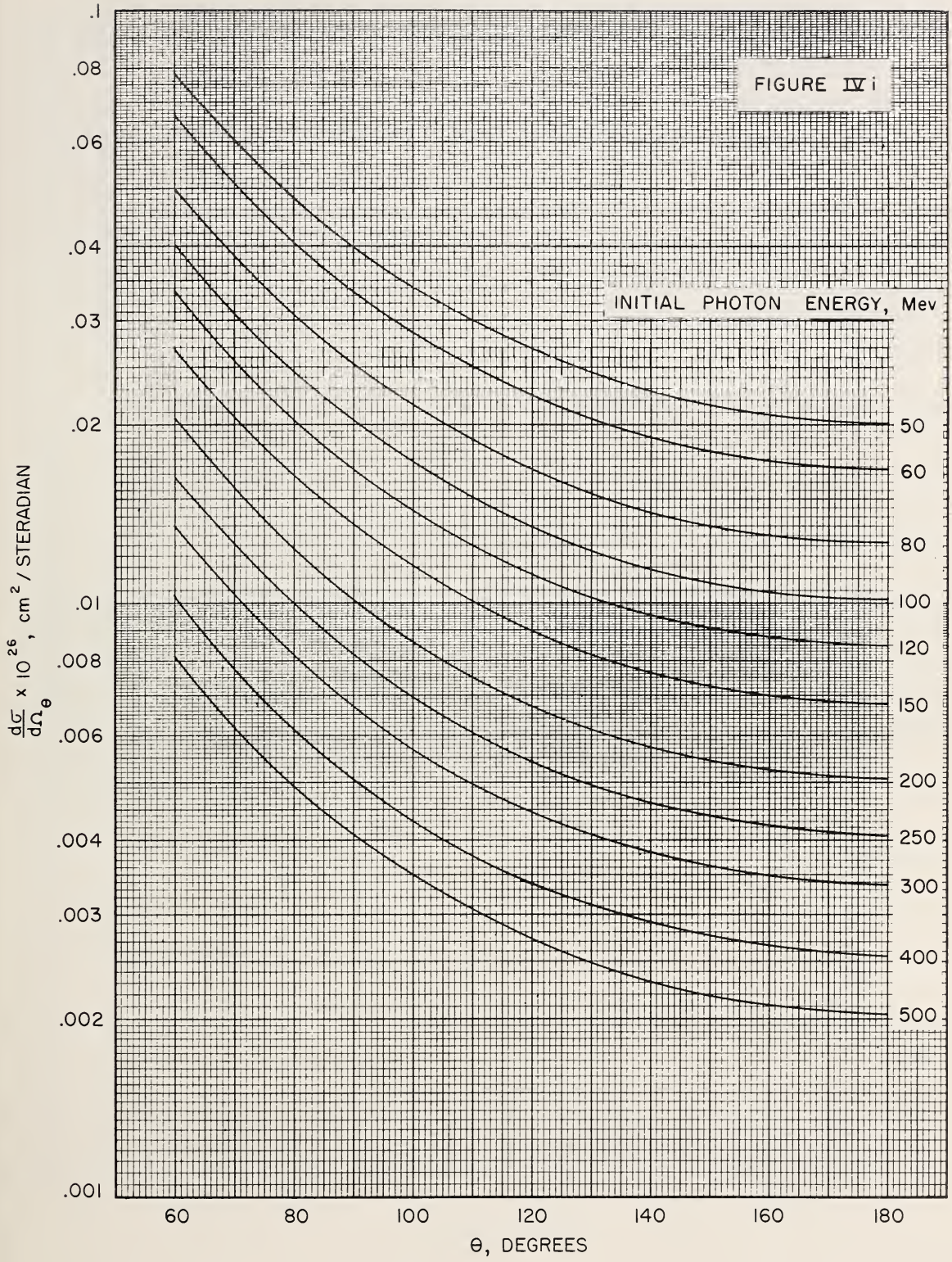
FIGURE IV i
INITIAL PHOTON ENERGY, Mev
50
60
80
100
120
150
200
250
300
400
500
.1
.08
.06
.04
.03
.02
.01
.008
.006
.004
.003
.002
.001
60
80
100
120
140
160
180
θ, DEGREES
dσ/dΩθ x 10^26, cm^2 / STERADIAN

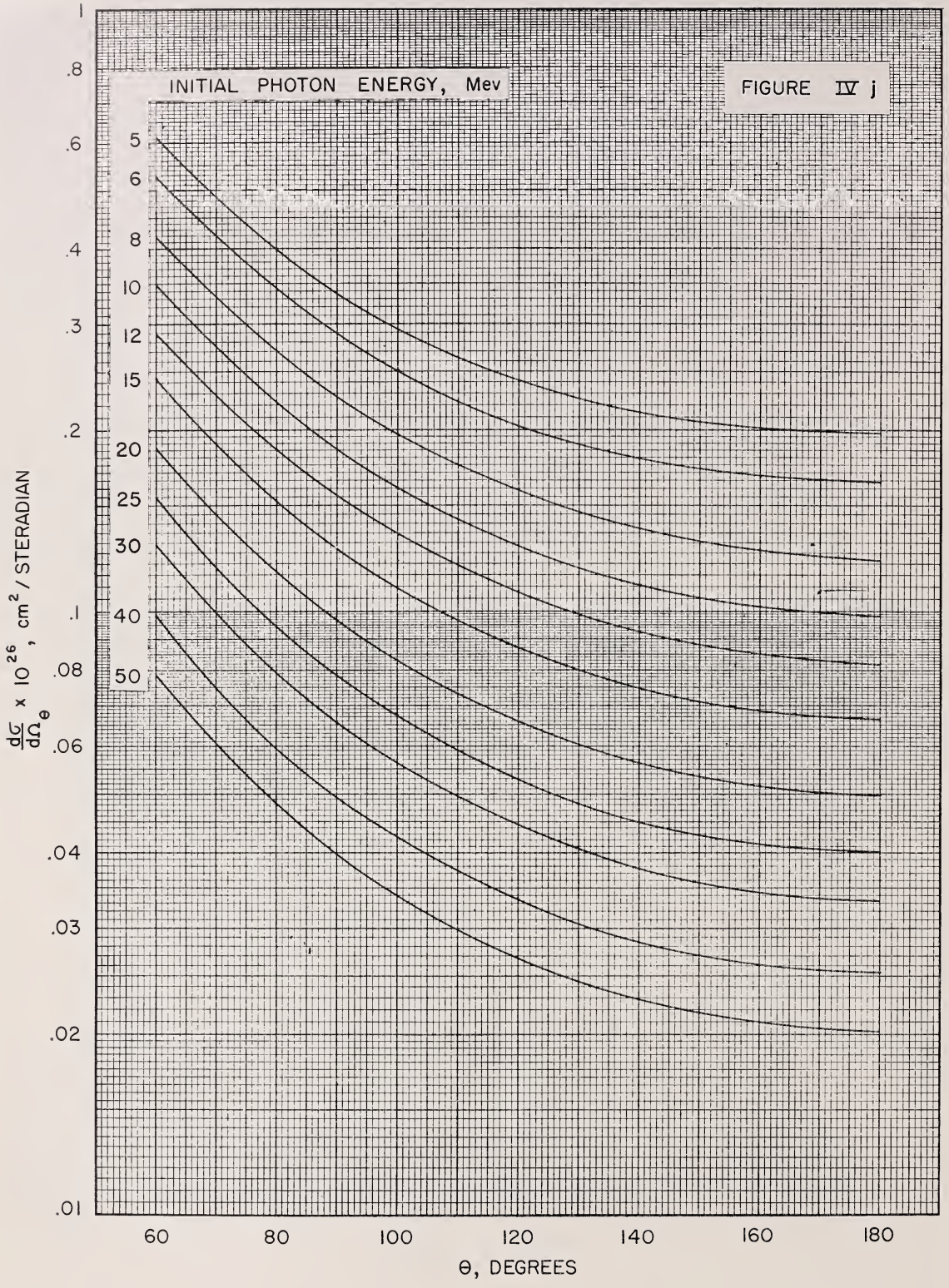
FIGURE IV j
INITIAL PHOTON ENERGY, Mev
5
6
8
10
12
15
20
25
30
40
50
1
.8
.6
.4
.3
.2
.1
.08
.06
.04
.03
.02
.01
$\frac{d\sigma}{d\Omega_\theta} \times 10^{26}$, cm^2 / STERADIAN
60
80
100
120
140
160
180
θ, DEGREES

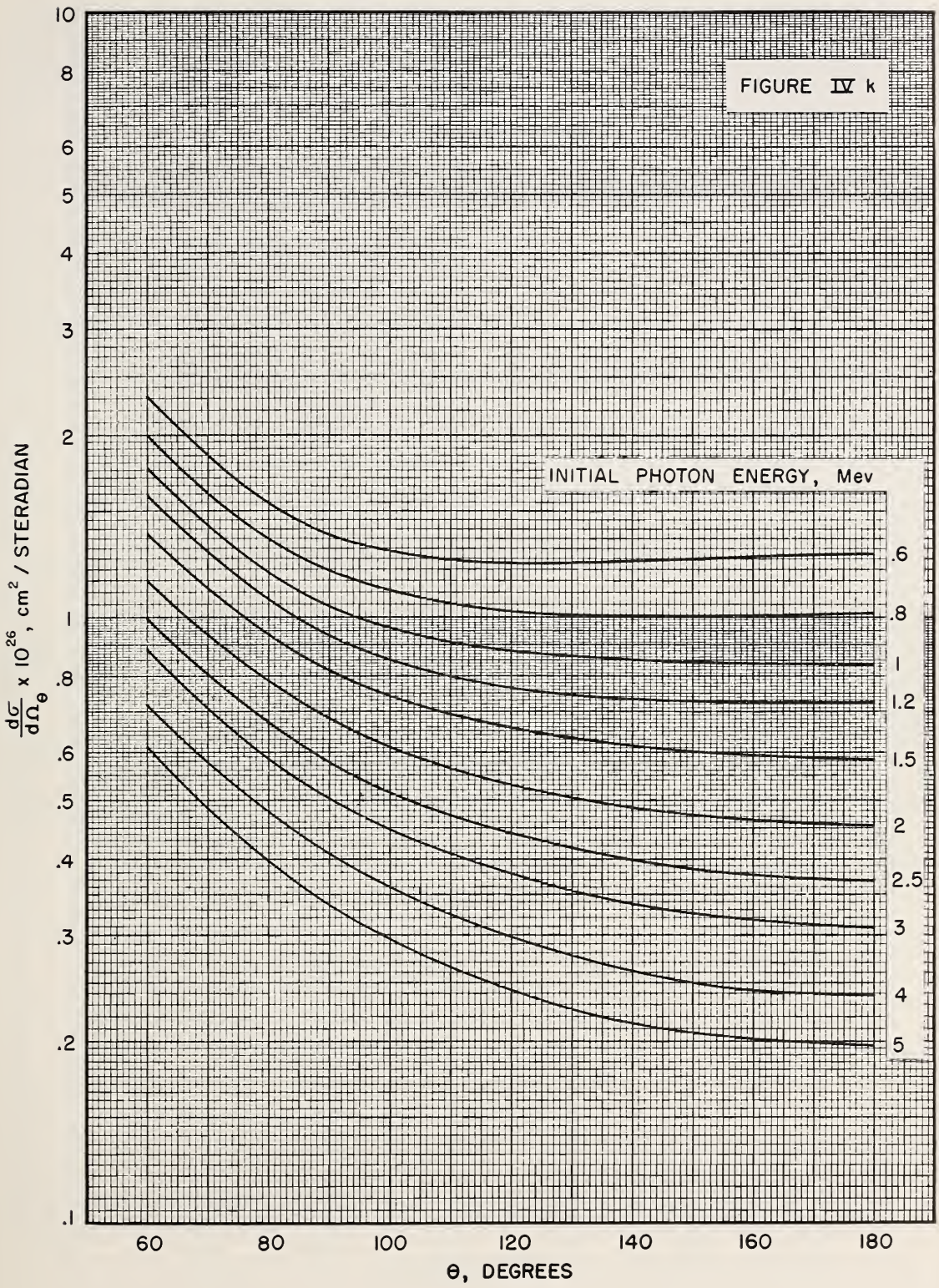
FIGURE IV k
INITIAL PHOTON ENERGY, Mev
.6
.8
1
1.2
1.5
2
2.5
3
4
5
$\frac{d\sigma}{d\Omega_\theta}$ x 10^{26}, cm^2 / STERADIAN
θ, DEGREES
10
8
6
5
4
3
2
1
.8
.6
.5
.4
.3
.2
.1
60
80
100
120
140
160
180

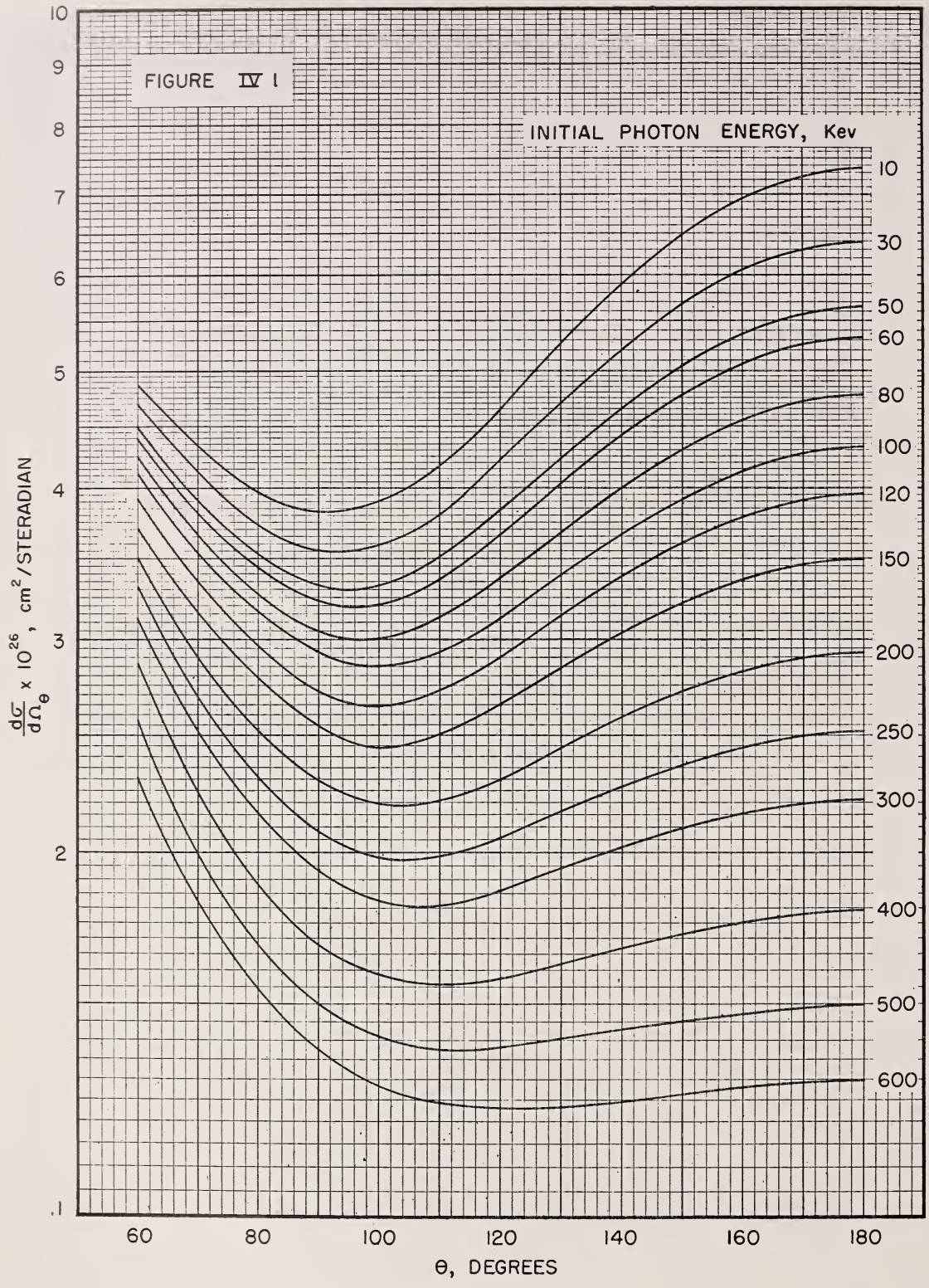
FIGURE IV 1
INITIAL PHOTON ENERGY, Kev
10
30
50
60
80
100
120
150
200
250
300
400
500
600
$\frac{d\sigma}{d\Omega_\theta} \times 10^{26}$, cm^2/STERADIAN
θ, DEGREES
10
9
8
7
6
5
4
3
2
.1
60
80
100
120
140
160
180

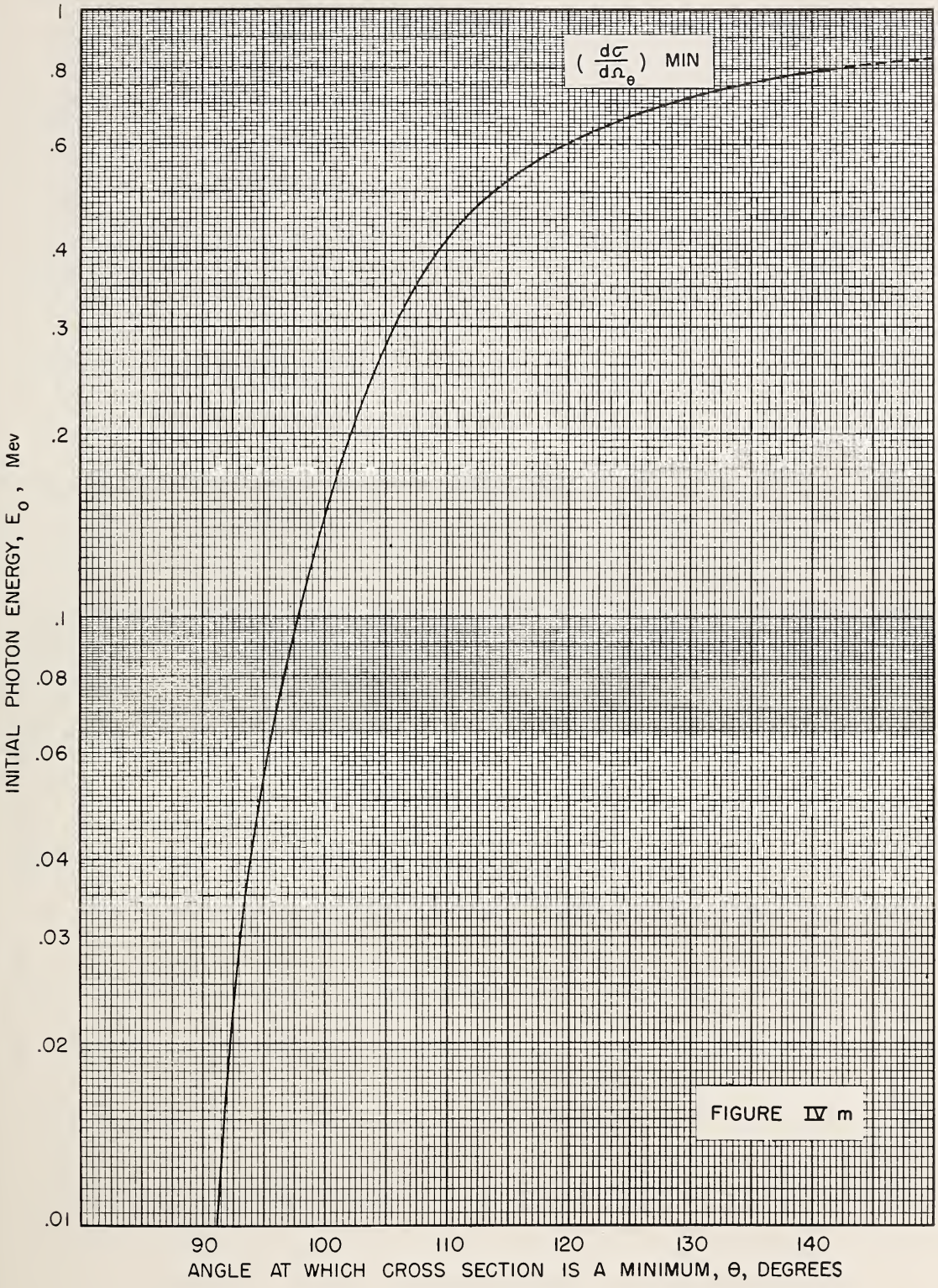
$\left(\frac{d\sigma}{d\Omega_\theta}\right)$ MIN
INITIAL PHOTON ENERGY, E_o, Mev
1
.8
.6
.4
.3
.2
.1
.08
.06
.04
.03
.02
.01
90
100
110
120
130
140
ANGLE AT WHICH CROSS SECTION IS A MINIMUM, θ, DEGREES

FIGURE IV m

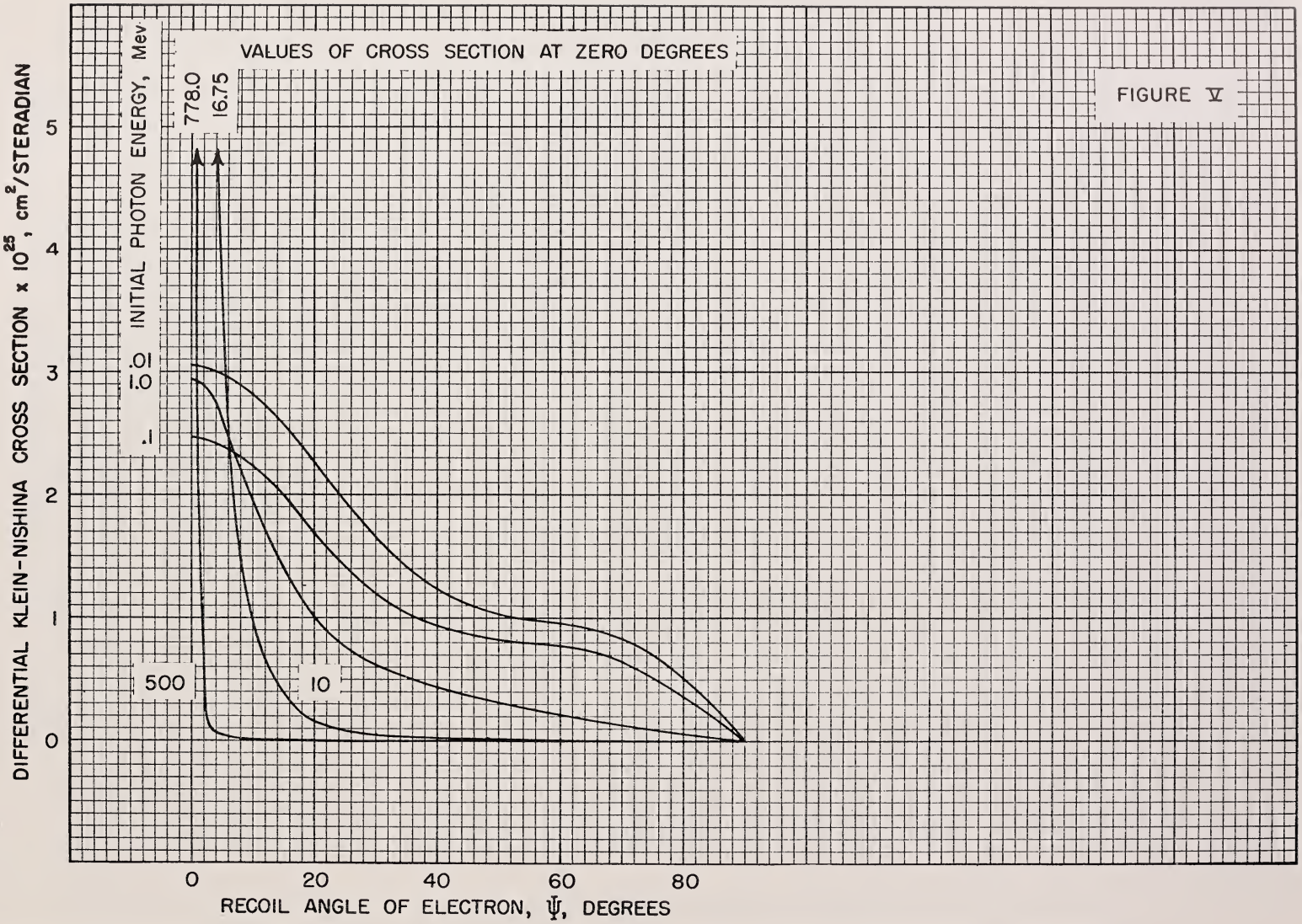
VALUES OF CROSS SECTION AT ZERO DEGREES
778.0
16.75
INITIAL PHOTON ENERGY, Mev
.1
.5
1.0
500
10
DIFFERENTIAL KLEIN-NISHINA CROSS SECTION x 10^{25}, cm^2/STERADIAN
0
1
2
3
4
5
0
20
40
60
80
RECOIL ANGLE OF ELECTRON, Ψ, DEGREES

FIGURE V

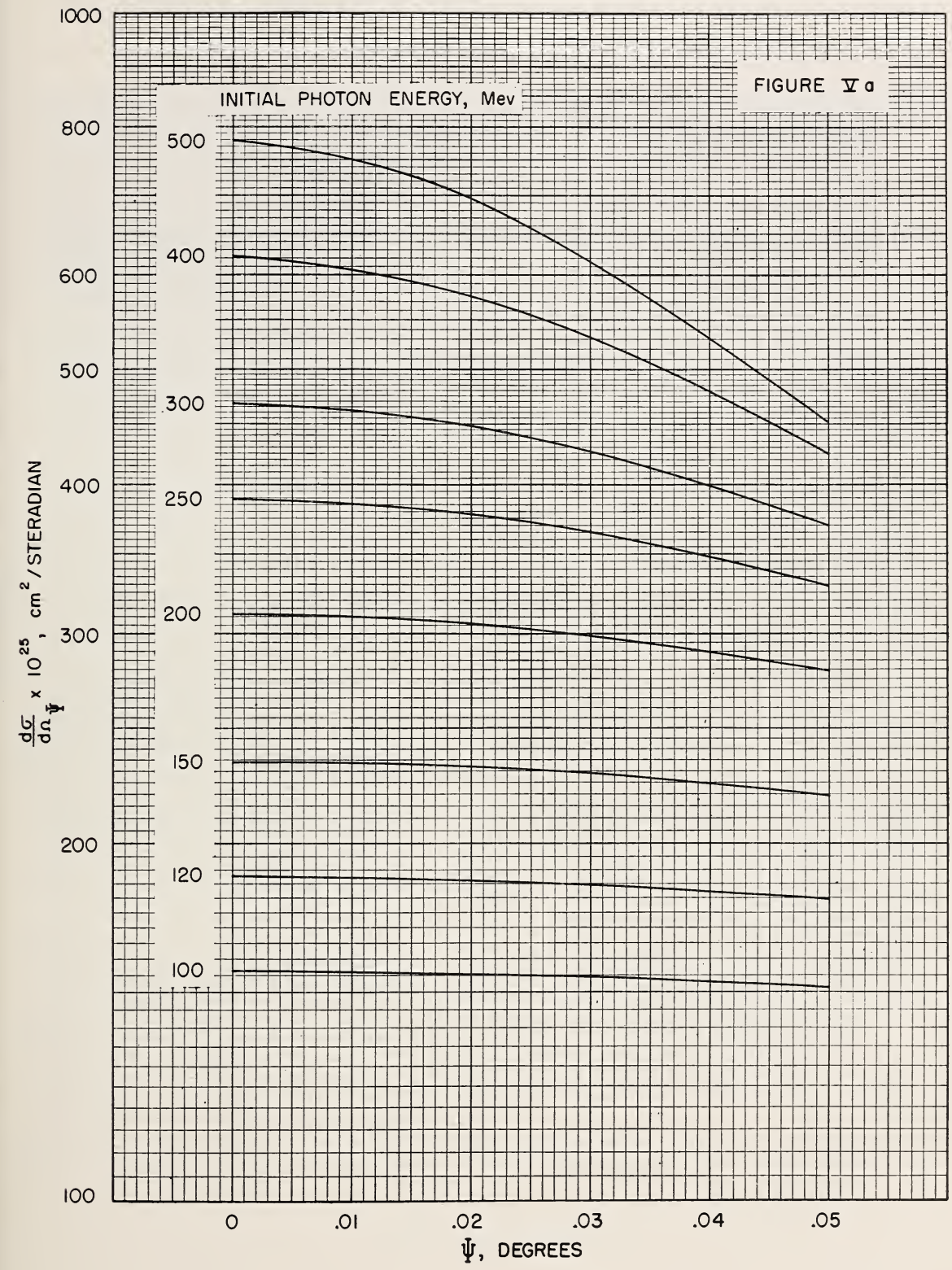
FIGURE V a
INITIAL PHOTON ENERGY, Mev
500
400
300
250
200
150
120
100
1000
800
600
500
400
300
200
100
0
.01
.02
.03
.04
.05
Ψ, DEGREES
dσ/dΩ_Ψ x 10^25, cm^2/STERADIAN

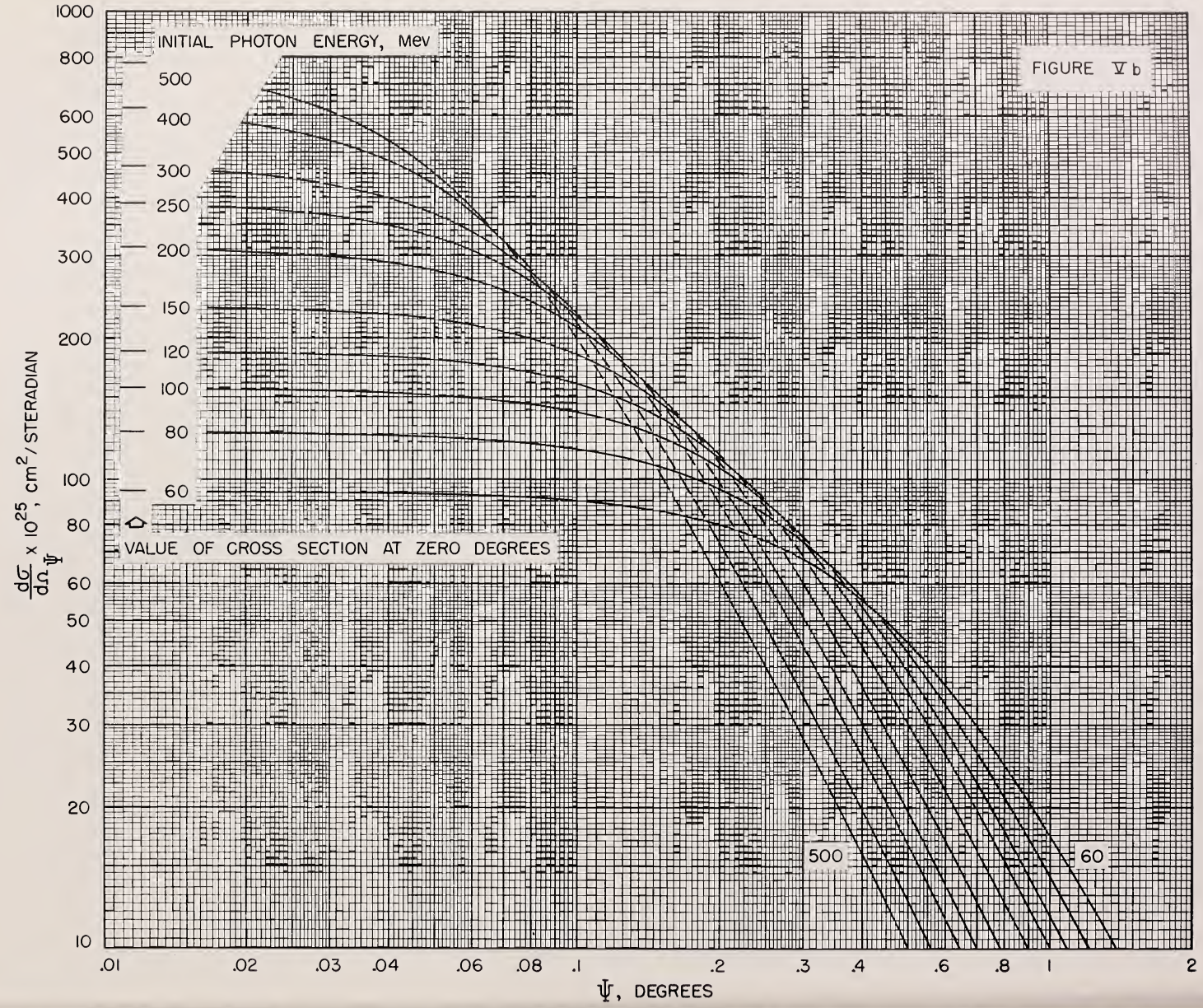
INITIAL PHOTON ENERGY, Mev
500
400
300
250
200
150
120
100
80
60
VALUE OF CROSS SECTION AT ZERO DEGREES
500
60
1000
800
600
500
400
300
200
100
80
60
50
40
30
20
10
.01
.02
.03
.04
.06
.08
.1
.2
.3
.4
.6
.8
1
2
Ψ, DEGREES
dσ/dΩ_Ψ x 10^25, cm^2/STERADIAN

FIGURE V b

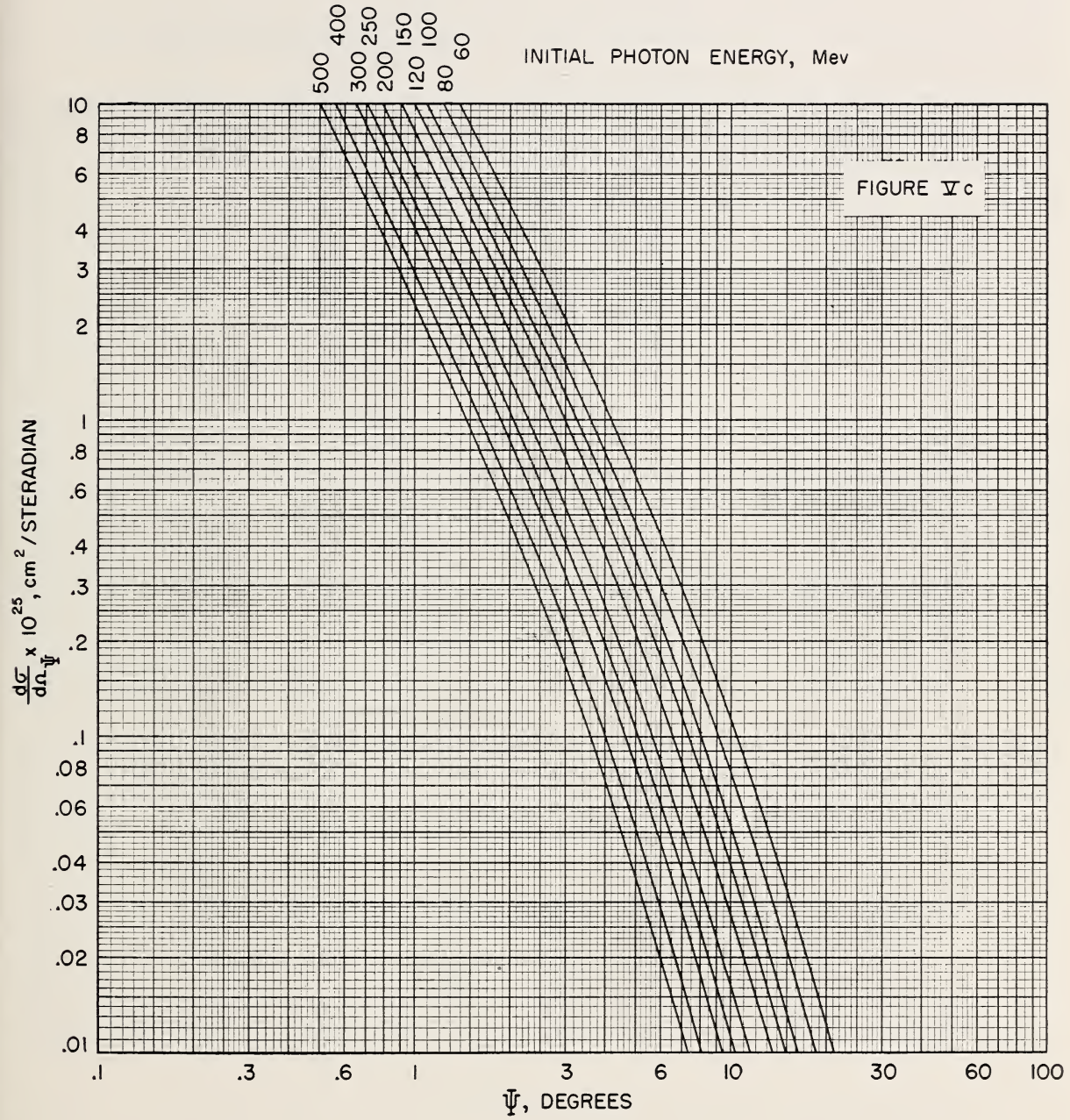
500 400 300 250 200 150 120 100 80 60
INITIAL PHOTON ENERGY, Mev
FIGURE V c
10 8 6 4 3 2 1 .8 .6 .4 .3 .2 .1 .08 .06 .04 .03 .02 .01
$\frac{d\sigma}{d\Omega_\Psi}$ x 10^{25}, cm^2 / STERADIAN
.1 .3 .6 1 3 6 10 30 60 100
Ψ, DEGREES

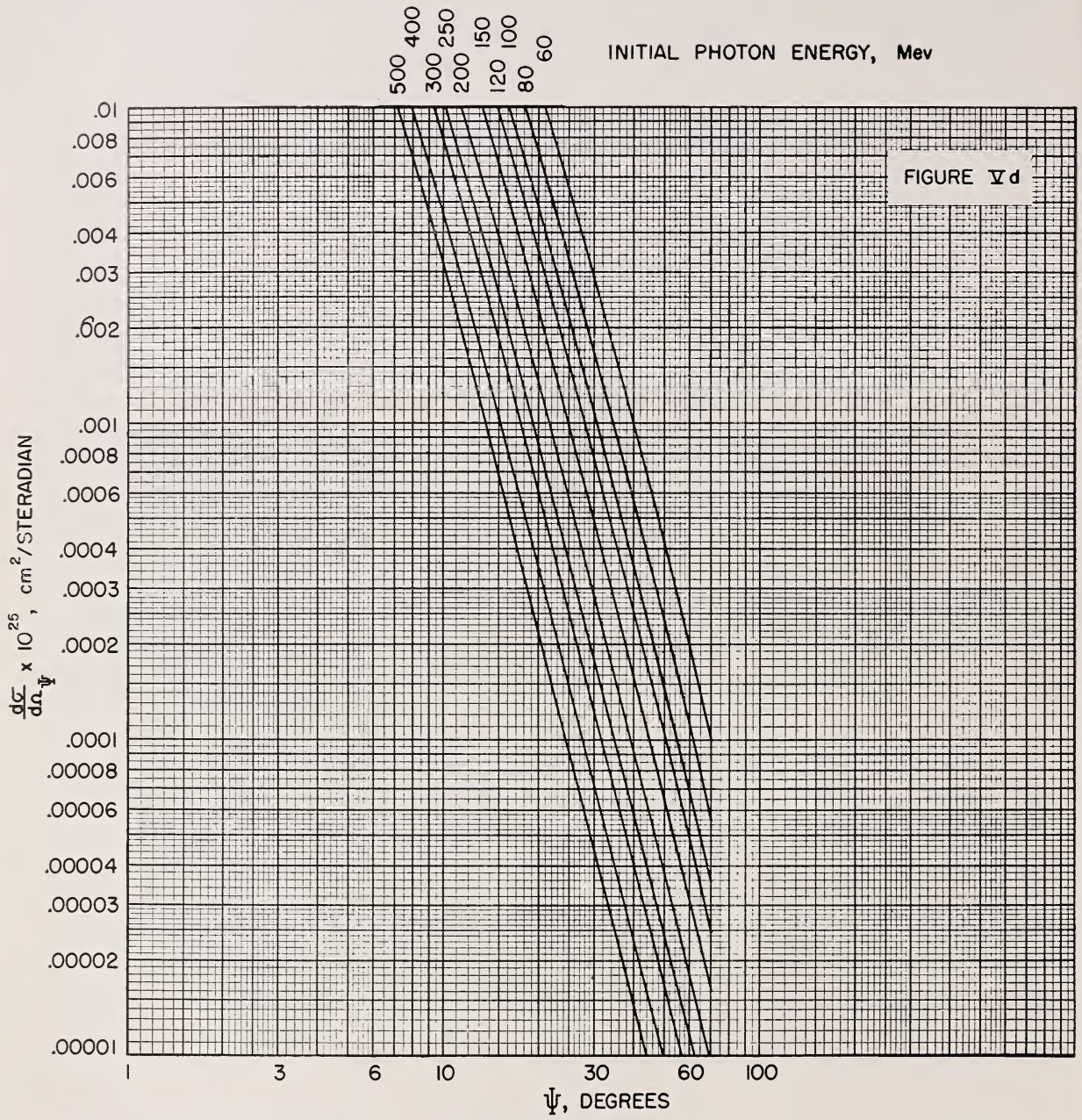
INITIAL PHOTON ENERGY, Mev
500 400 300 250 200 150 120 100 80 60
FIGURE V d
.01 .008 .006 .004 .003 .002 .001 .0008 .0006 .0004 .0003 .0002 .0001 .00008 .00006 .00004 .00003 .00002 .00001
$\frac{d\sigma}{d\Omega_\Psi} \times 10^{25}$, cm^2/STERADIAN
1 3 6 10 30 60 100
Ψ, DEGREES

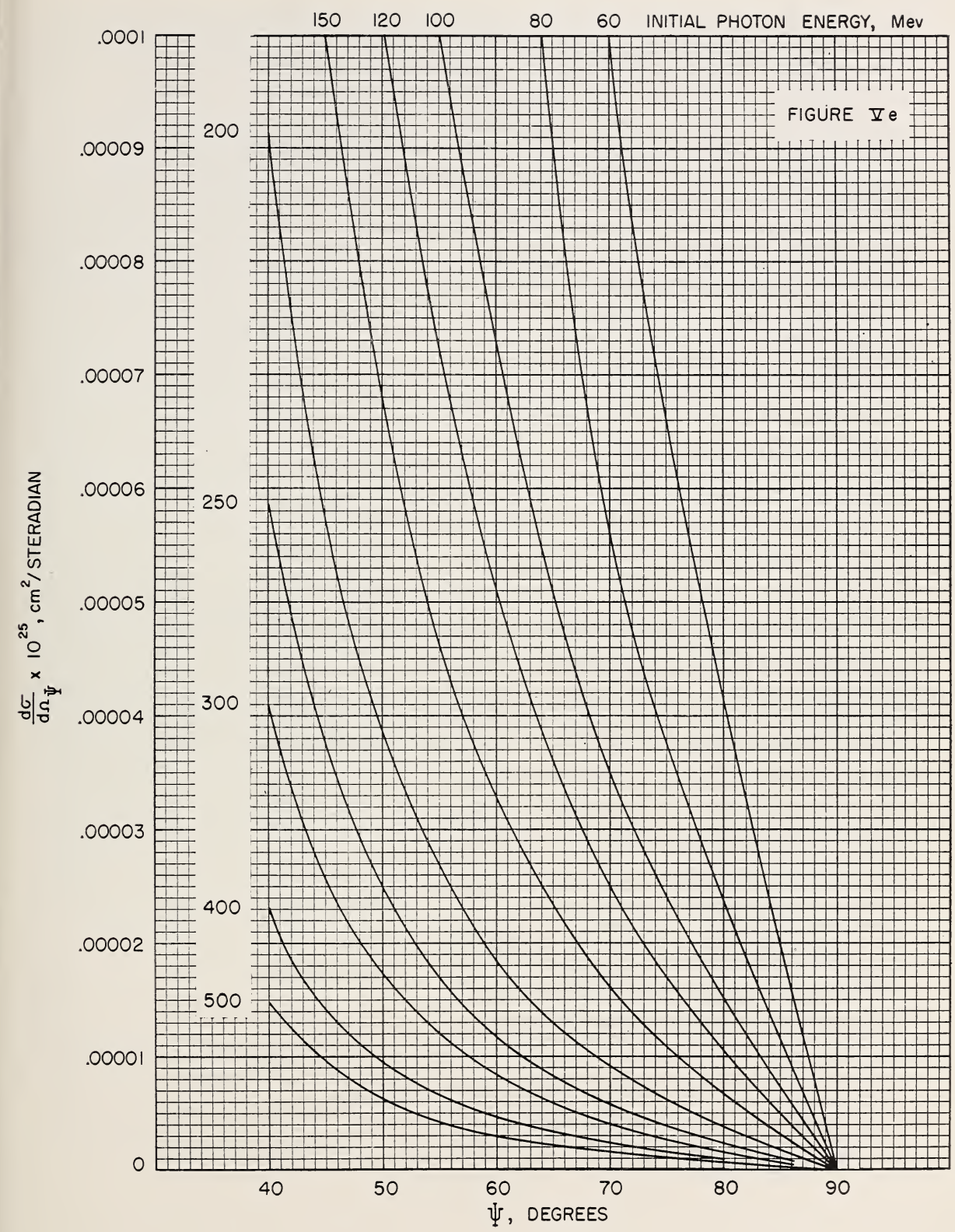
150 120 100 80 60 INITIAL PHOTON ENERGY, Mev
FIGURE Ve
.0001
.00009
.00008
.00007
.00006
.00005
.00004
.00003
.00002
.00001
0
200
250
300
400
500
40 50 60 70 80 90
Ψ, DEGREES
dσ/dΩΨ x 10^25, cm^2/STERADIAN

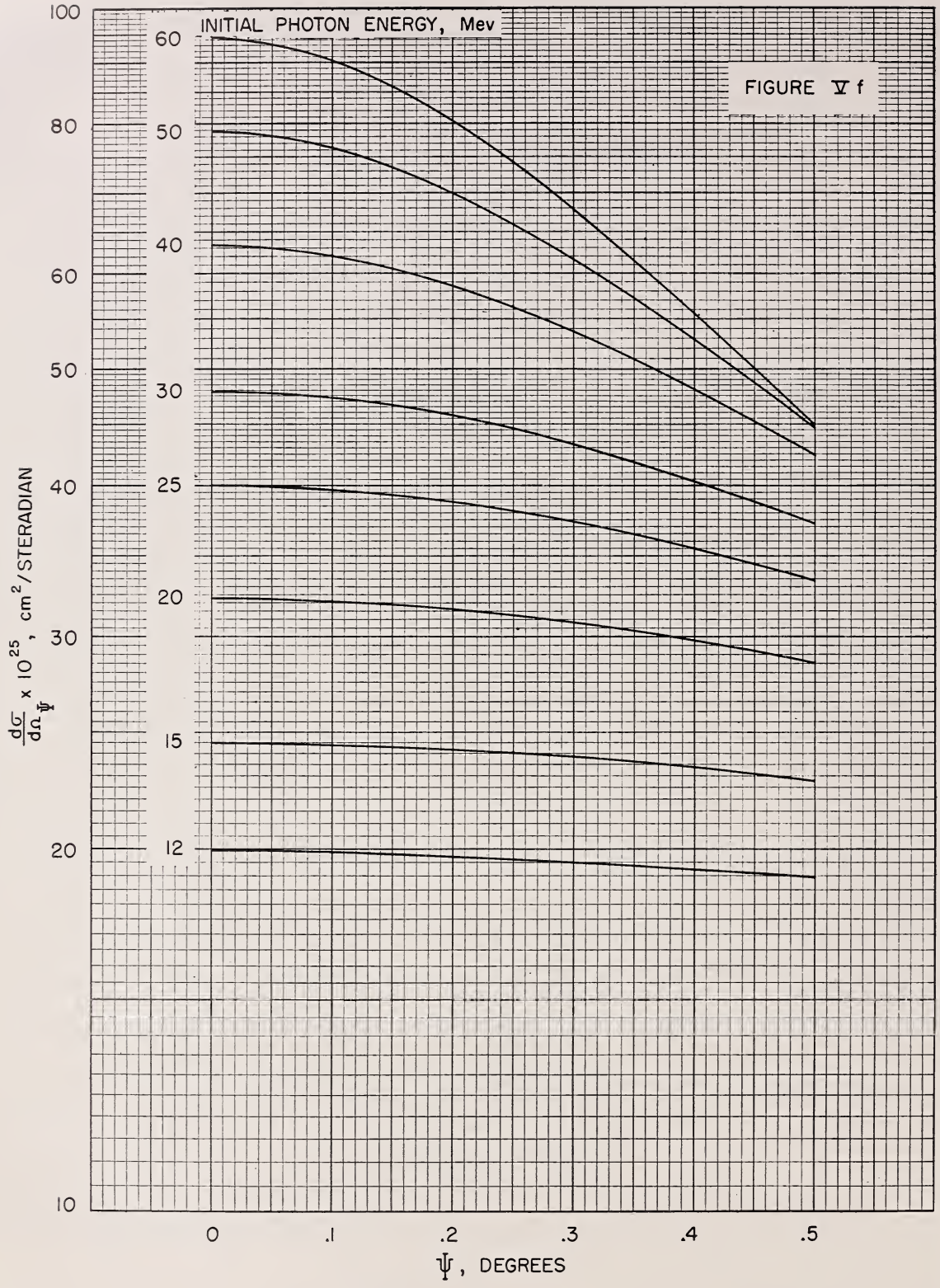
INITIAL PHOTON ENERGY, Mev
60
50
40
30
25
20
15
12
FIGURE V f
100
80
60
50
40
30
20
10
$\frac{d\sigma}{d\Omega_\Psi} \times 10^{25}$, cm^2/STERADIAN
0
.1
.2
.3
.4
.5
Ψ, DEGREES

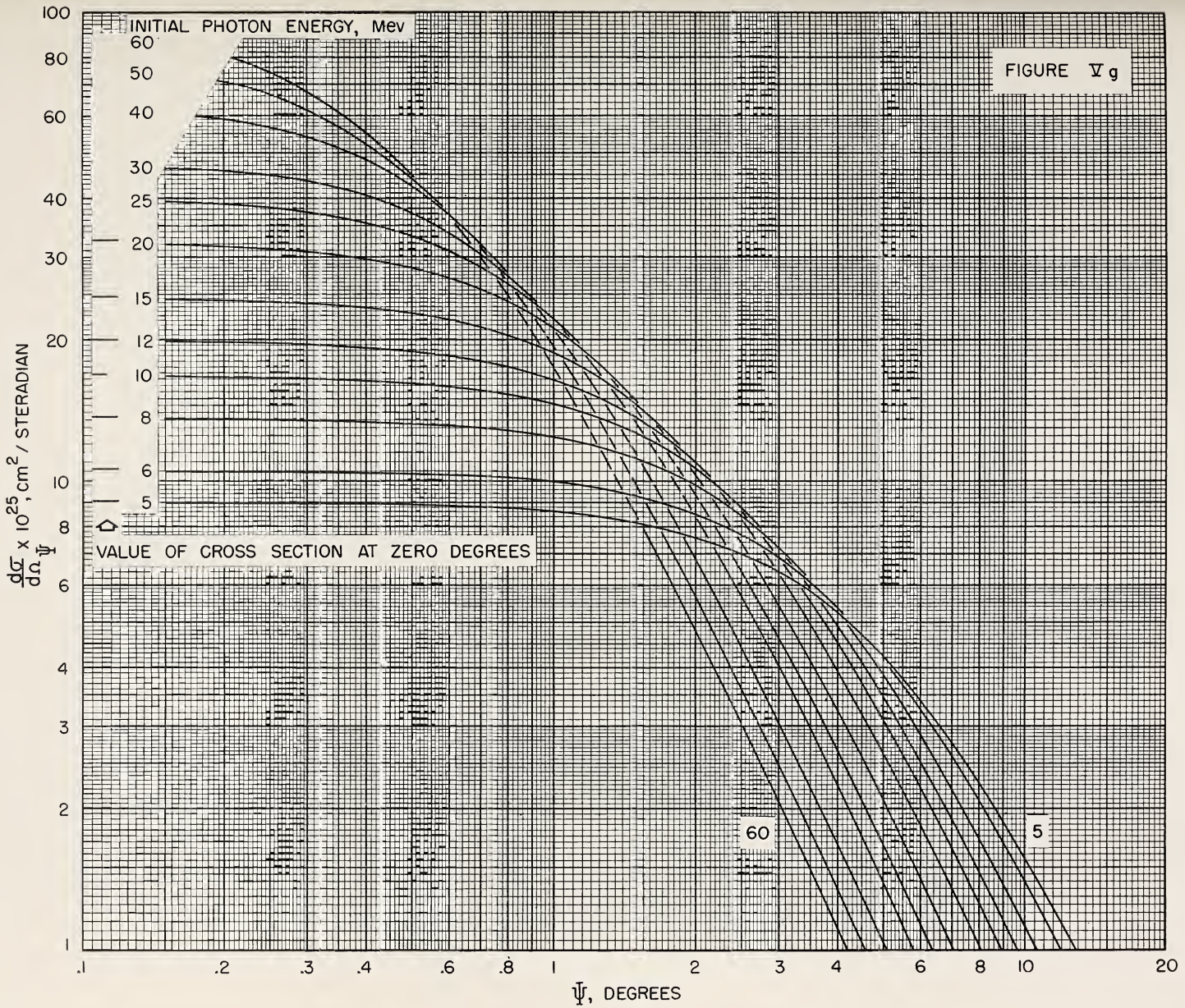
INITIAL PHOTON ENERGY, Mev
60
50
40
30
25
20
15
12
10
8
6
5
VALUE OF CROSS SECTION AT ZERO DEGREES
FIGURE V g
100
80
60
40
30
20
10
8
6
4
3
2
1
$\frac{d\sigma}{d\Omega}_{\Psi}$ x 10^{25}, cm^2 / STERADIAN
.1
.2
.3
.4
.6
.8
1
2
3
4
6
8
10
20
Ψ, DEGREES
60
5

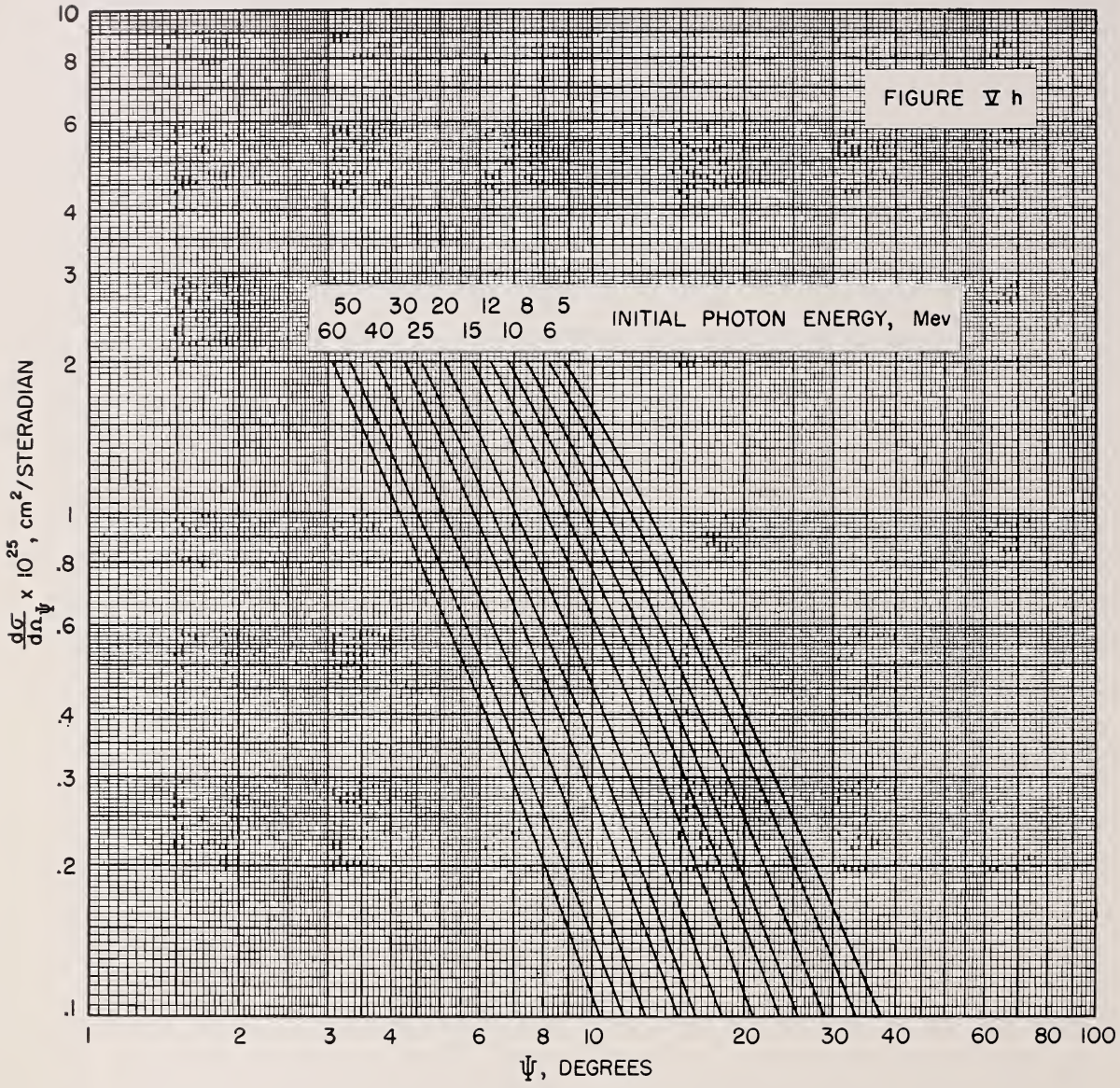
FIGURE V h
50 30 20 12 8 5
60 40 25 15 10 6
INITIAL PHOTON ENERGY, Mev
$\frac{d\sigma}{d\Omega_\Psi} \times 10^{25}$, cm²/STERADIAN
10
8
6
4
3
2
1
.8
.6
.4
.3
.2
.1
1
2
3
4
6
8
10
20
30
40
60
80
100
Ψ, DEGREES

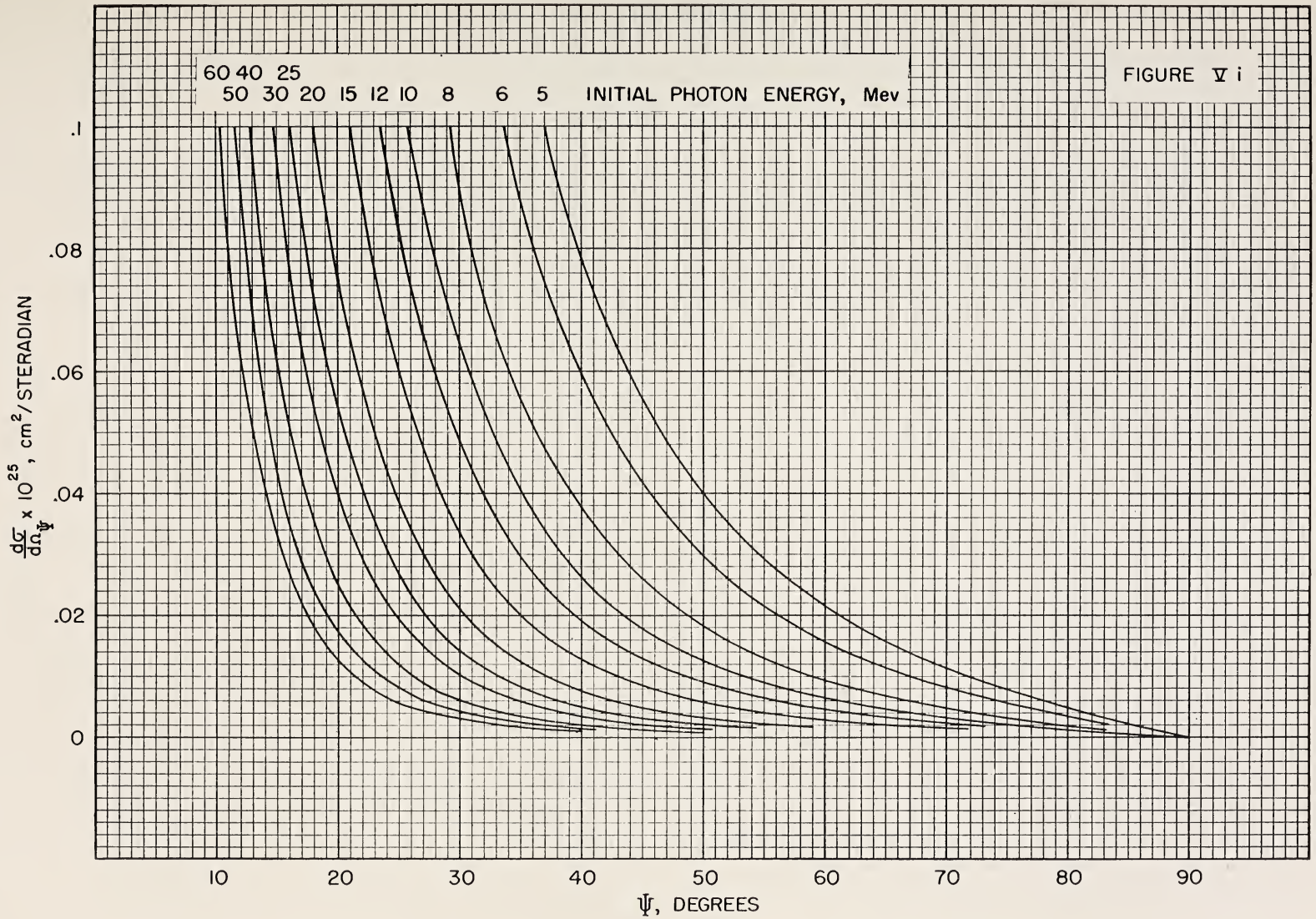
60 40 25
50 30 20 15 12 10 8 6 5 INITIAL PHOTON ENERGY, Mev
FIGURE V i
.1
.08
.06
.04
.02
0
$\frac{d\sigma}{d\Omega_\Psi} \times 10^{25}$, cm^2/ STERADIAN
10
20
30
40
50
60
70
80
90
Ψ, DEGREES

INITIAL PHOTON ENERGY, Mev
60 50 40 30 25 20 15 12 10 8 6 5
$\frac{d\sigma}{d\Omega_\psi} \times 10^{25}$, cm²/STERADIAN
.010
.008
.006
.004
.002
0
10 20 30 40 50 60 70 80 90
ψ, DEGREES

FIGURE XI j

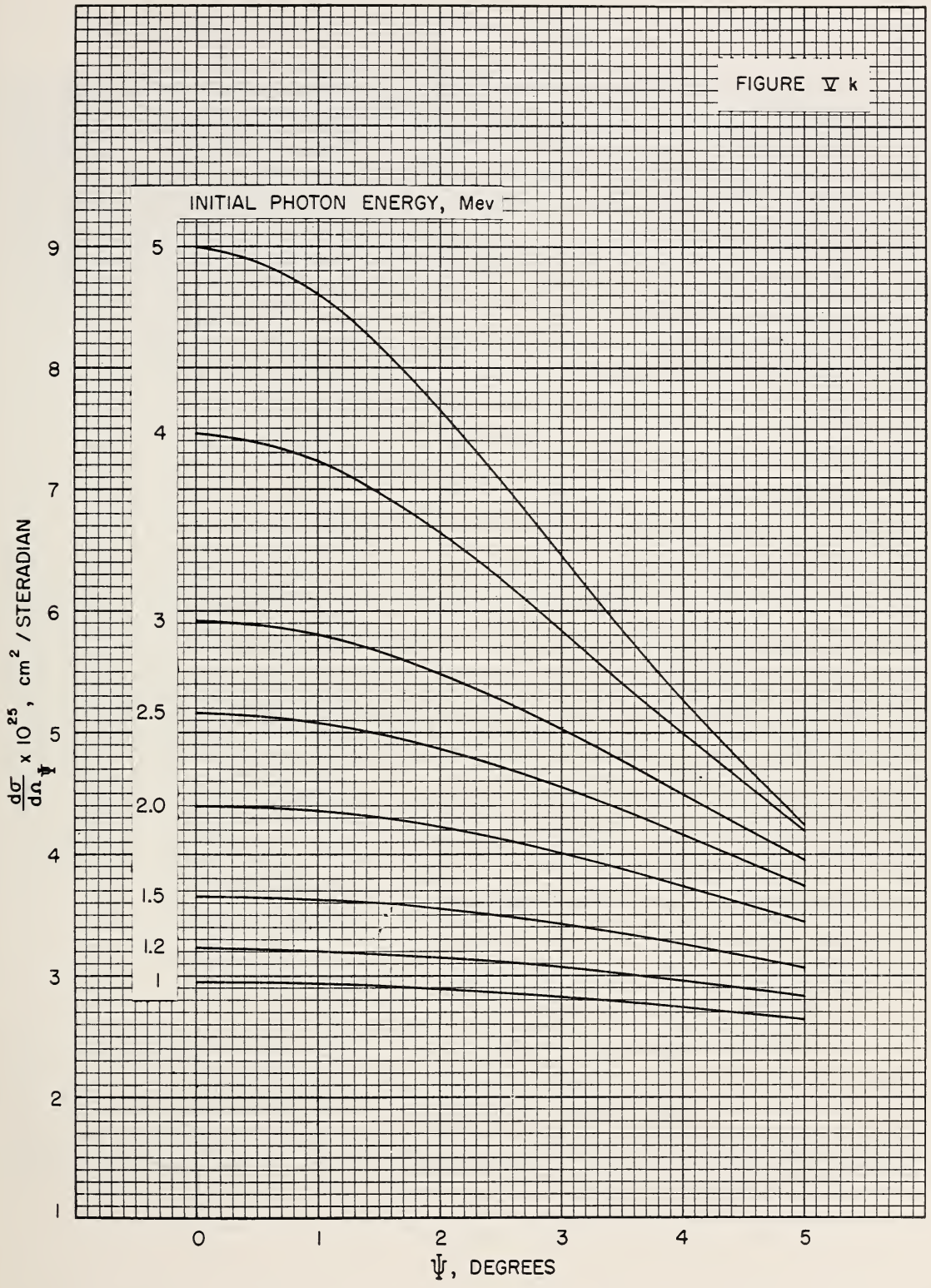
FIGURE V k
INITIAL PHOTON ENERGY, Mev
5
4
3
2.5
2.0
1.5
1.2
1
$\frac{d\sigma}{d\Omega_\Psi} \times 10^{25}$, cm^2 / STERADIAN
9
8
7
6
5
4
3
2
1
0
1
2
3
4
5
Ψ, DEGREES

FIGURE VI I
INITIAL PHOTON ENERGY, Mev
5.0
4.0
3.0
2.5
2.0
1.5
1.2
1.0
VALUE OF CROSS SECTION AT ZERO DEGREES
5.0
1.0
$\frac{d\sigma}{d\Omega_\Psi}$ x 10^{25}, cm^2/STERADIAN
Ψ, DEGREES

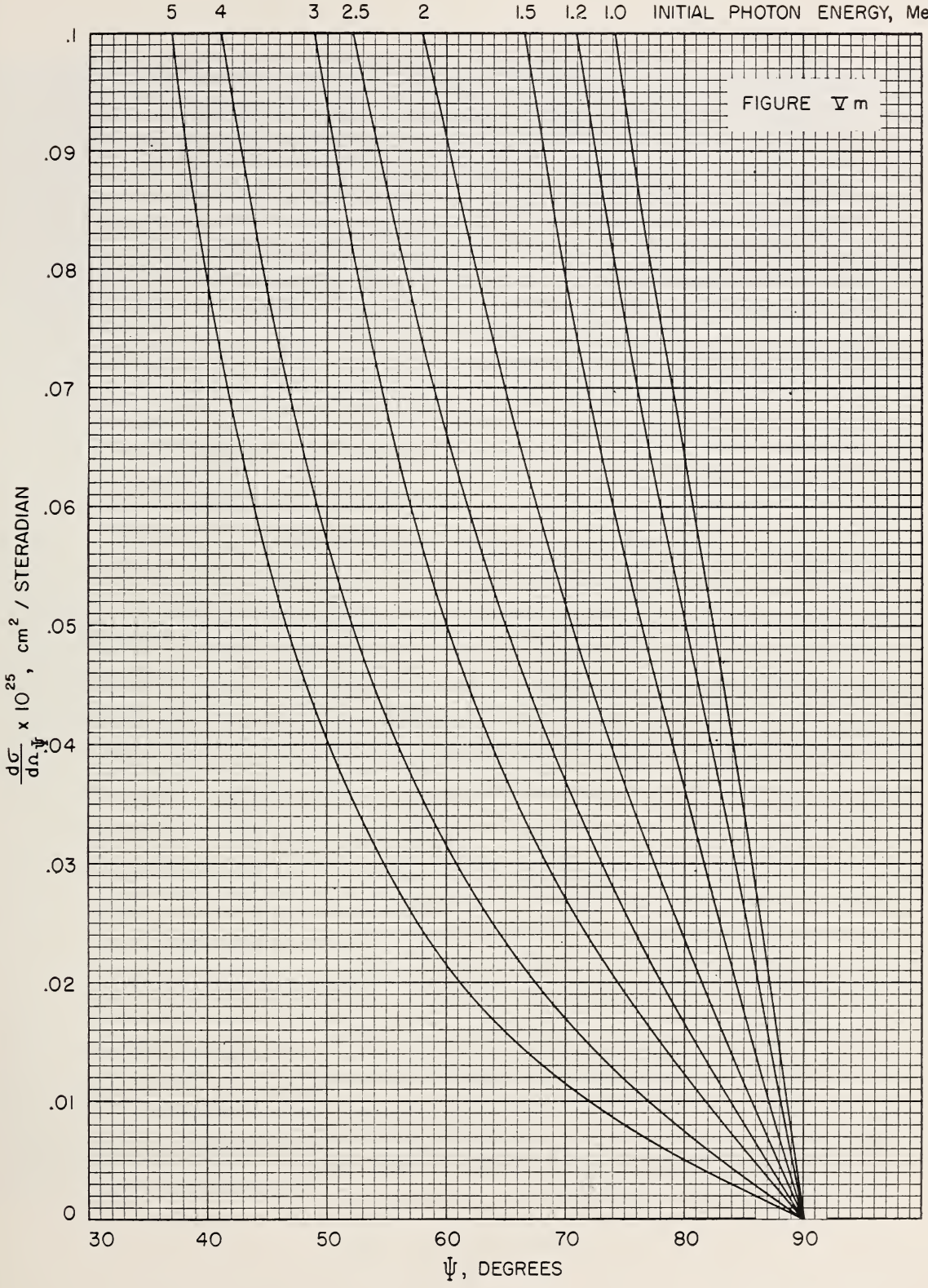
5 4 3 2.5 2 1.5 1.2 1.0 INITIAL PHOTON ENERGY, Mev
FIGURE V m
.1
.09
.08
.07
.06
.05
.04
.03
.02
.01
0
$\frac{d\sigma}{d\Omega_\Psi} \times 10^{25}$, cm^2 / STERADIAN
30 40 50 60 70 80 90
Ψ, DEGREES

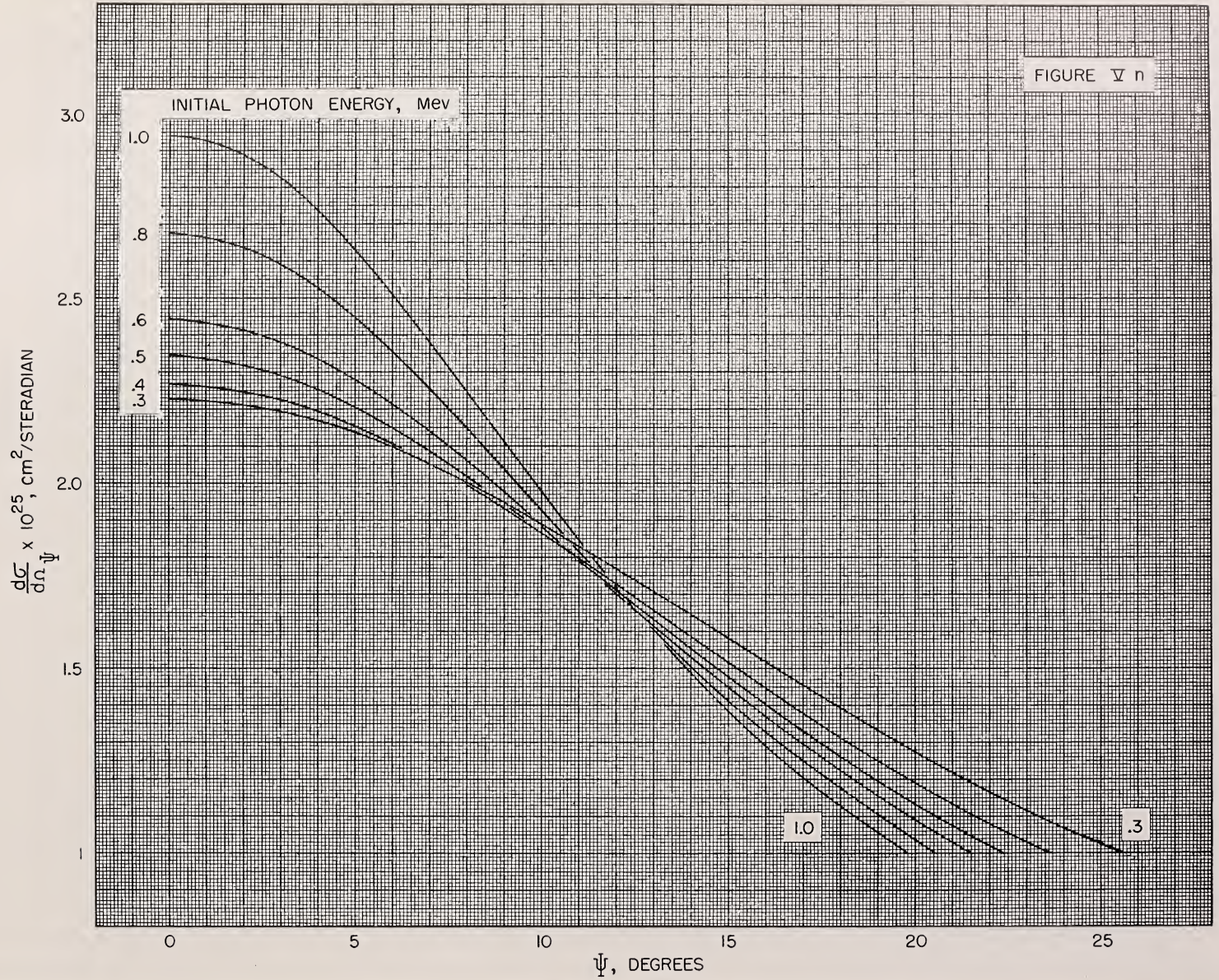
FIGURE V n
INITIAL PHOTON ENERGY, Mev
1.0
.8
.6
.5
.4
.3
3.0
2.5
2.0
1.5
1
$\frac{d\sigma}{d\Omega_\Psi} \times 10^{25}$, cm^2/STERADIAN
0
5
10
15
20
25
Ψ, DEGREES
1.0
.3

FIGURE V o
1.0 .8 .6 .5 .4 .3 INITIAL PHOTON ENERGY, Mev
$\frac{d\sigma}{d\Omega_\Psi} \times 10^{25}$, cm^2/STERADIAN
0 .1 .2 .3 .4 .5 .6 .7 .8 .9 1.0
15 20 25 30 35 40 45 50 55 60 65 70 75 80 85 90
Ψ, DEGREES

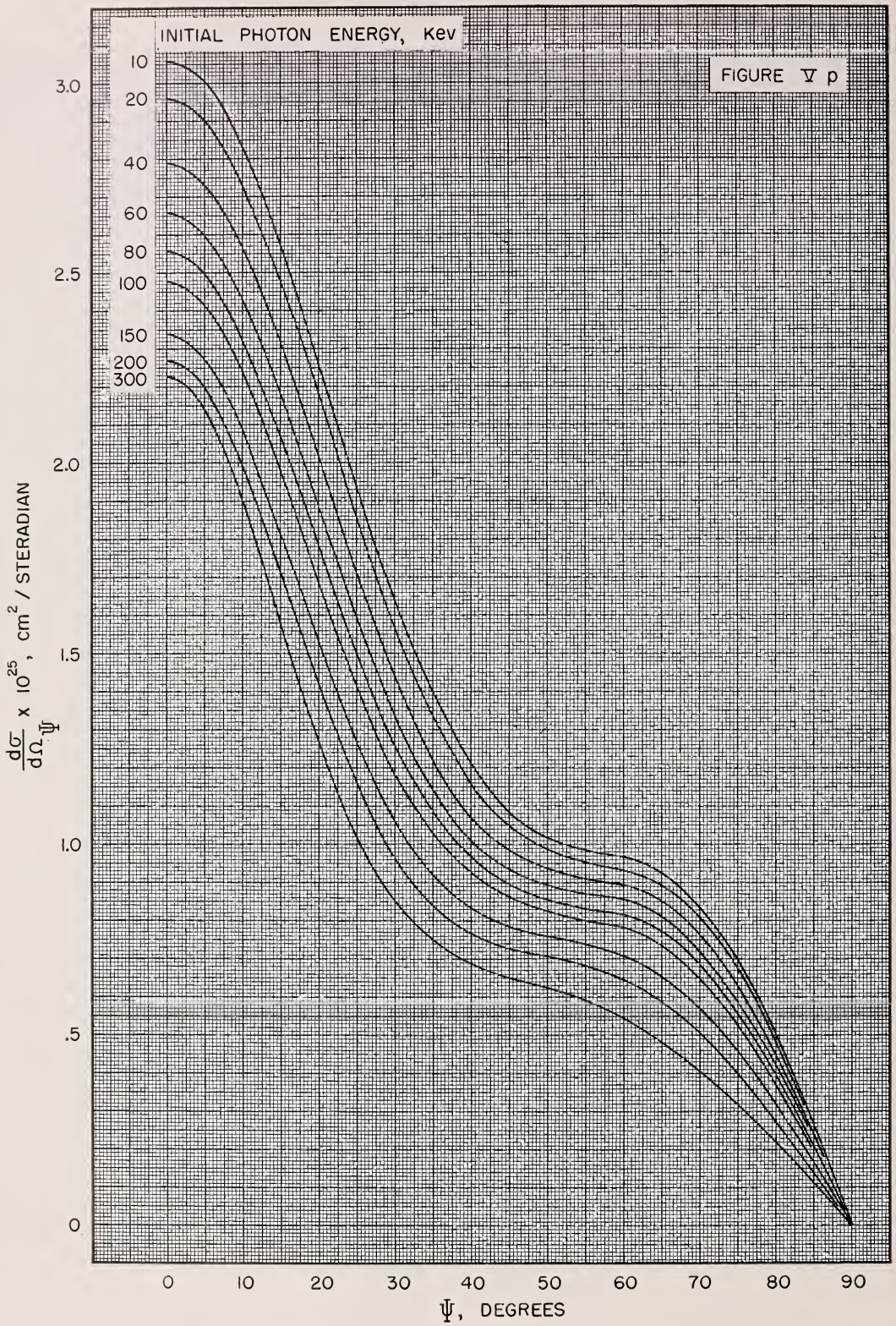
INITIAL PHOTON ENERGY, Kev
10
20
40
60
80
100
150
200
300
FIGURE ∇ p
3.0
2.5
2.0
1.5
1.0
.5
0
$\frac{d\sigma}{d\Omega_\Psi}$ x 10^{25}, cm^2 / STERADIAN
0
10
20
30
40
50
60
70
80
90
Ψ, DEGREES

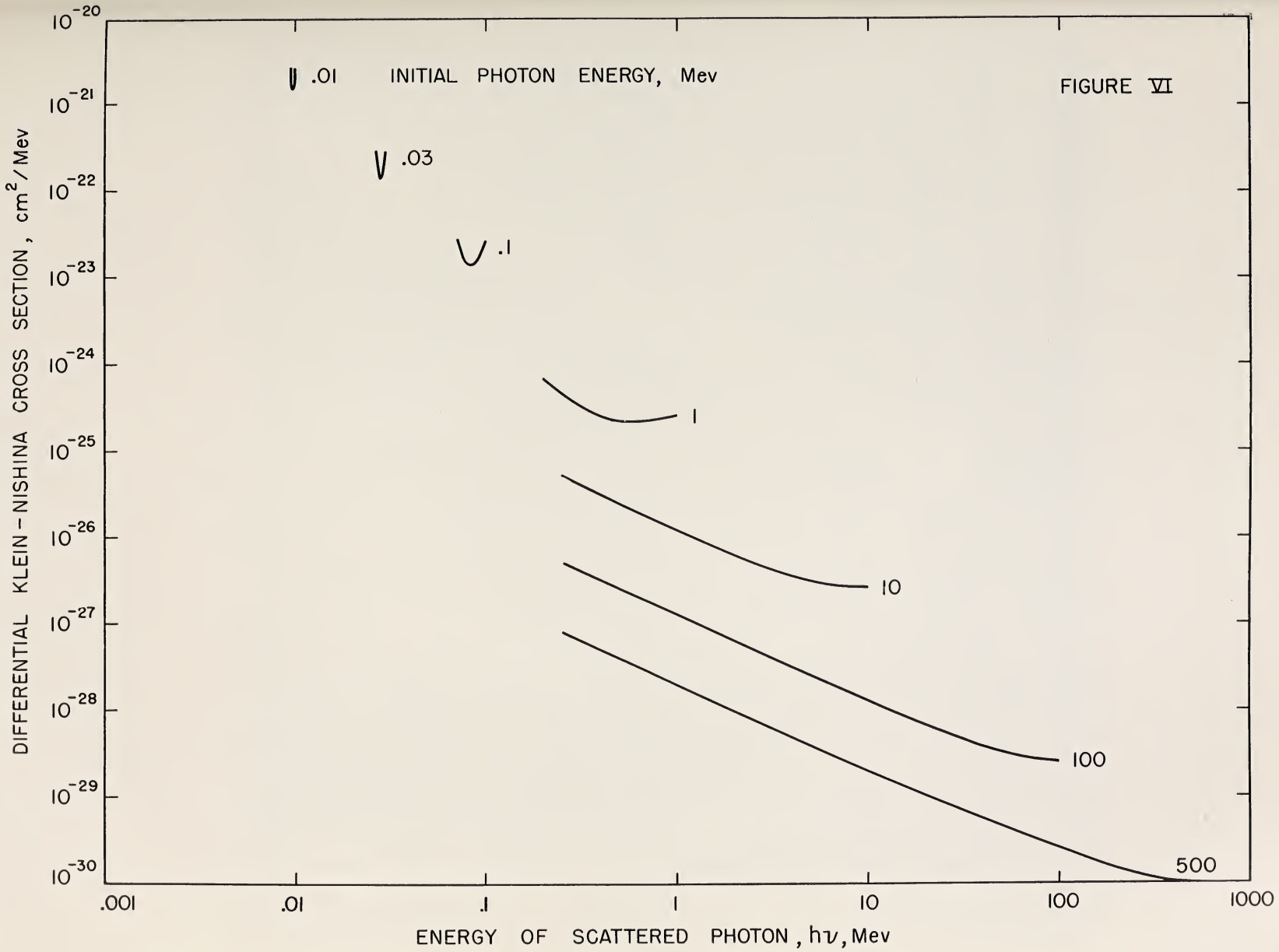
.01
INITIAL PHOTON ENERGY, Mev
.03
.1
1
10
100
500
DIFFERENTIAL KLEIN-NISHINA CROSS SECTION, cm²/Mev
ENERGY OF SCATTERED PHOTON, hν, Mev
10⁻²⁰
10⁻²¹
10⁻²²
10⁻²³
10⁻²⁴
10⁻²⁵
10⁻²⁶
10⁻²⁷
10⁻²⁸
10⁻²⁹
10⁻³⁰
.001
.01
.1
1
10
100
1000

FIGURE VI

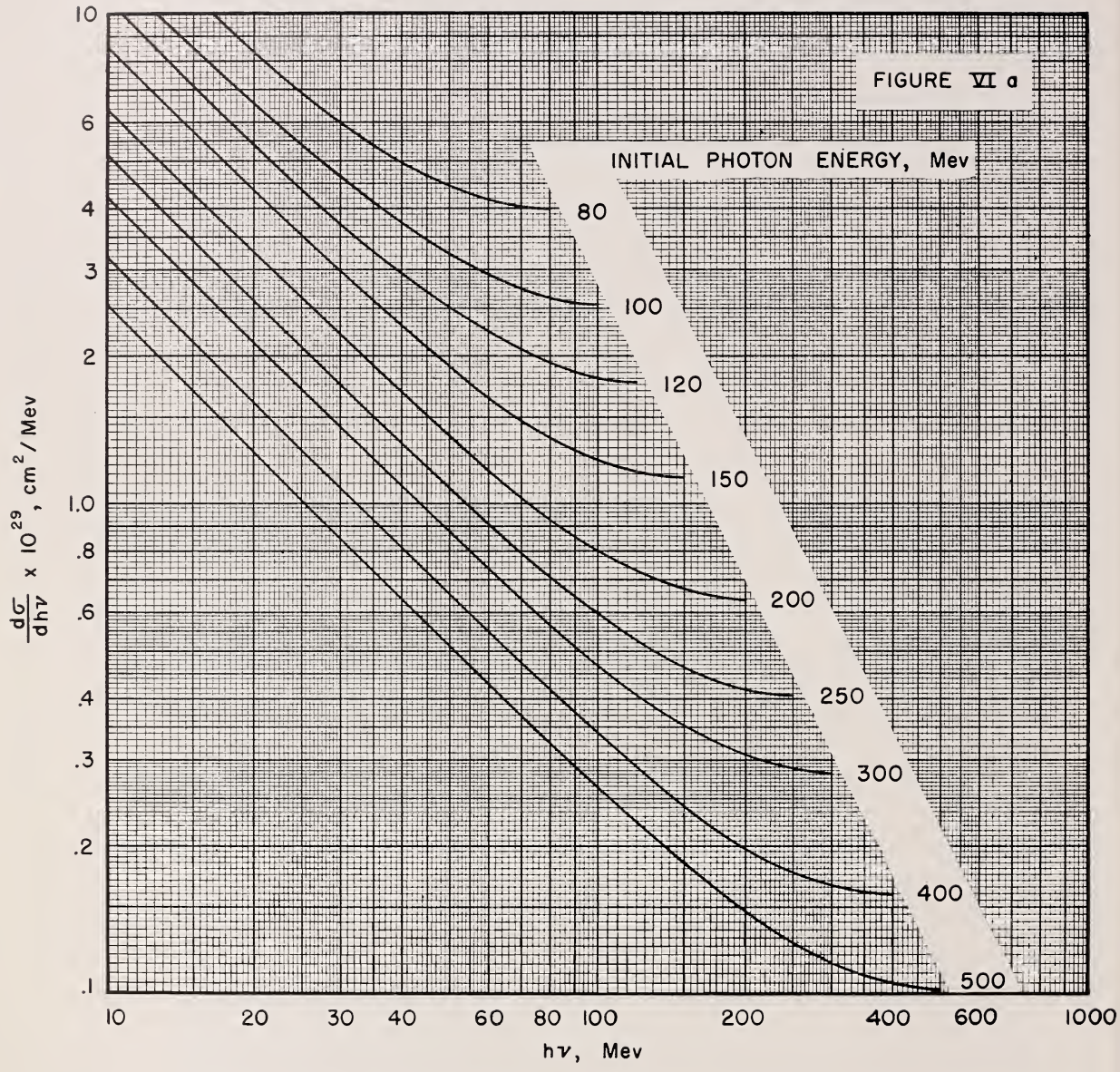
FIGURE VI a
INITIAL PHOTON ENERGY, Mev
80
100
120
150
200
250
300
400
500
10
6
4
3
2
1.0
.8
.6
.4
.3
.2
.1
$\frac{d\sigma}{dh\nu}$ x 10^{29}, cm^2 / Mev
10
20
30
40
60
80
100
200
400
600
1000
$h\nu$, Mev

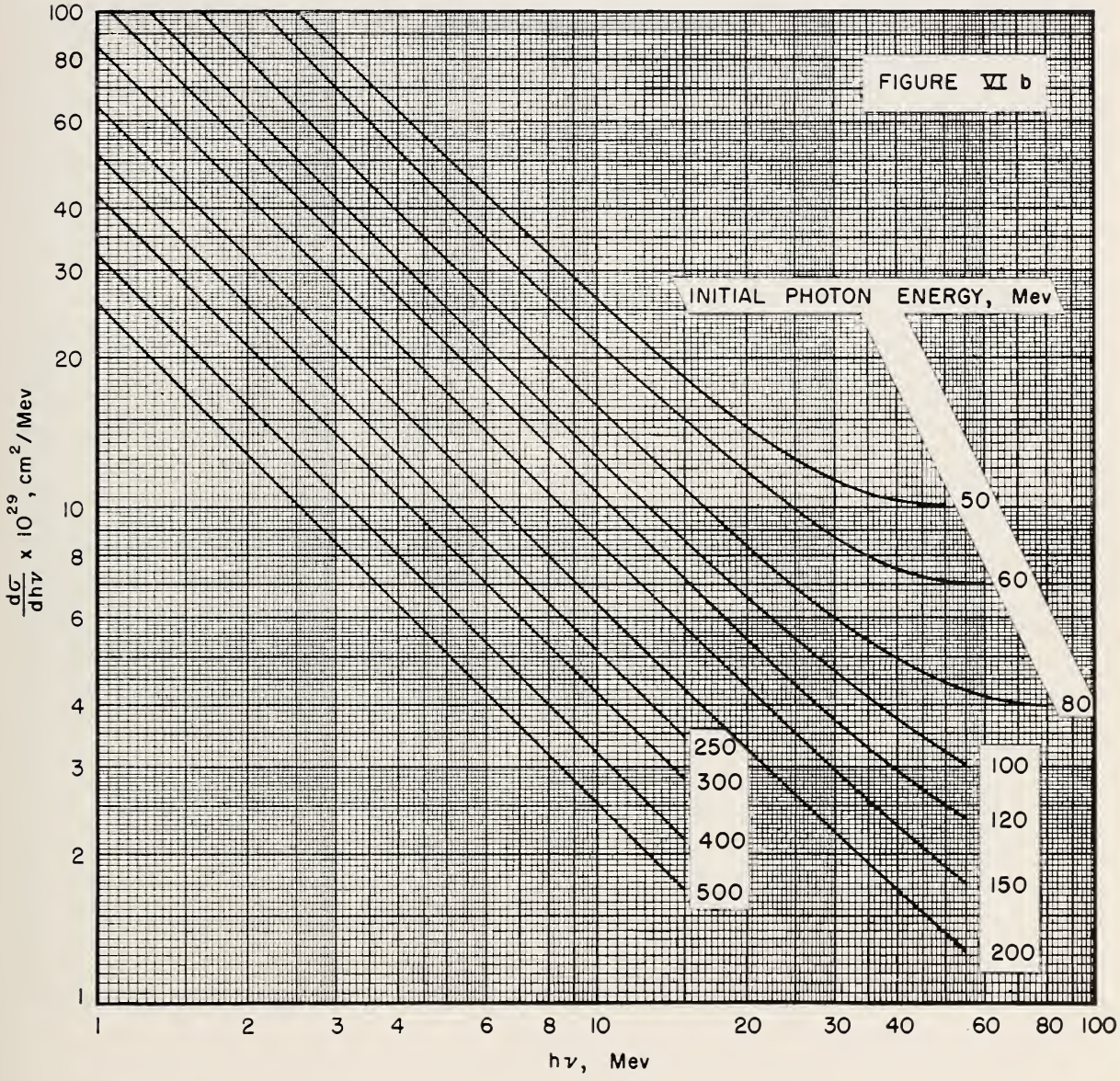
FIGURE VI b
INITIAL PHOTON ENERGY, Mev
50
60
80
100
120
150
200
250
300
400
500
$\frac{d\sigma}{dh\nu} \times 10^{29}$, cm^2/Mev
100
80
60
40
30
20
10
8
6
4
3
2
1
1
2
3
4
6
8
10
20
30
40
60
80
100
$h\nu$, Mev

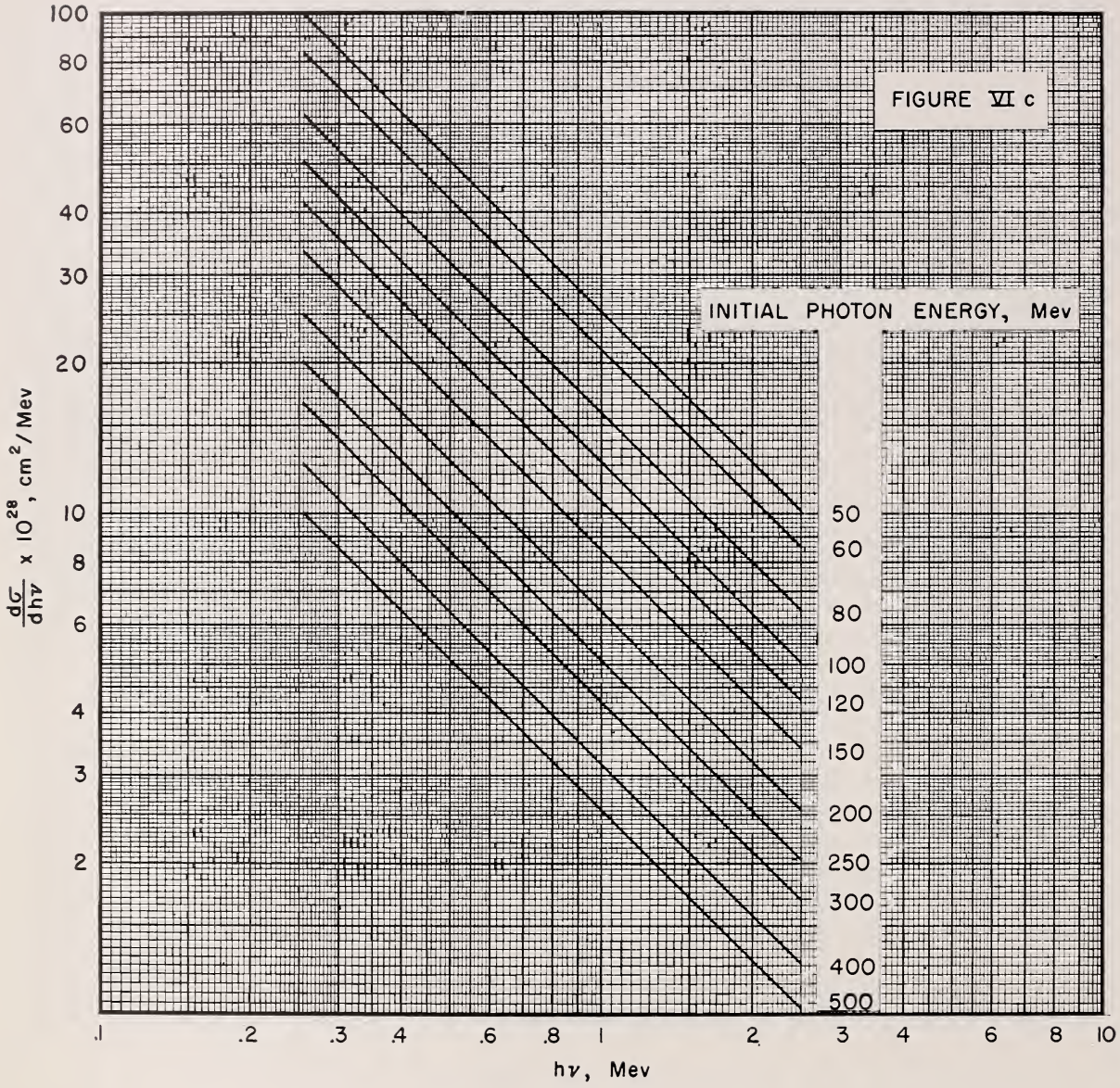
FIGURE VI c
INITIAL PHOTON ENERGY, Mev
50
60
80
100
120
150
200
250
300
400
500
100
80
60
40
30
20
10
8
6
4
3
2
.1
.2
.3
.4
.6
.8
1
2
3
4
6
8
10
hν, Mev
dσ/dhν x 10^28, cm^2/Mev

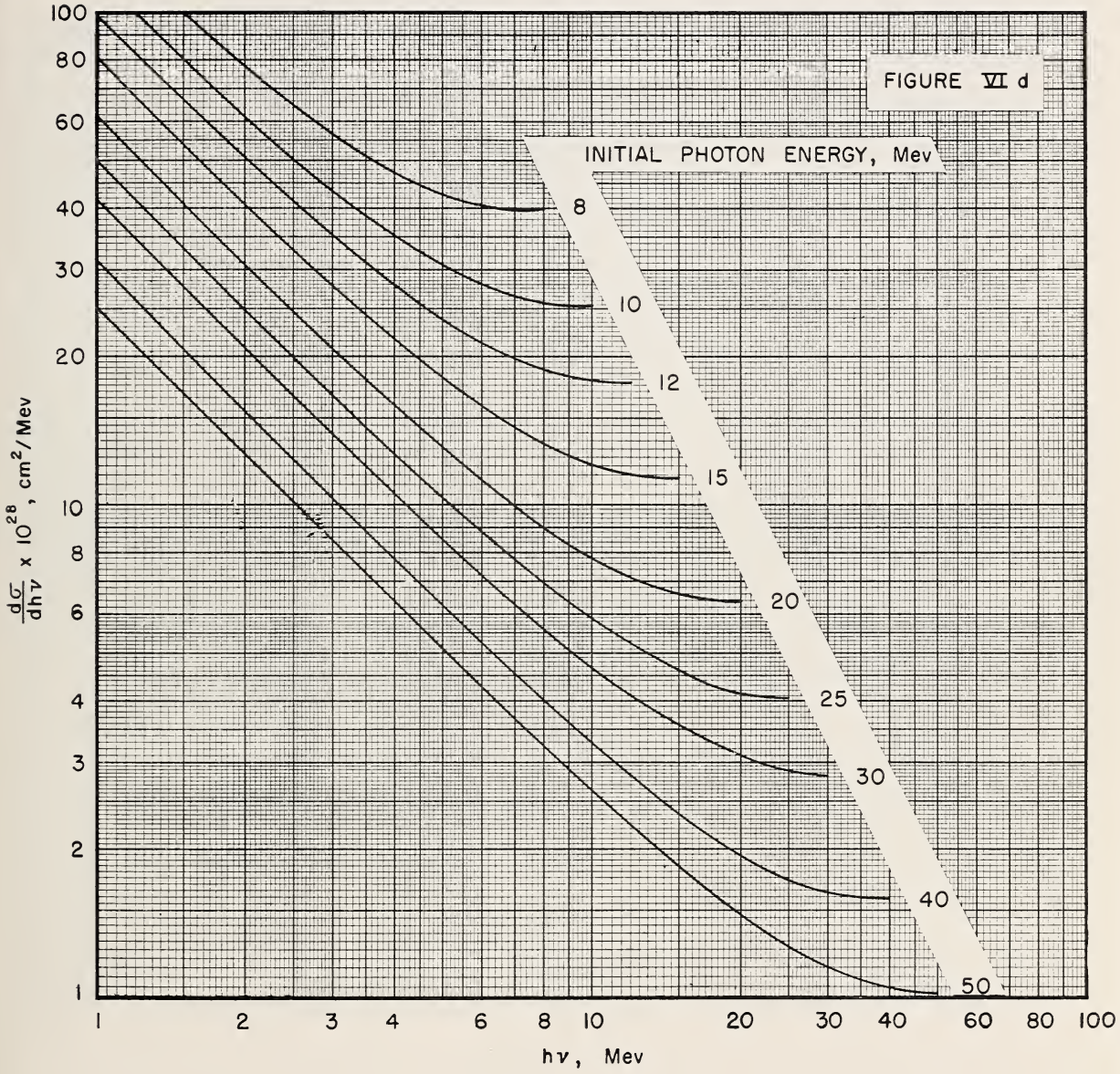
FIGURE VI d
INITIAL PHOTON ENERGY, Mev
8
10
12
15
20
25
30
40
50
100
80
60
40
30
20
10
8
6
4
3
2
1
1
2
3
4
6
8
10
20
30
40
60
80
100
hν, Mev
dσ/dhν x 10^28, cm^2/Mev

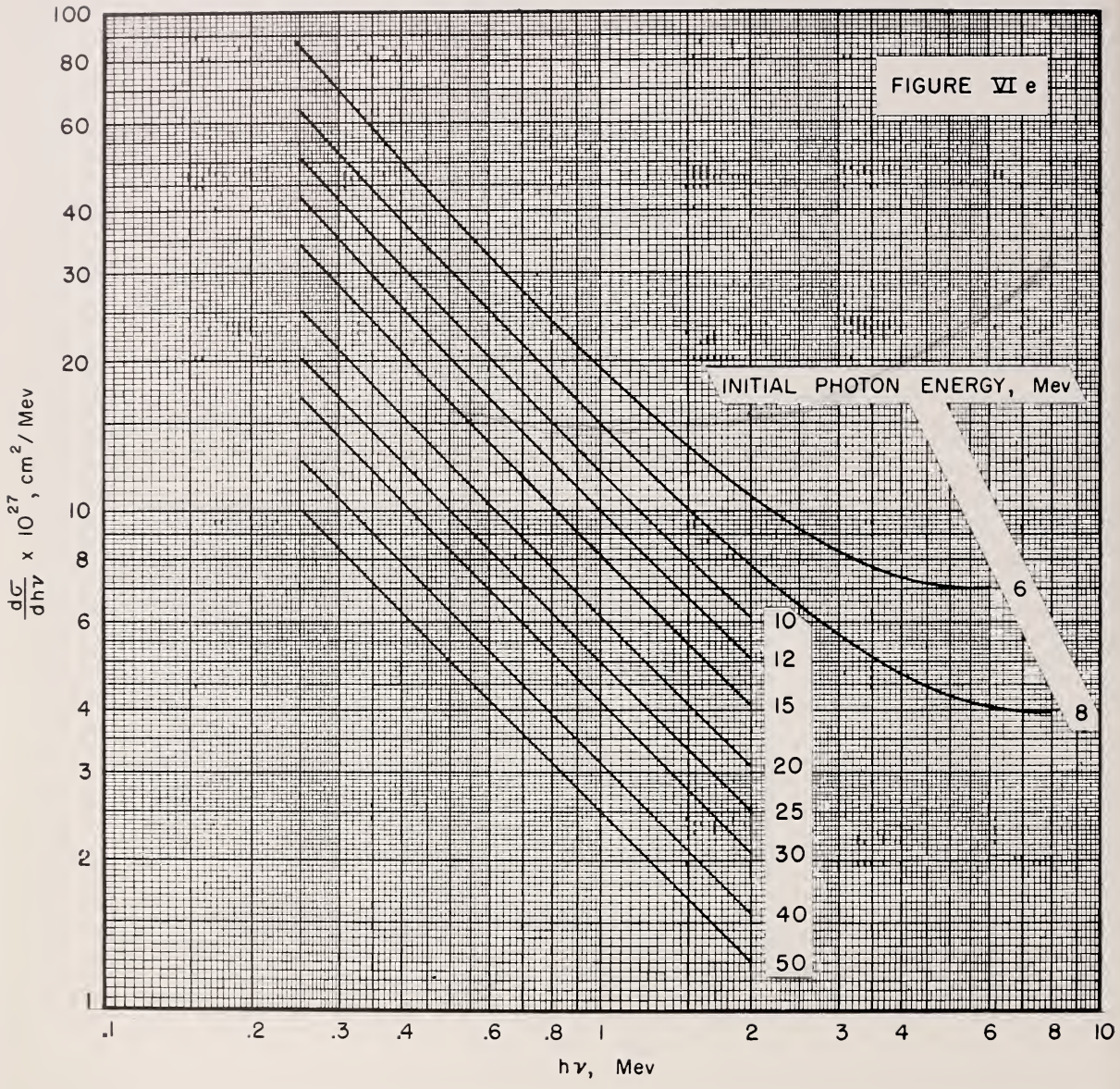
FIGURE VI e
INITIAL PHOTON ENERGY, Mev
6
8
10
12
15
20
25
30
40
50
100
80
60
40
30
20
10
8
6
4
3
2
1
.1
.2
.3
.4
.6
.8
1
2
3
4
6
8
10
hν, Mev
dσ/dhν x 10^27, cm^2/Mev

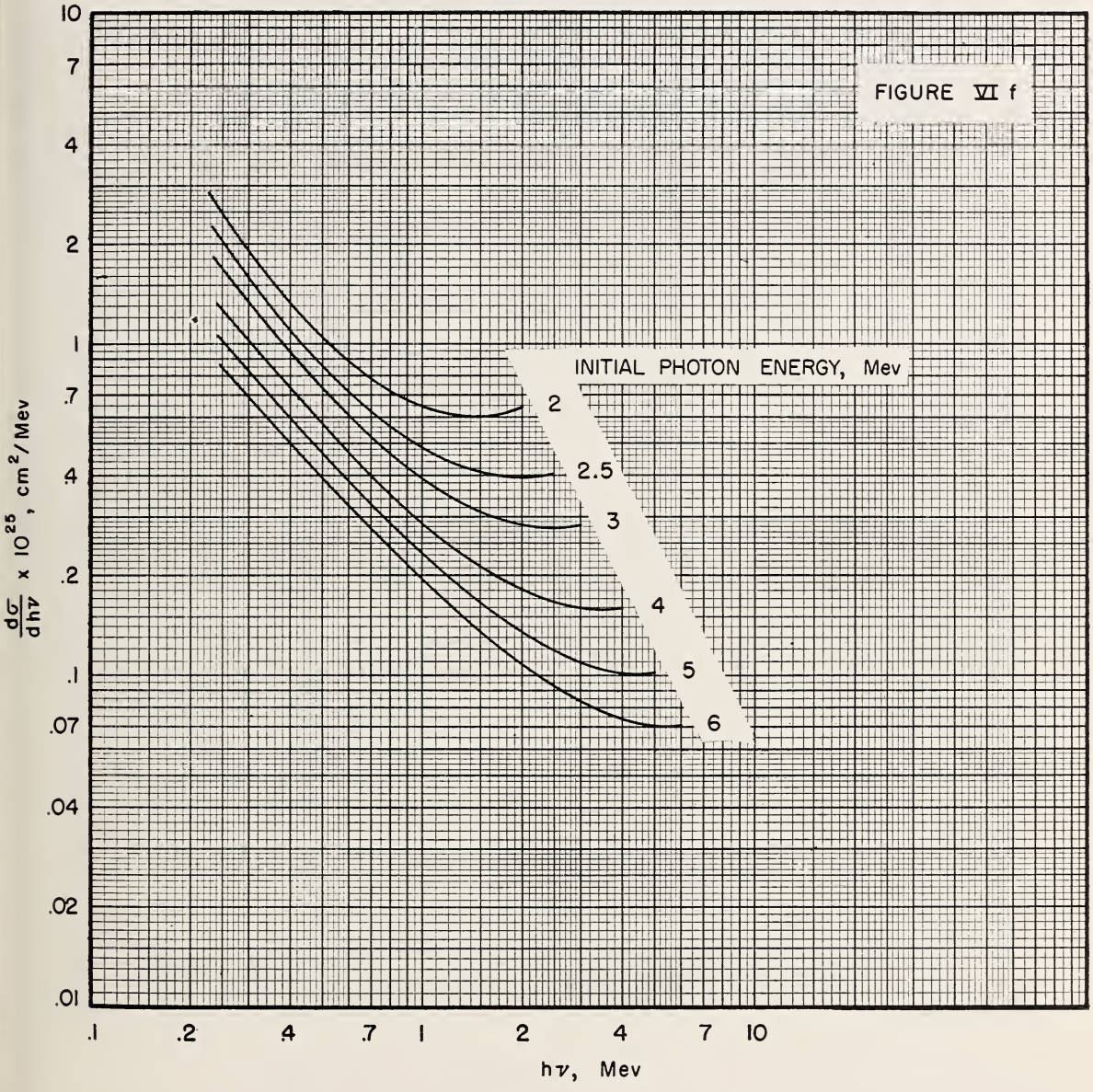
FIGURE VI f
INITIAL PHOTON ENERGY, Mev
2
2.5
3
4
5
6
10
7
4
2
1
.7
.4
.2
.1
.07
.04
.02
.01
.1
.2
.4
.7
1
2
4
7
10
hν, Mev
dσ/dhν x 10^25, cm^2/Mev

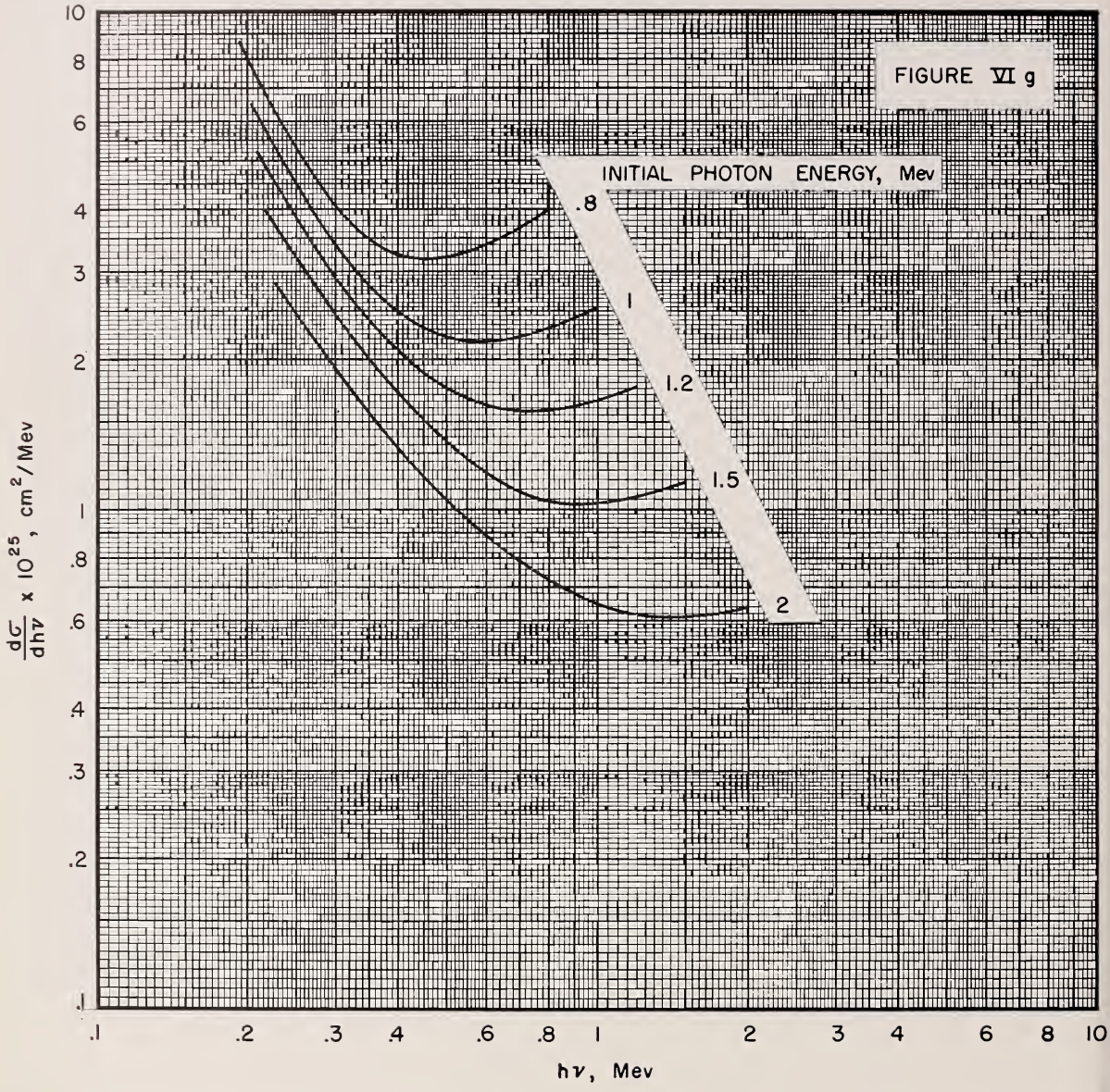
FIGURE VI g
INITIAL PHOTON ENERGY, Mev
.8
1
1.2
1.5
2
$\frac{d\sigma}{dh\nu} \times 10^{25}$, cm^2/Mev
10
8
6
4
3
2
1
.8
.6
.4
.3
.2
.1
.1
.2
.3
.4
.6
.8
1
2
3
4
6
8
10
$h\nu$, Mev

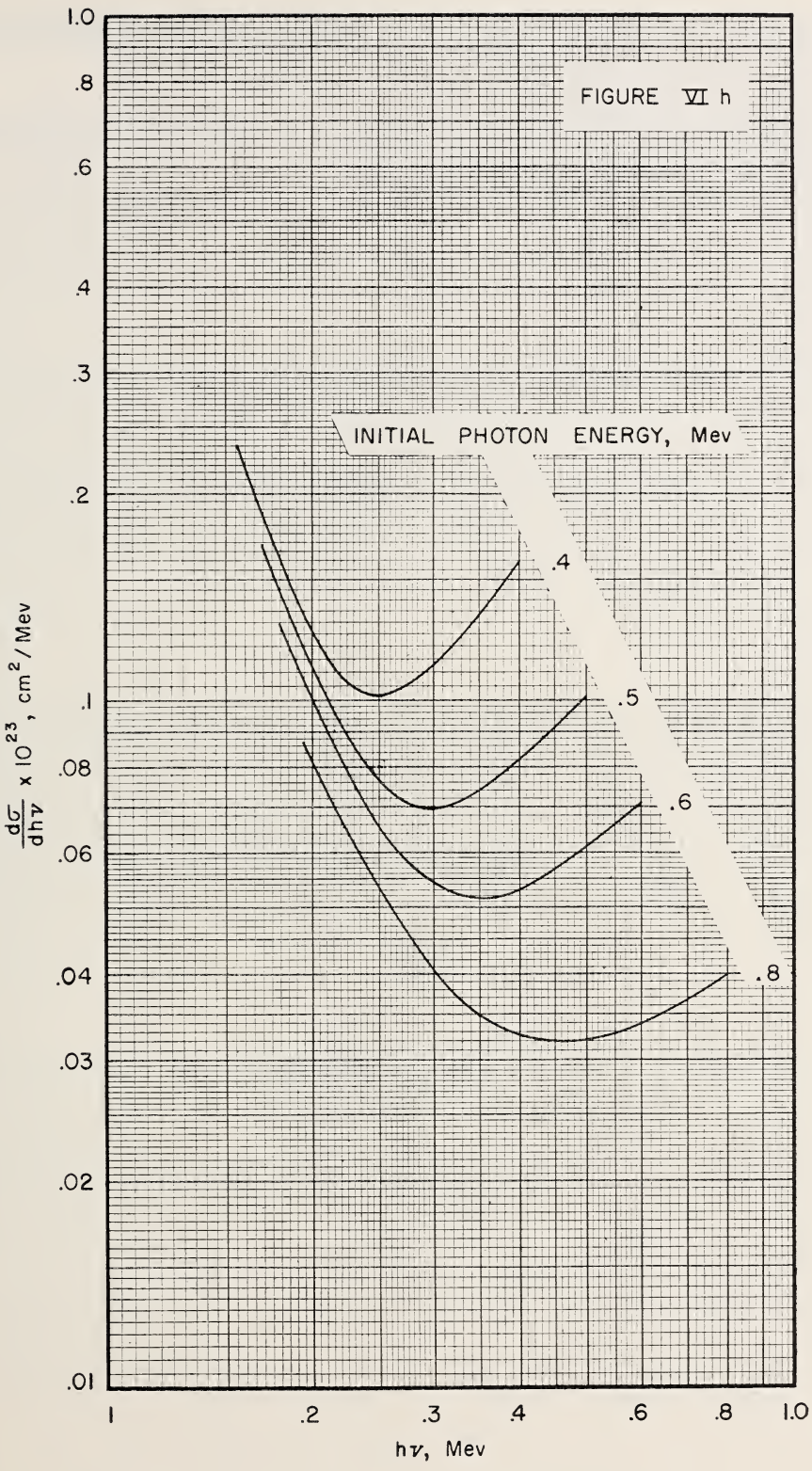
FIGURE VI h
INITIAL PHOTON ENERGY, Mev
.4
.5
.6
.8
1.0
.8
.6
.4
.3
.2
.1
.08
.06
.04
.03
.02
.01
1
.2
.3
.4
.6
.8
1.0
$\frac{d\sigma}{dh\nu} \times 10^{23}$, cm^2/Mev
$h\nu$, Mev

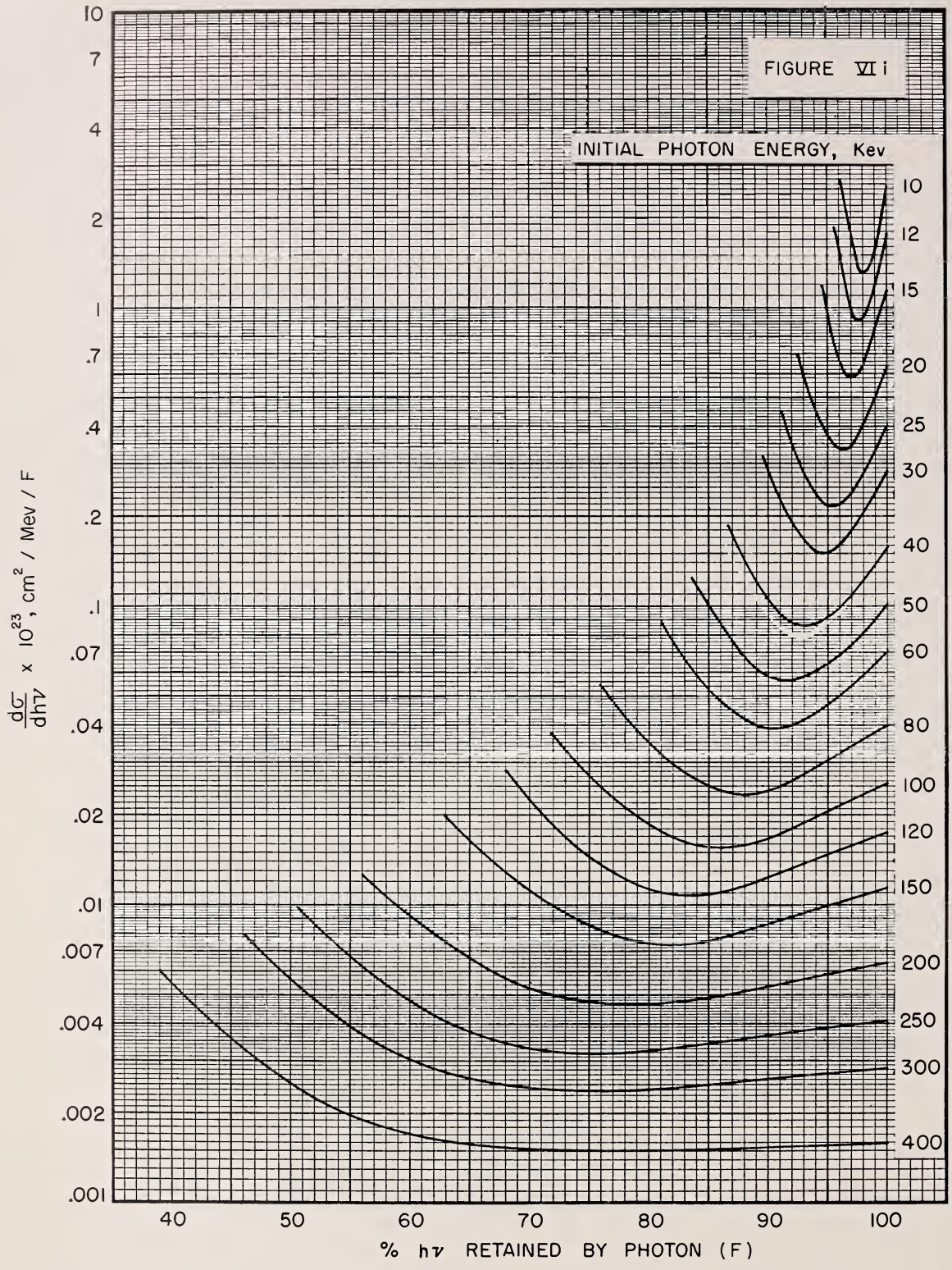
FIGURE VII
INITIAL PHOTON ENERGY, Kev
10
12
15
20
25
30
40
50
60
80
100
120
150
200
250
300
400
$\frac{d\sigma}{dh\nu}$ x 10^{23}, cm^2 / Mev / F
10
7
4
2
1
.7
.4
.2
.1
.07
.04
.02
.01
.007
.004
.002
.001
40
50
60
70
80
90
100
% $h\nu$ RETAINED BY PHOTON (F)

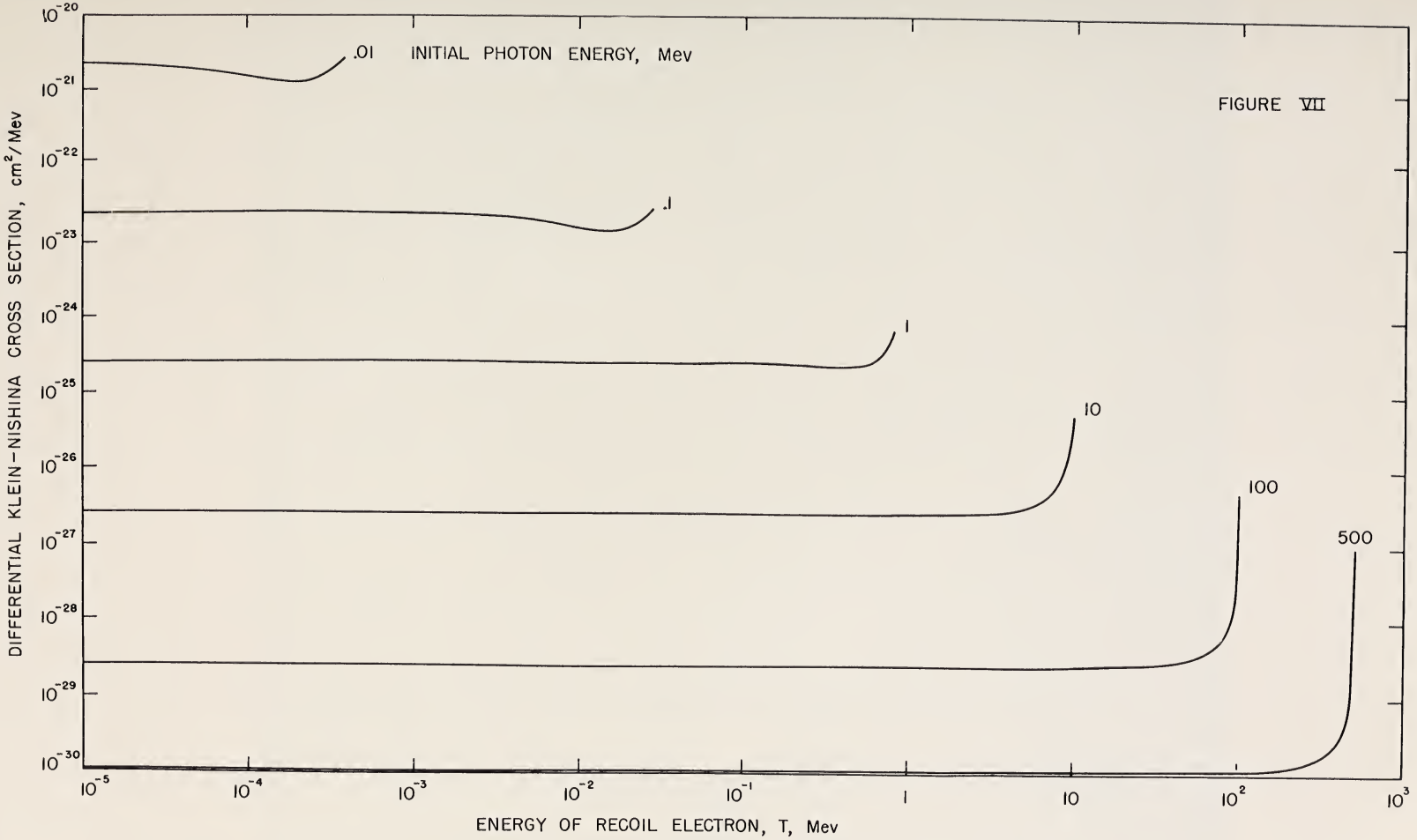
FIGURE VII
INITIAL PHOTON ENERGY, Mev
.01
.1
1
10
100
500
DIFFERENTIAL KLEIN-NISHINA CROSS SECTION, cm²/Mev
ENERGY OF RECOIL ELECTRON, T, Mev
10⁻²⁰
10⁻²¹
10⁻²²
10⁻²³
10⁻²⁴
10⁻²⁵
10⁻²⁶
10⁻²⁷
10⁻²⁸
10⁻²⁹
10⁻³⁰
10⁻⁵
10⁻⁴
10⁻³
10⁻²
10⁻¹
1
10
10²
10³

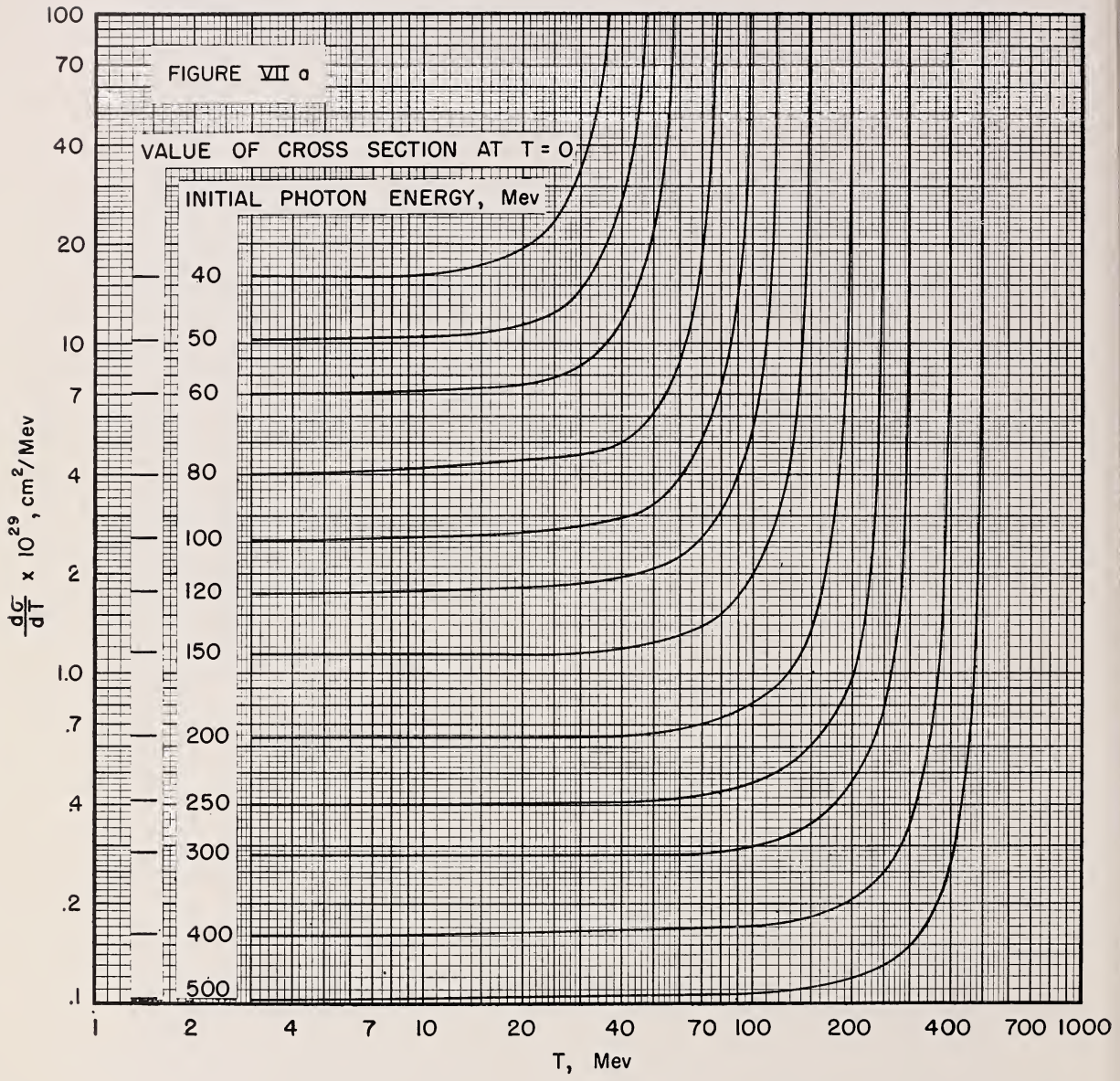
FIGURE VII a
VALUE OF CROSS SECTION AT T = 0
INITIAL PHOTON ENERGY, Mev
40
50
60
80
100
120
150
200
250
300
400
500
100
70
40
20
10
7
4
2
1.0
.7
.4
.2
.1
$\frac{d\sigma}{dT} \times 10^{29}$, cm^2/Mev
1
2
4
7
10
20
40
70
100
200
400
700
1000
T, Mev

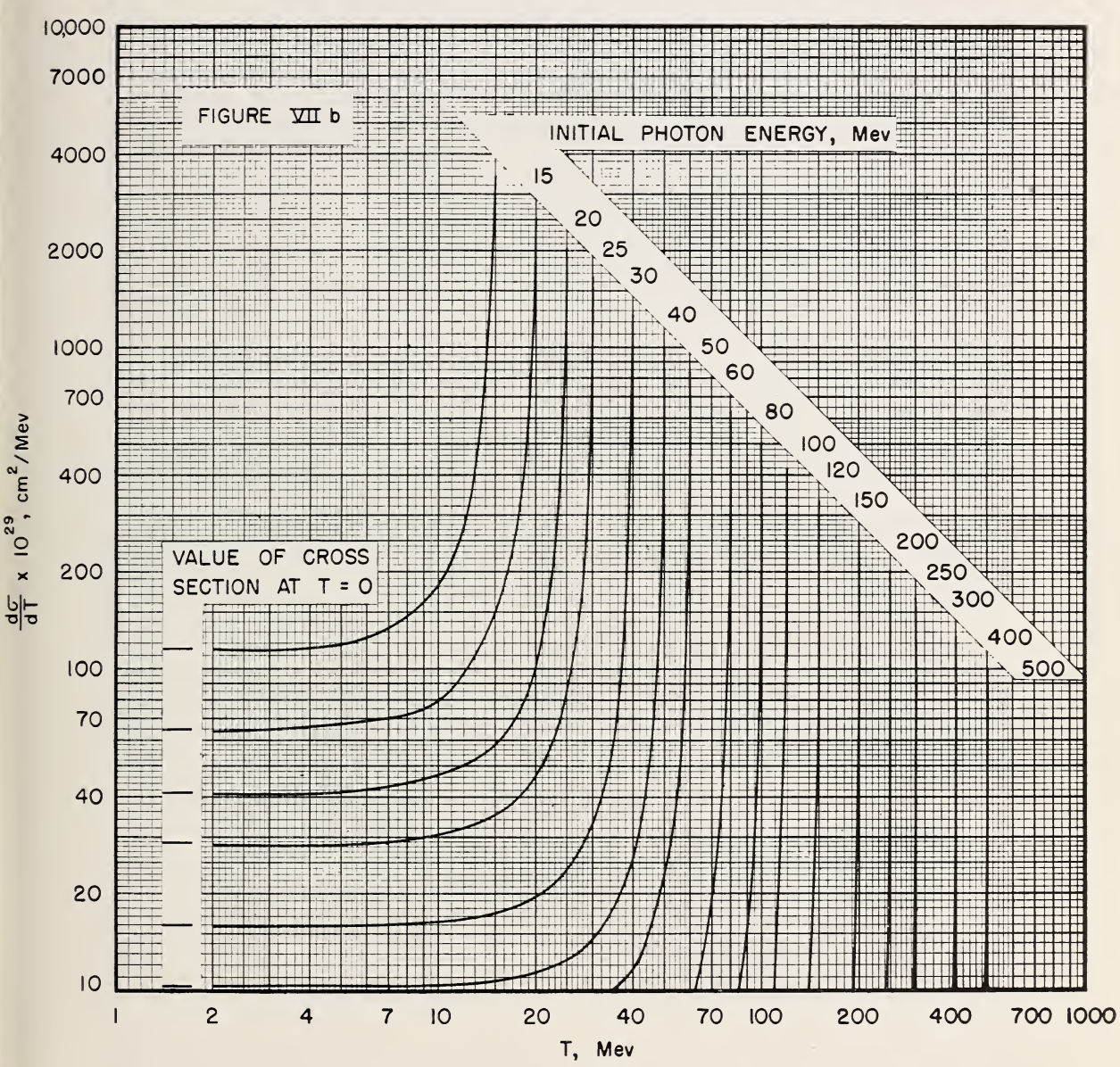
FIGURE VII b
INITIAL PHOTON ENERGY, Mev
15
20
25
30
40
50
60
80
100
120
150
200
250
300
400
500
VALUE OF CROSS SECTION AT T = 0
$\frac{d\sigma}{dT} \times 10^{29}$, cm^2/Mev
10,000
7000
4000
2000
1000
700
400
200
100
70
40
20
10
1
2
4
7
10
20
40
70
100
200
400
700
1000
T, Mev

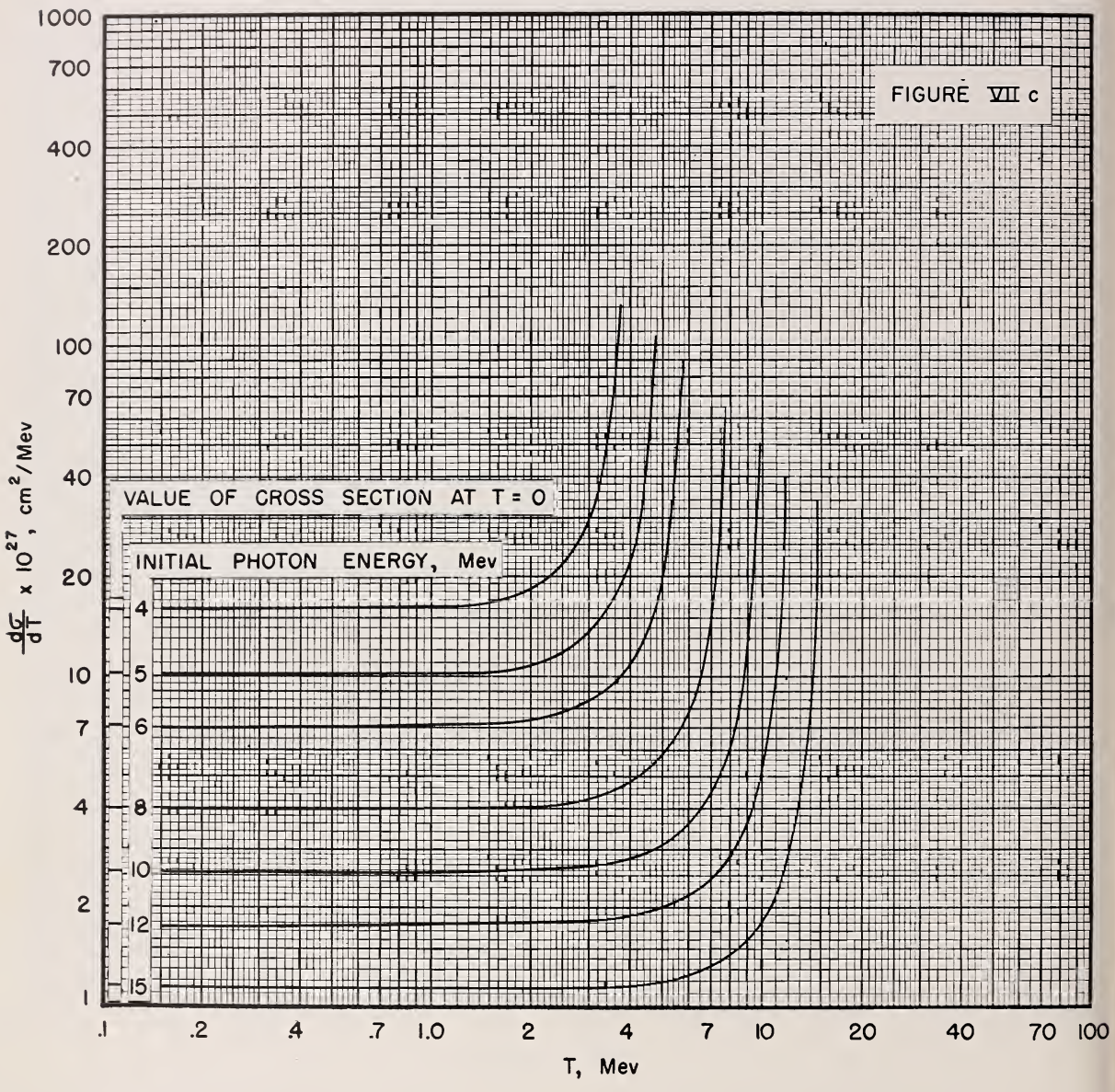
FIGURE VII c
1000
700
400
200
100
70
40
20
10
7
4
2
1
$\frac{d\sigma}{dT} \times 10^{27}$, cm^2/Mev
VALUE OF CROSS SECTION AT T = 0
INITIAL PHOTON ENERGY, Mev
4
5
6
8
10
12
15
.1
.2
.4
.7
1.0
2
4
7
10
20
40
70
100
T, Mev

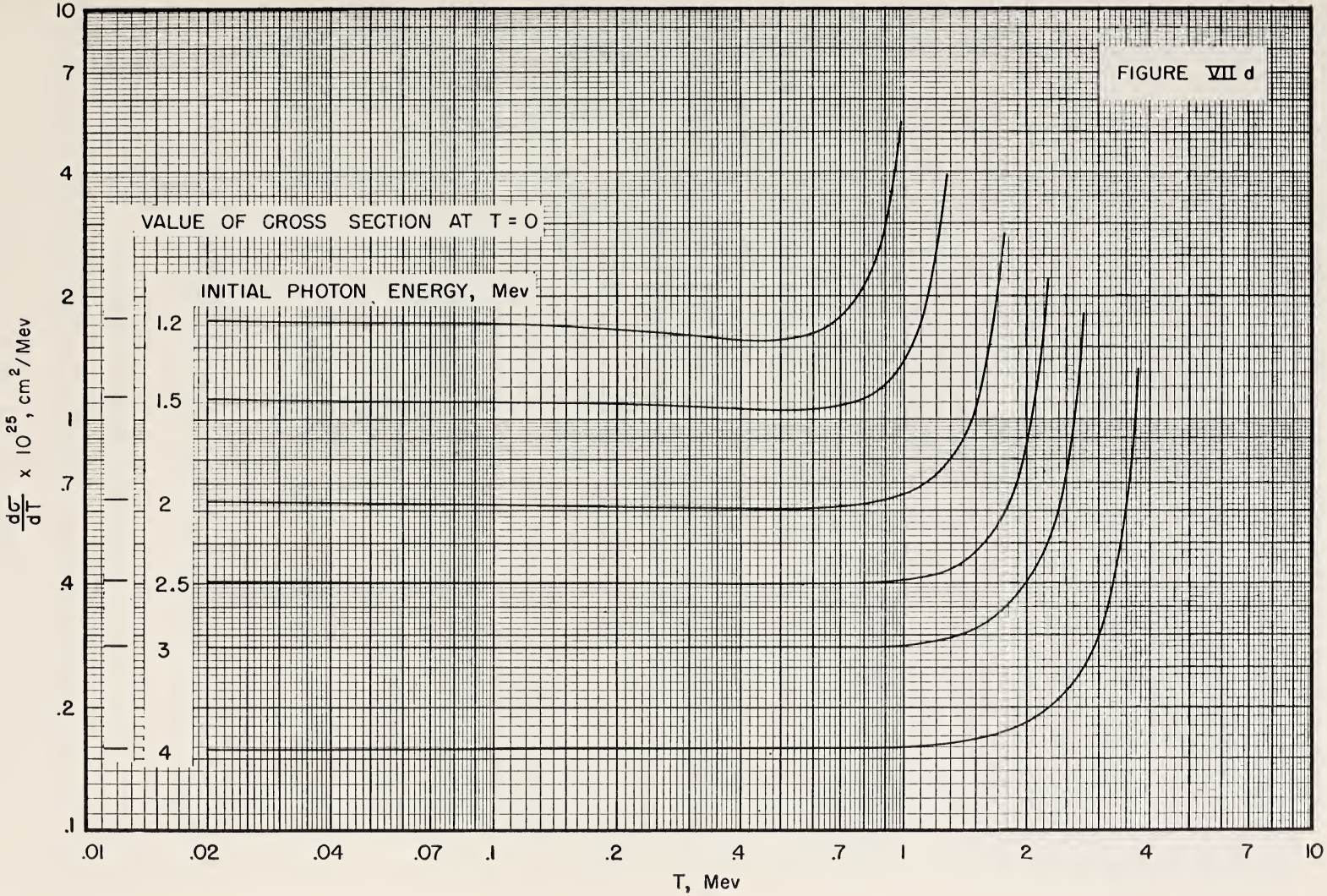
FIGURE VII d
VALUE OF CROSS SECTION AT T = 0
INITIAL PHOTON ENERGY, Mev
1.2
1.5
2
2.5
3
4
$\frac{d\sigma}{dT} \times 10^{25}$, cm^2/Mev
10
7
4
2
1
.7
.4
.2
.1
.01
.02
.04
.07
.1
.2
.4
.7
1
2
4
7
10
T, Mev

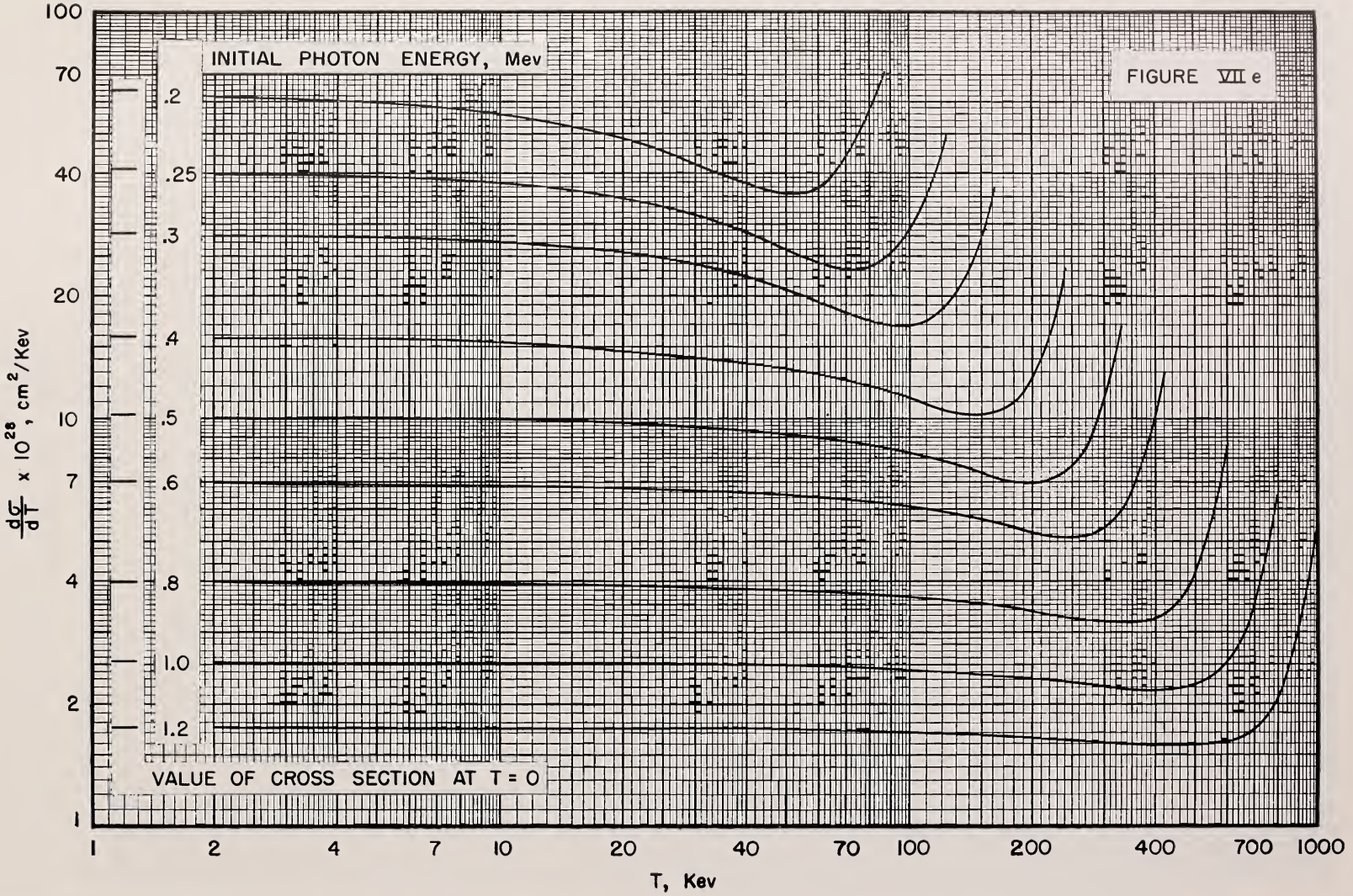
FIGURE VII e
INITIAL PHOTON ENERGY, Mev
.2
.25
.3
.4
.5
.6
.8
1.0
1.2
VALUE OF CROSS SECTION AT T = 0
$\frac{d\sigma}{dT} \times 10^{28}$, cm²/Kev
100
70
40
20
10
7
4
2
1
1
2
4
7
10
20
40
70
100
200
400
700
1000
T, Kev

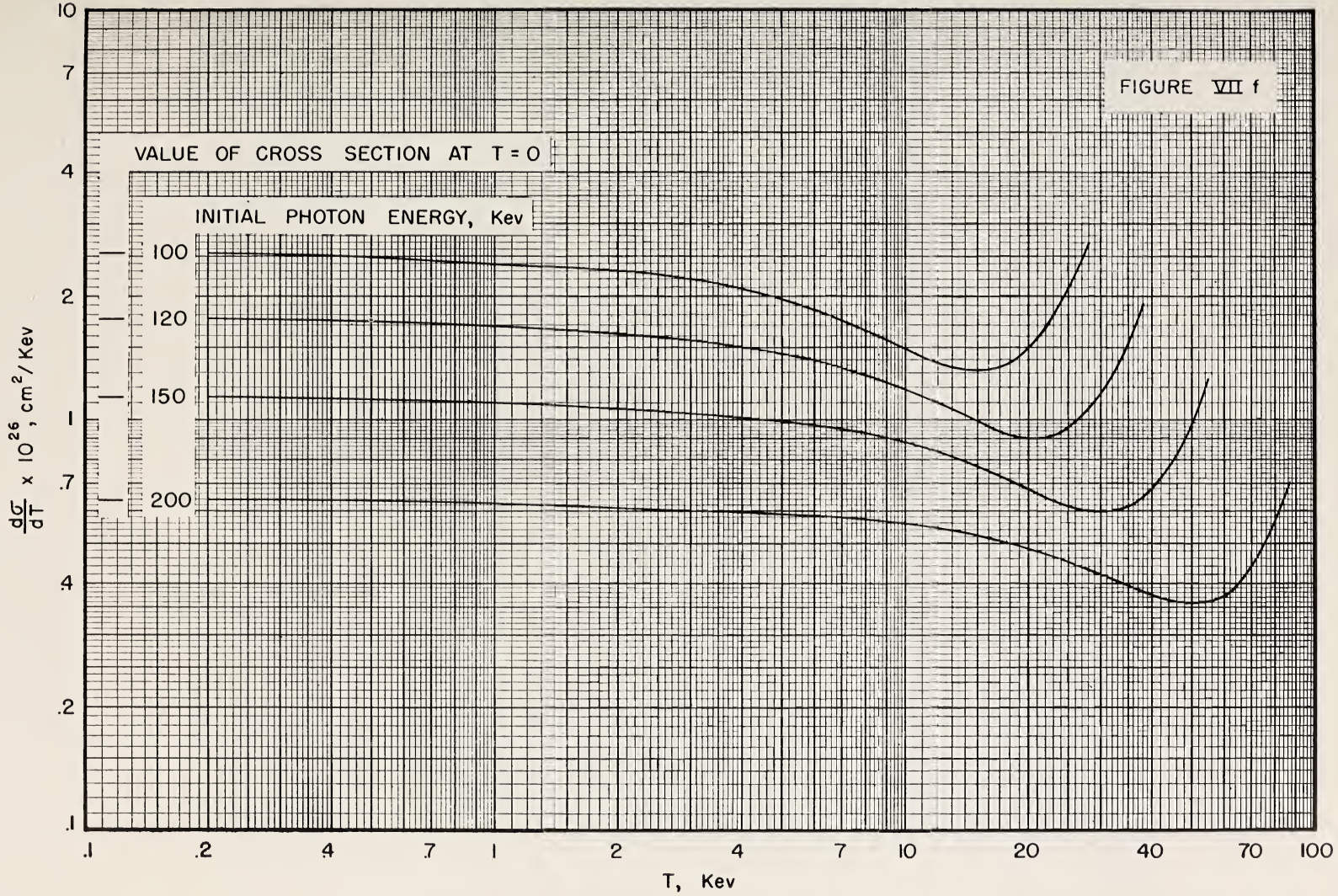
FIGURE VII f
VALUE OF CROSS SECTION AT T = 0
INITIAL PHOTON ENERGY, Kev
100
120
150
200
$\frac{d\sigma}{dT} \times 10^{26}$, cm²/Kev
10
7
4
2
1
.7
.4
.2
.1
.1
.2
.4
.7
1
2
4
7
10
20
40
70
100
T, Kev

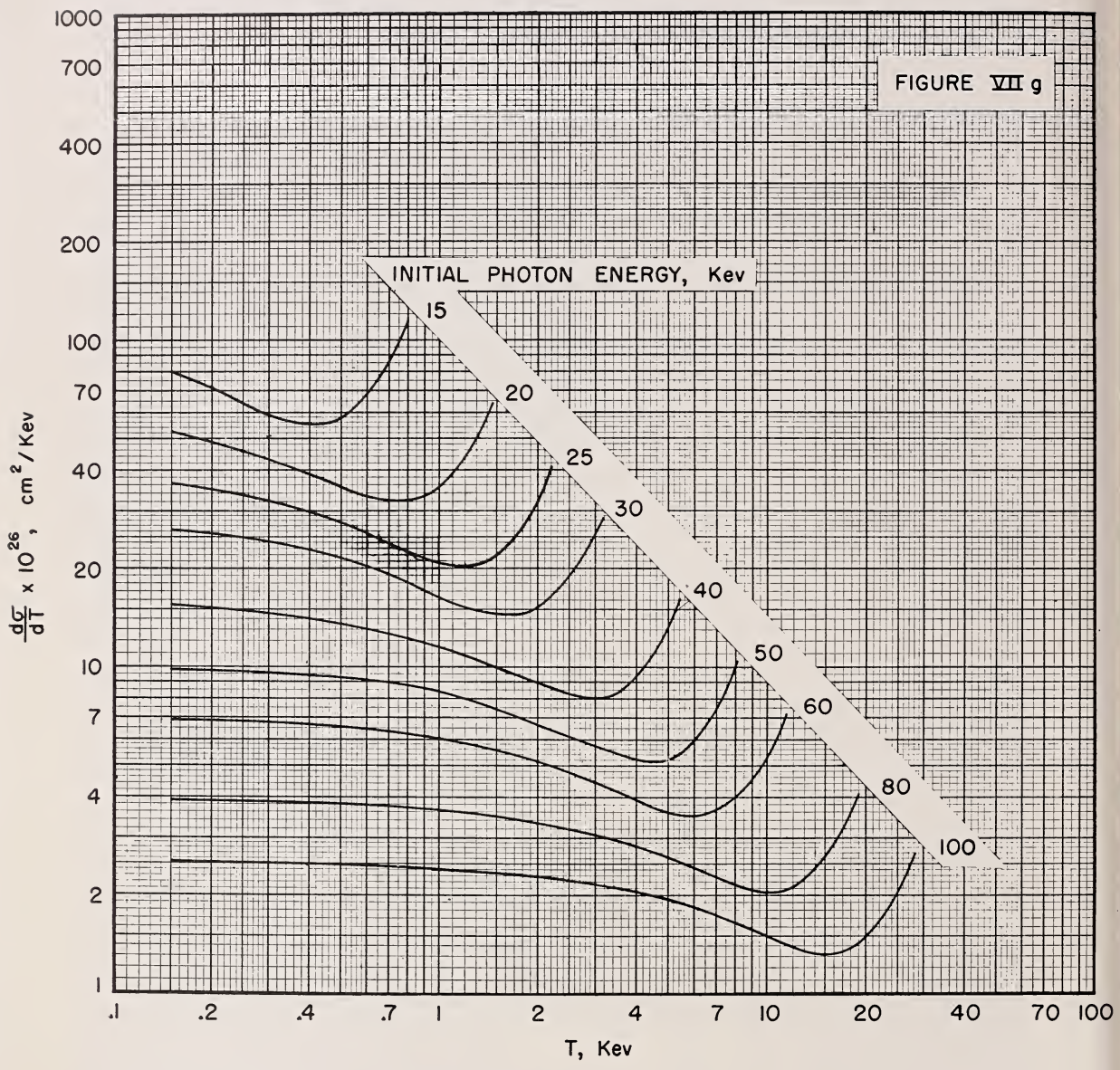
FIGURE VII g
INITIAL PHOTON ENERGY, Kev
15
20
25
30
40
50
60
80
100
1000
700
400
200
100
70
40
20
10
7
4
2
1
.1
.2
.4
.7
1
2
4
7
10
20
40
70
100
T, Kev
dσ/dT x 10^26, cm^2/Kev

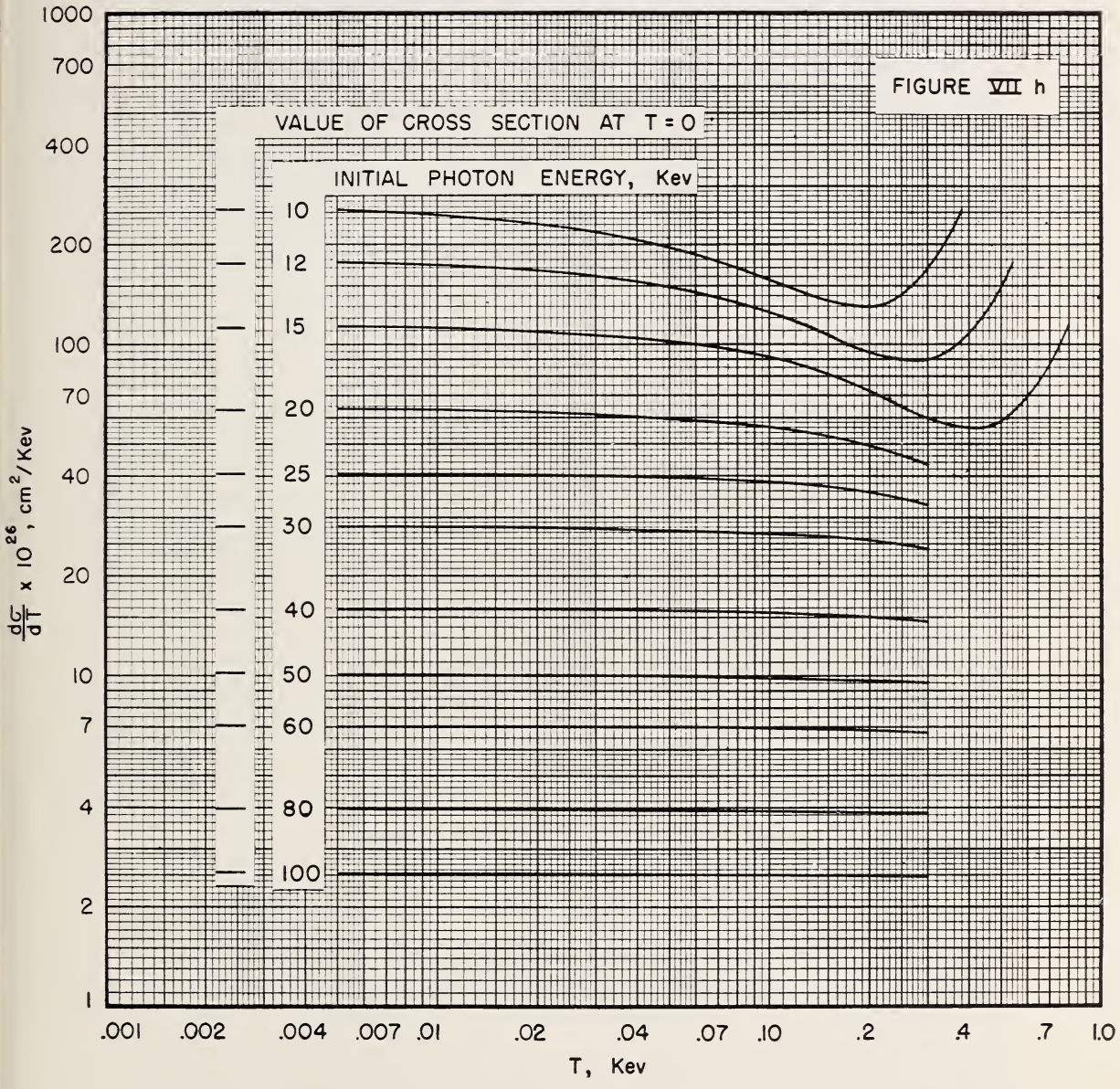
FIGURE VII h
VALUE OF CROSS SECTION AT T = 0
INITIAL PHOTON ENERGY, Kev
10
12
15
20
25
30
40
50
60
80
100
1000
700
400
200
100
70
40
20
10
7
4
2
1
.001
.002
.004
.007
.01
.02
.04
.07
.10
.2
.4
.7
1.0
T, Kev
dσ/dT x 10^26, cm^2/Kev

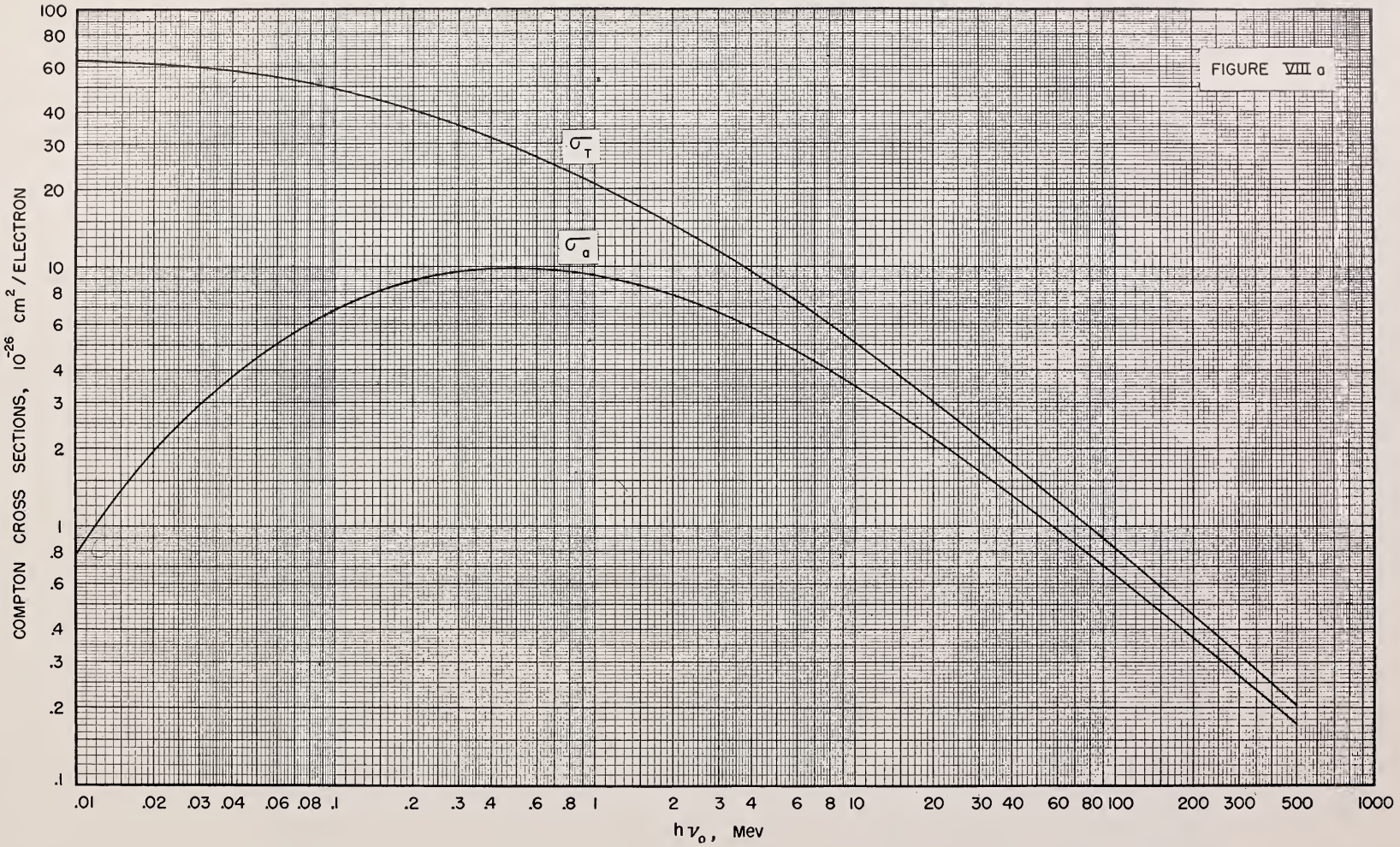
FIGURE VIII a
COMPTON CROSS SECTIONS, 10^{-26} cm^2 / ELECTRON
100
80
60
40
30
20
10
8
6
4
3
2
1
.8
.6
.4
.3
.2
.1
σ_T
σ_a
.01
.02
.03
.04
.06
.08
.1
.2
.3
.4
.6
.8
1
2
3
4
6
8
10
20
30
40
60
80
100
200
300
500
1000
$h\nu_o$, Mev

U. S. GOVERNMENT PRINTING OFFICE: 1953

DEPARTMENT OF COMMERCE
UNITED STATES OF AMERICA